CHORS TM 89-001
31 March 1989

BIOOPTICAL VARIABILITY IN THE GREENLAND SEA OBSERVED WITH THE MULTISPECTRAL AIRBORNE RADIOMETER SYSTEM (MARS) (21 MAY - 2 JUNE 1987)

by

James L. Mueller*

Charles C. Trees

Scripps Institution of Oceanography
University of California, San Diego
La Jolla, CA 92093

31 March 1989

Final Technical Report

NASA Grant NAG-5-1022
11/1/87 through 10/30/87,
extended through 30 April 1987

*Present Affiliation:

Center for Hydro-Optics and Remote Sensing
San Diego State University
6505 Alvarado Road; Suite 206
San Diego, CA 92128

Biooptical Variability in the Greenland Sea Observed with the Multispectral Airborne Radiometer System (MARS) (21 May - 2 June 1987)

BIOOPTICAL VARIABILITY in the GREENLAND SEA OBSERVED with the MULTISPECTRAL AIRBORNE RADIOMETER SYSTEM (MARS) (21 May - 2 June 1987)

1.0 INTRODUCTION and MISSION SUMMARY

A prototype Multispectral Airborne Radiometer System (MARS) was deployed aboard a survey aircraft to measure ocean color distributions in the Greenland Sea in conjunction with observations aboard the R/V Polarstern (cruise ARK IV/1) between 21 May and 2 June 1987. Dr. Nancy G. Maynard was the Principal Investigator responsible for acquisition and ecological analysis of the MARS ocean color data in this experiment, which has been supported jointly by NASA and ONR [via a contract with the Visibility Laboratory at Scripps Institution of Oceanography (SIO), the University of California, San Diego]. The aircraft was a twin-engine Dornier provided and operated by the Alfred Wegener Institute (AWI) in West Germany through collaboration with Dr. Hans-Juergen Hirche, a Principal Investigator for biological investigations aboard the R/V Polarstern. In situ spectral irradiance, spectral radiance, and spectral reflectance measurements, and phytoplankton pigment concentrations measured using the High-Performance Liquid Chromotography (HPLC) method were acquired aboard the R/V Polarstern by Dr. Charles C. Trees (of the SIO Visibility Laboratory), a Principal Investigator under a separate ONR contract.

The ARK IV/1 cruise track of the R/V Polarstern is illustrated in Appendix A (Fig. A-2), with the majority of stations concentrated in two study sites referred to as the "East Box" and "West Box". The date, GMT and geographic location of each R/V Polarstern ARK IV/1 station at which spectral reflectance and HPLC pigment concentrations were measured by Trees is listed in Table 1-1 and locations are illustrated in Figures 1-1 and 1-2. HPLC pigment concentration profiles from these stations are tabulated in Appendix A, and irradiance attenuation profiles K(488, z) are summarized in Appendix B.

The West German Dornier aircraft deployed the MARS on eight survey flights from the airport at Longyearbyen, Spitzbergen during the period between 21 May 1987 and 2 June 1987. The flightlines along which MARS data were acquired, together with locations of R/V Polarstern biooptical stations occupied within +/- two days of each flight, are discussed and illustrated in Section 6 below. Geographic positions were obtained from an inertial navigation system (INS) which was available as part of the West German Dornier airborne research facility; the MARS data

acquisition unit clock was synchronized to the INS clock, and after each flight, the INS data were downloaded to floppy discs on the MARS computer via an RS-232 interface at approximately 1 sec intervals for post-mission merger with the MARS data files. MARS radiometric data were continuously recorded as (approximately) 2-second averages during flight over each of the tracklines illustrated in Section 6, and during shorter flight segments over the Polarstern (some of which are not illustrated). Aircraft altitude during MARS data acquisition varied from approximately 500 feet to 1500 feet, and was measured with a radar altimeter recorded by the INS system for flights after 21 May 1987. Because the sun's elevation in the sky was low at this site during all flights, sun glint was not observed near nadir and the MARS view was directed at nadir (rather than tilted and directed away from the sun). Assuming a nominal altitude of 300 m and groundspeed of 85 m/sec, the spatial footprint associated with each MARS spectral radiance data point is an oval measuring approximately 160 m in the cross-track direction, and approximately 330 m alongtrack. Successive observations overlap by approximately 80 m. The 6-point averages graphed in Section 8 are therefore associated nominally with a 160 m cross-track by 1 km alongtrack footprint on the sea surface.

The present NASA Grant (NAG-5-1022) was initiated by Dr. Maynard to provide support for Mueller and Trees to develop a site-specific ocean color remote sensing algorithm and use it to convert MARS spectral radiance measurements to chlorophyll-a concentration profiles along each of the aircraft tracklines described above. This report describes that analysis and presents the results in graphical and/or tabular form. The complete MARS calibrated radiance data, together with geolocation and aircraft velocity and altitude interpolated from the INS files, are provided separately as ASCII files on magnetic tape; for each data point not contaminated by clouds or ice reflectances, chlorophyll-a concentration (and lat, lon position) is provided within a companion ASCII file on the same data tape. Data formats of the digital ASCII files, and a table of file contents for the MARS GSP-87 Data Tape, are presented in Appendix D.

The program of presentation in this report is as follows. In Section 2 we briefly describe the salient characteristics and history of development of the MARS instrument, up to the time of the observational work presented here. In Section 3 we describe our analyses of MARS flight segments over consolidated sea ice, with the end result being a set of altitude dependent ratios used (over water) to estimate radiance reflected by the surface and atmosphere in channels 1 through 9 (408 nm to 680 nm) from total radiance measured in channel 10 (725 nm). In Section 4 we present optically weighted pigment concentrations (Gordon and Clark, 1980) calculated from the profile data in Appendices A and

B, and spectral reflectances measured in situ from the Polarstern in the top meter of the water column; we then describe our analyses of this data to develop an algorithm relating chlorophyll-a concentrations to the ratio of radiance reflectances at 441 and 550 nm [with a selection of coefficients dependent upon whether significant gelvin presence is implied by a low ratio of reflectances at 410 and 550 nm]. In Section 5 we describe the scaling adjustments which were derived to reconcile the MARS upwelled radiance ratios at 410:550 nm and 441:550 nm to in situ reflectance ratios measured simultaneously during overflights of the R/V Polarstern at six intercomparison stations. In Section 6 we graphically present the locations of MARS data tracklines and positions of Polarstern stations occupied within two days of each flight. In Section 7 we present "stick-plots" of MARS tracklines selected to illustrate two-dimensional spatial variability within the "box" covered by each day's flight. Finally in Section 8, we present curves of chlorophyll-a concentration profiles derived from MARS data along survey tracklines.

We now briefly summarize the significant results of our investigation:

a. An algorithm was developed to correct MARS radiance measurements for atmospheric backscatter and surface reflection contributions, based on the assumption that at 725 nm (MARS channel 10) there is no upwelled radiance contribution from beneath the sea surface. This approach follows what has become common practice in atmospheric corrections to Nimbus-7 CZCS data (Gordon, 1978; Gordon, et al., 1983). Because the MARS could not be equipped with downwelling (incident) irradiance channels in time for the 1987 deployment, we were forced to use a small set of MARS radiance measurements over sea ice to estimate the spectral quality of the components due to atmospheric backscatter and sea-surface reflections in spectral radiance measured by MARS over water. In this approach we assumed that the reflectance of sea ice is grey, i.e. not wavelength dependent. We also assumed that the cloud cover and solar elevation conditions, and resultant spectral quality of incident daylight, which prevailed during the sea ice reflectance measurements were representative of conditions during the entire sequence of eight flights on different days. We recognize that both of these assumptions are suspect, but we have no better source of information on which to base analyses of the present data set.

b. An algorithm for calculating chlorophyll-a concentration from the ratio of radiance reflectance R(441) at 441 nm to R(550) at 550 nm was developed by regression analyses

of HPLC pigment concentrations on in-situ reflectances measured with a Biospherical Instrument Inc. MER-1032 submersible radiometer. Two separate regression equations were derived to separate cases influenced by apparently high concentrations of decayed organic material in freshly melted sea-ice, as indicated by low reflectance ratios R(410):R(550). A classification algorithm (to select the appropriate chlorophyll-a vs R(441):R(550) coefficients) was derived through separate regressions of ratios R(410):R(550) vs R(441):R(550) for subsamples of stations known to be unaffected by ice melt ("East Box" stations only), and stations known to be so affected (a subset of "West Box" Stations characterized by low salinity at 10 m and by obviously low R(410):R(550) ratios). When this two-step algorithm (classification followed by chlorophyll-a computation) is applied to all biooptical stations, the squared correlation coefficient is 0.71 (squared correlation improves to 0.86 if one apparent outlier - station 168 - is excluded, and to 0.91 if stations 168 and 143 are both excluded).

c. Inspection of MARS calibrated radiance spectra over both ice and water persistently contain unrealistically high relative values of L(410) (channel 1 radiance). L(441) (channel 2 radiance) is also persistently greater than might be expected, but by a much smaller amount (relative to radiances in the other channels) than is L(410). The instrument did not display these tendencies in calibration tests under laboratory conditions at room temperature. We speculate that these two channels, which are both at wavelengths where detector sensitivity is low and signal to noise ratios are small, may be sensitive to ambient operating temperature, but we've not yet had time and resources to test the instrument for these tendencies. We expect to do so in the near future. We also note that the MARS had a new Barium-Sulfate coating applied in West Germany during the deployment (see Section 2 below), and that the MARS was not recalibrated until more that a month later when the instrument was returned to San Diego. During the first few weeks after application, new coatings tend to age and reduce reflectance especially rapidly, and the effect is greatest at the shorter wavelengths. This aging tendency could explain the anomalously high relative radiance levels in these channels (i.e. for a given aperture radiance, a higher coating reflectance at the time of the field observations whould produce a larger irradiance in the sphere than would the same aperture radiance and reduced coating reflectance at the time of calibration. We can only speculate at this point, however. To allow

analysis of the 1987 GSP MARS data, we chose to reconcile the MARS water leaving radiance ratio estimates Lw(410):Lw(550) and Lw(441):Lw(550) to in situ reflectance ratios R(410):R(550) and R(441):R(550) respectively at the 6 simultaneous comparison stations with the Polarstern. Through a post hoc trial and error adjustment, the best agreement between the respective MARS radiance and in situ MER reflectance ratios was obtained when MARS calibrated radiances were reduced by the scale factors 0.83 in channel 1 and 0.95 in channel 2.

d. Despite a limited number of simultaneous ground truth stations and our post-hoc adjustment of MARS calibration factors in channels 1 and 2 (above), the chlorophyll-a distributions calculated from MARS data are plausible and agree at least semi-quantitatively with alongtrack chlorophyll-a fluorescence measured aboard Polarstern. An exhaustive comparison between MARS and Polarstern observations, and the associated descriptive oceanographic analysis, are beyond the scope of the present grant. We offer, however, two brief intercomparisons. Chlorophyll-a concentration calculated for MARS Trackline B of 23 May 1987 (see also Sections 6, 7 and 8 for other presentations of this data) is illustrated in the upper panel of Figure 1-3. In the lower panel are shown graphs of alongtrack values of particle counts (2 sizes), sea surface temperature (line without symbols), and un-normalized chlorophyll-a fluorescence (triangles) measured aboard Polarstern along the same transect on 21 May 1987. The two tracklines both show the same ocean front near 5.5 E longitude, with higher chlorophyll concentrations (approximately 1.5 ug/l) to the west and lower concentrations (approximately 0.75 ug/l) to the east. The MARS values agree in magnitude with HPLC pigment concentrations measured from samples at stations in the two separate water masses, and were the fluorescence values also normalized to the discrete concentrations, they would also. These patterns are representative of the structure and amplitude of chlorophyll-a variability observed in the "East Box" by MARS (Sections 7 and 8, tracklines from 21, 23 and 25 May 1987) and at Polarstern stations (Appendix A and Hirche, 1987). The "West Box" (Secs. 6, 7 and 8, plots for 29 May thru 2 June 1987) was characterized by more dramatic frontal structure in both the MARS and Polarstern chlorophyll-a data, with concentrations ranging from 0.25 to more than 5.0 ug/l. Figure 1-4 compares the alongtrack chlorophyll-a fluorescence (again not normalized to concentration) measured aboard Polarstern on 31 May 1987 with chlorophyll-a calculated from MARS

along the same transect (Trackline A of 31 May 1987). The bottom solid curve is MARS chlorophyll concentration, and the upper dashed curve (which we transferred by hand from Hirche 1987) represents in situ fluorescence. The detailed agreement between MARS and in situ fluorescence along this trackline is remarkable. Both observations show the intense front near 0.5 E longitude with minimum chlorophyll-a concentration (< 0.5 ug/l) immediately east of the front, high concentrations to the west of the front organized in a sharply sharply banded structure, and low concentrations increasing weakly with distance east of the minimum. Both curves also decrease abruptly near 2 W near the marginal ice zone (segment denoted "MIZ") and show remarkably similar spatial structures in and near the MIZ.

REFERENCES:

Gordon, H. R., 1978. Removal of atmospheric effects from satellite imagery of the oceans. Applied Optics, 17:1631-1636.

Gordon, H. R. and D. K. Clark, 1980. Remote sensing optical properties of a stratified ocean: an improved interpretation. Applied Optics, 19:3428-3430.

Gordon, H. R., et al., 1983. Phytoplankton pigment concentrations in the Middle Atlantic Bight: comparison between ship determinations and Coastal Zone Color Scanner estimates. Applied Optics, 22:20-36.

Hirche, H-J., 1987. Data Report of RV "Polarstern" Cruise ARK IV/1, 1987 to the Arctic and Polar Fronts. Alfred Wegener Institute for Polar and Marine Research, Bremerhaven, FRG. 228p

Fig. 1-1: Polarstern Stations "West Box"
29 May 1987 - 4 June 1987

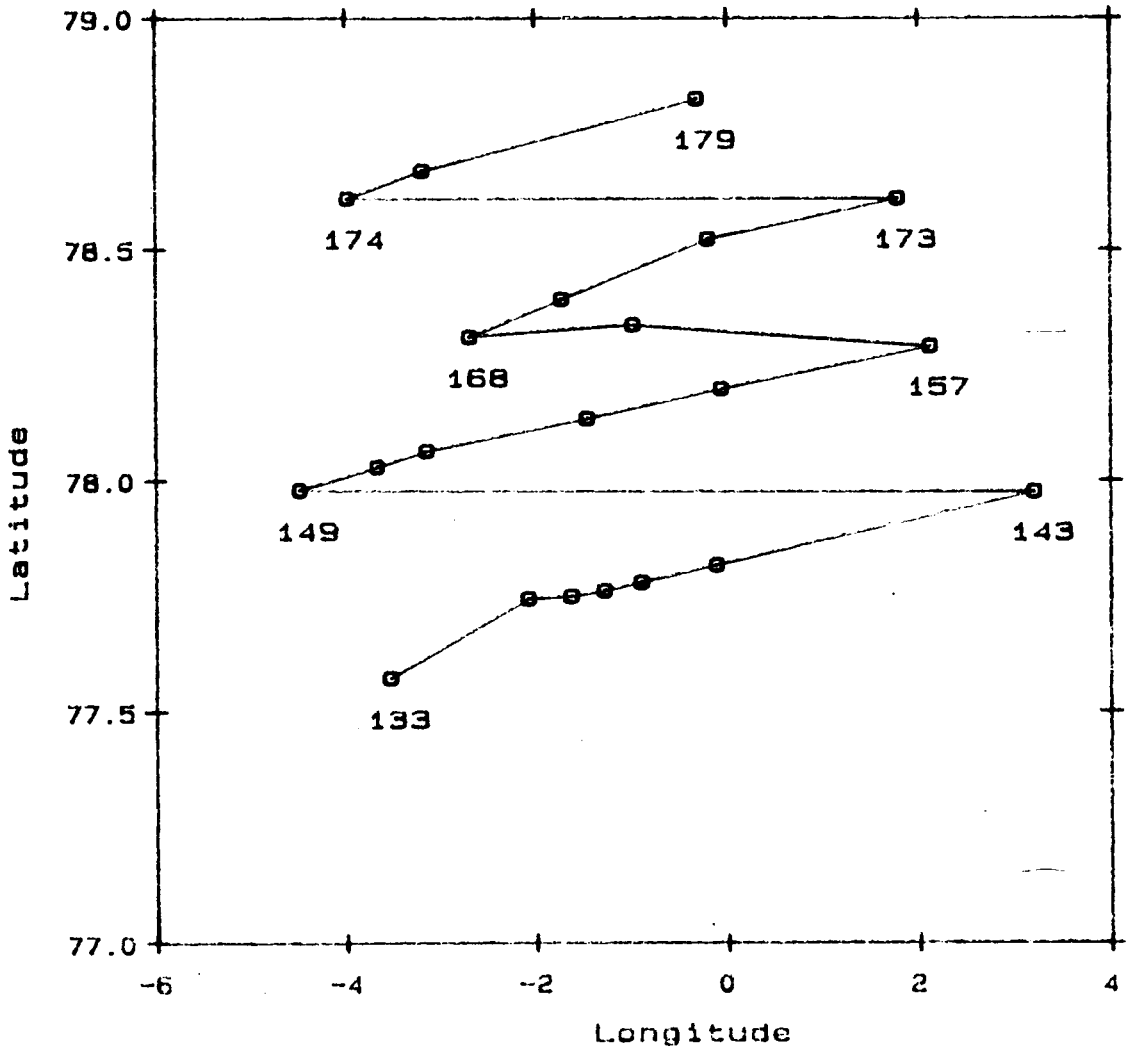

Fig. 1-2: Polarstern Stations "East Box"
19 May 1987 - 27 May 1987

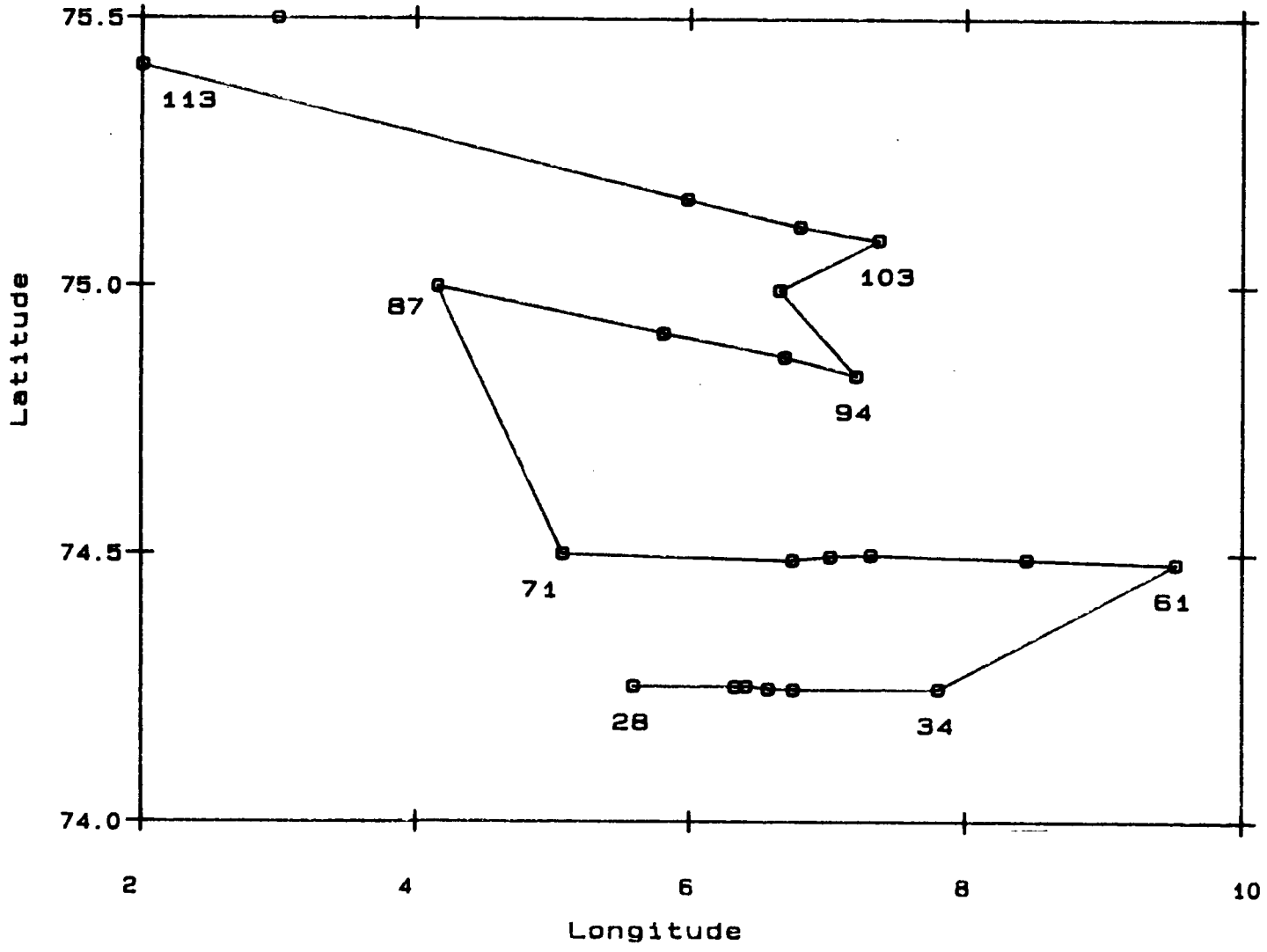

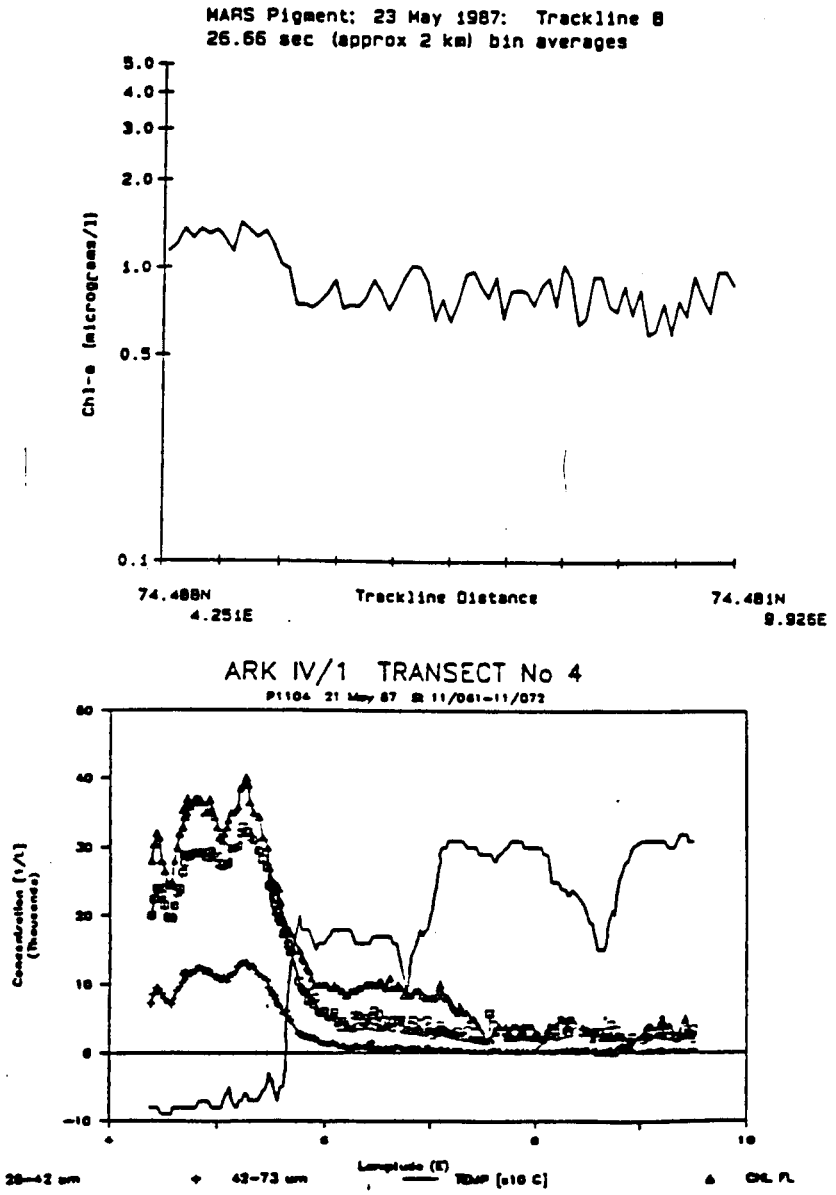

Figure 1-3: Comparison of chlorophyll-a estimated from MARS1 (top) with chl fluorescence & SST measured aboard R/V Polarstern along an E-W transect in the eastern Greenland Sea; "East Box".

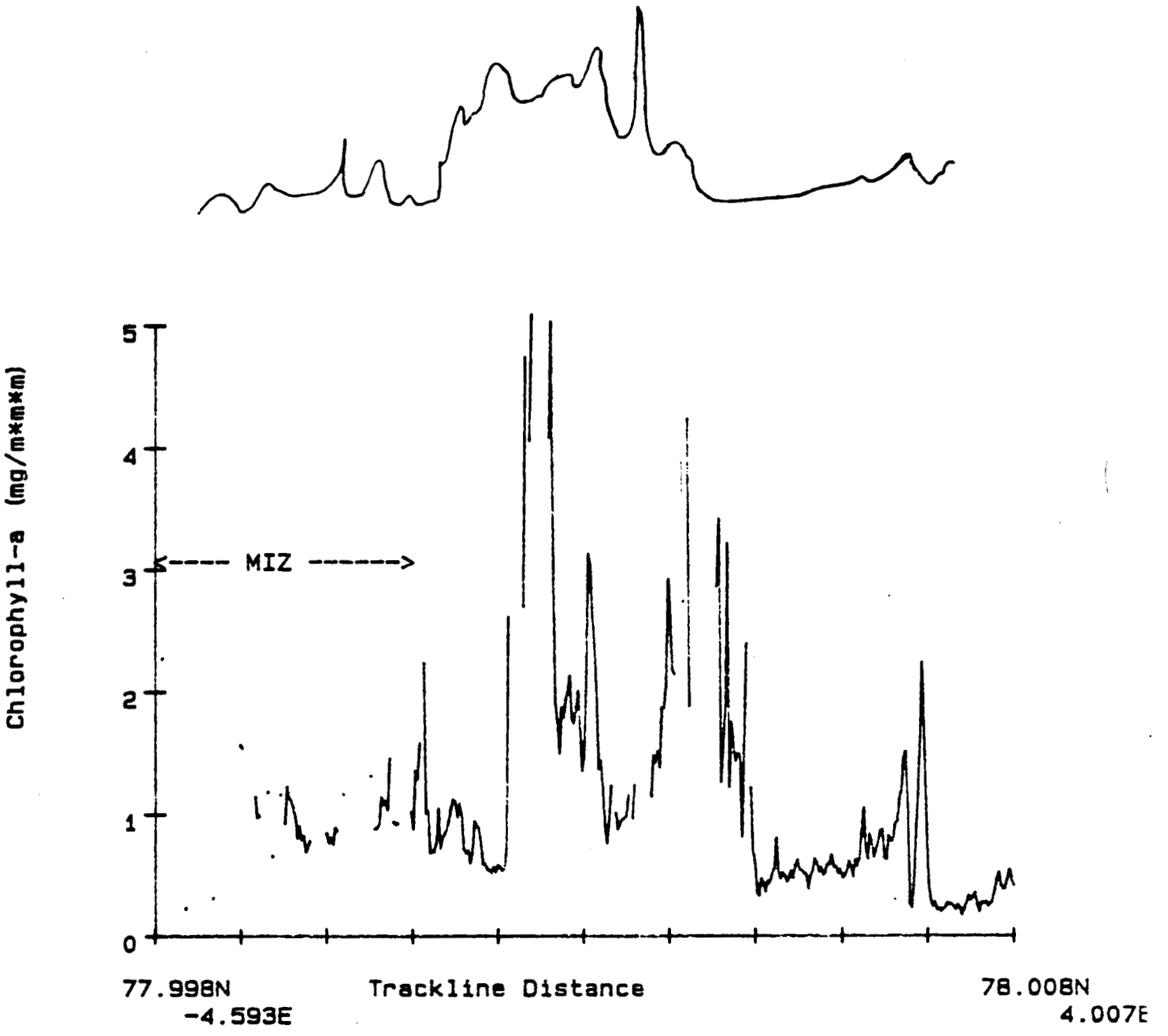

Figure 1-4: Comparison between MARS chlorophyll-a concentration (lower solid curve; Trackline A of 31 May 1987, see also sections 6,7 and 8) and un-normalized raw fluorescence measured along the same trackline aboard R/V Polarstern on 31 May 1987 (Hirche, 1987).

2.0 MULTISPECTRAL AIRBORNE RADIOMETER SYSTEM DESCRIPTION

The Multispectral Airborne Radiometer System (MARS) is a self-contained, portable, ten channel radiometer designed to measure ocean color from aircraft of opportunity. In flight, the MARS views the sea surface through a camera window at fixed nadir and azimuth angles, and thus measures a single horizontal profile of ocean color along the trackline followed by the aircraft. The MARS mounting assembly allows the viewing nadir angle to be adjusted from 0 to 20 degrees, and the viewing azimuth angle may be adjusted through 360 degrees to avoid sun-glint.

The core of the MARS optical assembly is an integrating sphere, the interior of which is illuminated through a 50mm f1.2 camera lens and a removable field stop. As configured for the Greenland Sea mission reported here, the field stop was sized to produce a 30-degree field-of-view. The interior surface of the sphere is coated with Barium-Sulfate, a white material with a reflectance of approximately 0.95, to uniformly diffuse light from the entrance aperture throughout the cavity. The uniform irradiance within the sphere is therefore proportional to radiance at the entrance aperture integrated over the entire field-of-view.

Ten silicon photodiode detectors, each covered with an interference filter, are mounted to view the interior of the integrating sphere through small ports. The wavelengths and spectral bandpasses (half-power, full-width) of the 10 MARS channels, as configured for the GSP mission, are listed in Table 2-1. The electronic assembly for amplifying the detector signals, analog-to-digital conversion, instrument control, and data communication are slightly modified versions of the electronics boards in the MER-1015 underwater radiometer manufactured by Biospherical Instruments, Inc., of San Diego, CA. The electronic boards provide additional channels, four of which were intended to be used to measure downwelling irradiance at four wavelengths through a cosine collector on top of the airplane; unfortunately, time did not permit adding this capability to MARS for the 1987 GSP mission. Instrument control and data logging are performed by a laptop IBM Personal Computer via an RS-232-C interface, using software provided by Biospherical Instruments, Inc. (who also aided in adapting it to the airborne application).

The ouput from each of the 10 channels is calibrated to radiance at the entrance aperture of the sphere by viewing a diffuse reflectance plate illuminated at 45-degrees by a laboratory working standard lamp (traceable to an NBS irradiance standard lamp through periodic comparison experiments). MARS was calibrated before the 1987 deployment to Spitzbergen via West

Germany, but the original PTFE coating detached from the interior of the sphere during shipment to West Germany. The present Barium-Sulfate coating was, therefore, applied at a laboratory in West Germany before installation aboard the Dornier and deployment to Spitzbergen. This instrument modification completely invalidated the predeployment calibration. MARS was calibrated again immediately following its return to the Visibility Laboratory in June 1987, with the results reported in Appendix C.

TABLE 2-1

Wavelength Characteristics of MARS Channels

Channel	Center Wavelength (nm)	Spectral Bandpass (HPFW) (nm)
1	408.6	13.9
2	437.5	11.3
3	486.8	10.5
4	518.6	10.0
5	548.8	9.9
6	586.3	12.1
7	629.8	13.0
8	665.6	13.8
9	679.6	14.4
10	726.4	19.0

3.0 MARS ATMOSPHERIC and SURFACE REFLECTION CORRECTIONS

The total radiance measured in each MARS channel represents the sum of upwelled radiance leaving the water from beneath the surface (as attenuated by the intervening atmosphere) and path radiance due to incident daylight reflected from the sea surface and backscattered by the intervening atmosphere. Only the water leaving radiance is of interest for remotely sensed ocean color applications; the path radiance contributions must be estimated and removed from each channel. In the present work, the MARS data tracklines were flown at low enough altitudes (150 to 500 m) that we may safely neglect atmospheric attenuation. However, significant path radiance is present due both to atmospheric backscatter and surface reflections.

Following common practice in CZCS algorithms (Gordon, 1978; Gordon, et al 1980), we assume that at a wavelength of 725 nm (MARS channel 10) the ocean is black, i.e. that the water leaving radiance is zero. Under this assumption, the measured radiance L(725) is assumed to be solely due to surface reflectance and path radiance. To first order at these low altitudes, the combined surface reflectance and path radiance at the shorter wavelengths should scale to that at 725 nm in direct proportion to the ratio of downwelled irradiances at the wavelengths in question, with a small but significant coefficient variation with flight altitude. Were the MARS equipped with uplooking irradiance detectors, we could determine the appropriate scale factors directly, but as is noted in Section 2, we were unable to complete that subsystem of the instrument in time for the GSP mission.

Substantial subsegments of Trackline A from 29 May 1987 (4 segments) and of Trackline C from 1 June 1987 (2 segments) were identified from the flight logs and channel 10 brightness as being over 100% consolidated sea ice. We assume that the reflectance of sea ice is spectrally grey (i.e. equal at all wavelengths), and that the illumination conditions (as determined by cloud cover and solar elevation) during the data runs over the ice were representative of conditions throughout the entire set of flights. Given these assumptions, which are admittedly suspect, we may interpret the ratios of radiances in channels 1 through 9 (409 nm through 685 nm) relative to radiance in channel 10 (725 nm) as representing the spectral quality of surface reflectance plus path radiance over water. To correct data acquired over water, we subtract from radiance in each of channels 1 through 9 the product of channel 10 radiance and the respective radiance ratio derived from our analysis of the data runs over the ice; the residual signal is our estimate of water leaving radiance Lw for each channel.

The path radiance portion of this correction should increase with decreasing wavelength, and in the absence of aerosols would vary as the -4th power of wavelength. The spectral ratios of surface reflectance plus path radiance relative to 725 nm should, therefore, become larger with increasing altitude. By sorting the original sea ice segments by altitude, subsegment samples at eight different mean altitudes were extracted. The average reflectance ratios and altitudes for these segments are listed in Table 3-1, together with channel 10 radiance L(725). Least squares linear regression coefficients accounting for the apparent variation in reflectance with increasing altitude are summarized in Table 3-2 below, and the data for channels 1, 2 and 5 (410, 440 and 550 nm nominal wavelengths respectively) are illustrated in Figure 3-1. With the exception of channel 8, the slopes decrease monotonically with increasing wavelength, which is consistent with the increasing relative contribution of atmospheric backscatter to the surface reflection plus path radiance correction. We have no explanation for the apparent anomalous behaviour of channel 8 (667 nm).

The coefficients in Table 3-2 may be used to correct radiances in channels 1 through 9 for surface reflectance and atmospheric backscatter. Given flight altitude H in feet, estimate water leaving radiance Lw for each channel as

$$Lw(ch) = Lt(ch) - [\ a(ch) + b(ch) * H\ ] * Lt(10),$$

where Lt(ch) is the calibrated value of MARS radiance in channel ch. Based on our post-hoc analysis (Section 5), the calibrated radiances in channel 1 should be reduced to 0.83 * Lt(1) and in channel 2 to 0.95 * Lt(2) before applying this correction.

Table 3-1

Mean Reflectance Ratios L(ch)/L(10) for Eight MARS Data Track Segments over 100% Consolidated Sea Ice at Different Flight Altitudes

ch: 1 *	2 **	3	4	5	6	7	8	9	L(10)	Alt
409nm	438nm	487nm	519nm	549nm	586nm	630nm	666nm	680nm	726nm	ft
1.515	1.542	1.667	1.620	1.679	1.565	1.396	1.143	1.209	11.448	443
1.507	1.533	1.655	1.605	1.664	1.551	1.382	1.139	1.199	9.314	392
1.540	1.568	1.695	1.647	1.708	1.588	1.411	1.158	1.218	10.834	455
1.539	1.566	1.690	1.640	1.701	1.584	1.408	1.133	1.216	12.765	405
1.712	1.717	1.827	1.772	1.835	1.682	1.483	1.298	1.269	6.839	894
1.660	1.665	1.775	1.725	1.783	1.642	1.455	1.281	1.251	6.563	920
1.623	1.630	1.740	1.689	1.751	1.617	1.436	1.234	1.239	8.796	823
1.633	1.640	1.750	1.698	1.758	1.622	1.439	1.247	1.240	8.060	970

* Reduced by factor 0.83 (Section 5, below).

** Reduced by factor 0.95 (Section 5, below).

Table 3-2

Altitude Dependence of MARS Ice Reflectance Ratios from Least Squares Regression

$$\{ L(ch)/L(10) \} = a + b * \text{altitude (feet)}$$

channel	a	b (1/feet)
1	1.4121	2.70119E-4
2	1.4568	2.27577E-4
3	1.5933	1.98516E-4
4	1.5472	1.92134E-4
5	1.6068	1.93248E-4
6	1.5123	1.41902E-4
7	1.3524	1.11481E-4
8	1.0375	2.51472E-4
9	1.1766	0.80788E-4

Figure 3-1: MARS Reflectance Ratios over Sea Ice versus Flight Altitude

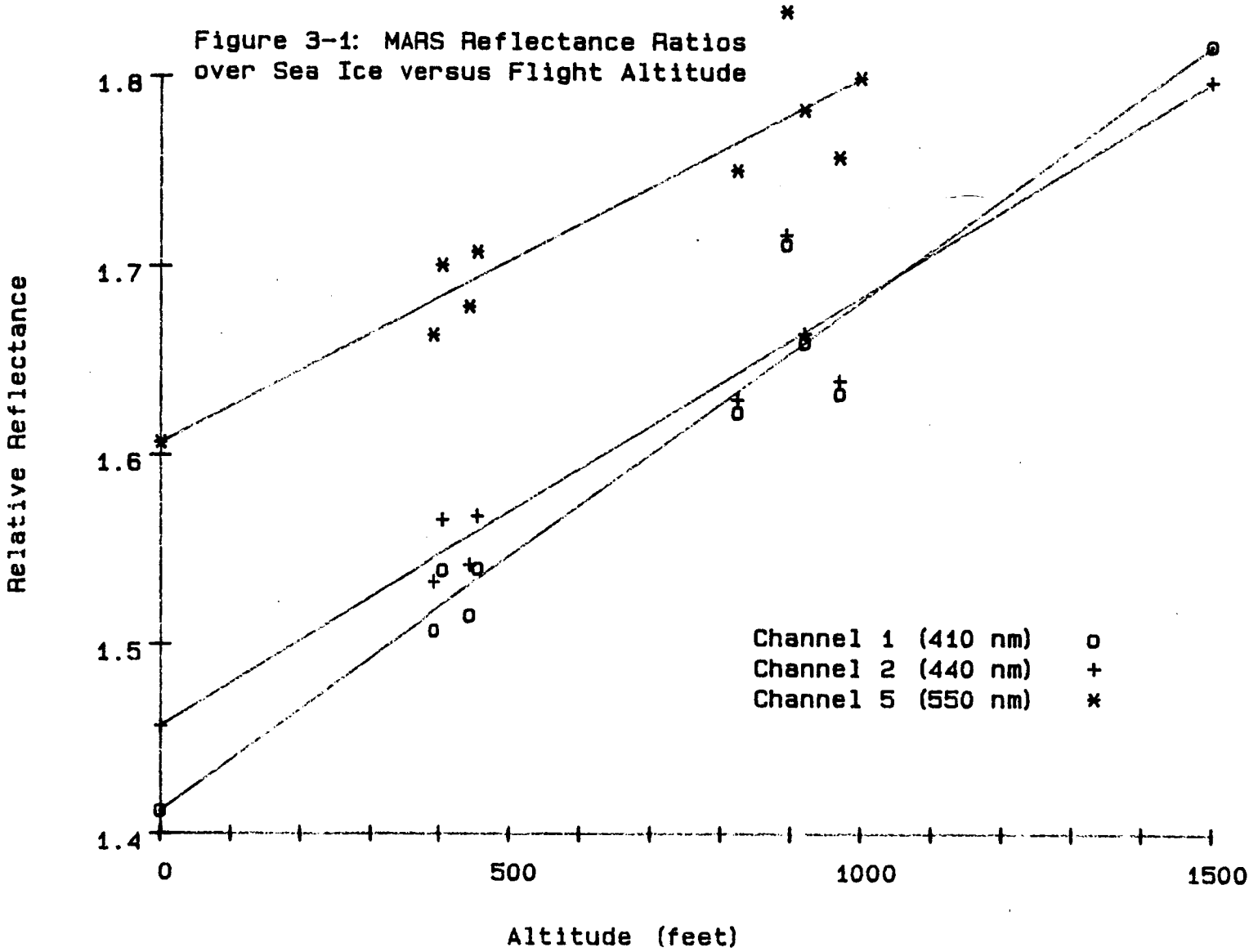

4.0 CHLOROPHYLL-A vs SPECTRAL REFLECTANCE RATIO ALGORITHM

Phytoplankton pigment concentrations were measured aboard the R/V Polarstern by C. Trees using HPLC methods (Appendix A). Trees also measured in situ profiles of downwelling irradiance Ed at 12 wavelengths, and of both spectral upwelling irradiance Eu and radiance Lu at 8 wavelengths. These measurements were made using an MER-1032 underwater radiometer manufactured by Biospherical Instruments Inc. of San Diego. Downwelling irradiance attenuation coefficient profiles are characterized in Appendix B.

Phytoplankton pigment concentration profiles (Appendix A) were optically weighted, using K(488) values for each station from Appendix B, using the method of Gordon and Clark (1980). The optically weighted surface concentrations of the 10 pigments are listed in Table 4-1 below. The concentrations listed in table 4-1 are given in pico-moles per liter. To convert these concentrations to micrograms per liter, simply multiply the values in table 4-1 by the molecular weight of the pigment in question and divide by 10**6. The molecular weights of these pigments are given here for convenience as: chlorophyll-a = 893.48; chlorophyll-b = 907.46; chlorophyll-c = 613.97; Fucoxanthin = 658.88; Beta-Carotene = 536.85; Hex. = 773.08; Chloropyllide-a = 614.97; Diadino = 582.00; and Peridinin = 630.00.

Surface radiance reflectance (Pi * Lu / Ed) values were calculated by averaging all MER-1032 readings from the top 1 m at each station. These spectral reflectances (Table 4-2) were then paired with optically weighted chlorophyll-a concentrations (Table 4-1) to derive an in-water algorithm to estimate chlorophyll from remotely sensed ocean color ratios measured by the airborne MARS. We follow the now common practice of parametrizing ocean color using the ratio

R(440 nm) : R(550 nm)

as a color index which is highly sensitive to surface chlorophyll-a concentration. On examining the overall scatter of data from "East Box" and "West Box" stations taken as a single sample, it became apparent that chlorophyll-a was not uniformly correlated with the R(440):R(550) color index over the entire data set. In particular, stations taken in the "West Box" very near the sea-ice edge (and presumably influenced by recently melted ice) followed a distinctively different scattergram than "East Box" stations, which were known to be free of recently melted sea ice.

Further examination of stations in the Marginal Ice Zone revealed that those stations closest to the ice edge were characterized by anomalously low values of the "yellow index"

R(410 nm) : R(550 nm)

which indicated that gelvin (decayed organic matter, whether particulate or dissolved) may have been present in significant quantities in areas influenced by recently melted sea ice. Trees examined CTD profiles from Hirche (1987) and found that stations characterized by low "yellow indices" R(410):R(550) were also characterized by depressed salinity at 10 m depth, indicating a clear associated with melted sea ice. We do not have independent corroborative evidence of elevated concentrations of decayed organic matter here, but the combination of low "yellow indices" and low salinity strongly suggests that decayed organic matter had been trapped in the ice and released to the upper water column in the MIZ.

We therefore extracted data from the sub-sample of the stations occupied in the "East Box", where melted sea ice could not reasonably have contributed elevated gelvin concentrations. The data from these stations (which in general evidenced low variability) are illustrated in Figure 4-1, together with the least-squares linear regression line

$$\log(\text{chlorophyll-a}) = 0.523 - 0.193 * \log(R(440) / R(550)), \quad (4\text{-}1)$$

which yields a squared correlation coefficient of 0.71 and residual standard deviation of 0.110 log-chl in micro-grams per liter.

A second subset of data from the 6 stations which were obviously influenced by melted sea ice was also extracted for a separate regression analysis. These data are illustrated in Figure 4-2, together with the regression line

$$\log(\text{chlorophyll-a}) = 0.081 - 0.278 * \log(R(440) / R(550)), \quad (4\text{-}2)$$

which yields a squared correlation coefficient of 0.99 and a residual standard deviation of 0.031.

The coefficients in equations (4-1) and (4-2) have been adjusted to reflect multiplication by the molecular weight of chlorophyll-a, and thus give the log of chlorophyll-a concentration in micro-grams per liter (rather than in pico-moles per liter, as given in Table 4-1).

Clearly the subsamples associated with equations (4-1) and (4-2) belong to statistically distinct biooptical water masses. To provide a basis for classifying a given Greenland Sea station as

belonging to one population or the other, we examined the above two subsets of the sample on the basis of correlations between the color index R(440):R(550) and the yellow index R(410):R(550). These stations are plotted in Figure 4-3, together with the regression fits relating the two indices in each population. Again, the two subsamples are clearly statistically distinguishable, with the "East Box" stations following the relationship

$$\log\{R(410) / R(550)\} = 1.054 + 0.773 * \log\{R(440) / R(550)\}, \quad (4\text{-}3)$$

with squared correlation 0.789 and residual standard deviation 0.475, and the "West Box" "Yellow Stations" follow the relationship

$$\log\{R(410) / R(550)\} = -0.243 + 0.607 * \log\{R(440) / R(550)\}, \quad (4\text{-}4)$$

with squared correlation 0.936 and residual standard deviation 0.177.

For a given station, if the index pair

$$\{ \log[R(410)/R(550)], \log[R(440)/R(550)] \}$$

falls closer to the line (4-3), we use the algorithm (4-1), and if it falls closer to the line (4-4) we use the algorithm (4-2), to compute chlorophyll-a concentration from the remotely sensed ocean color index R(440):R(550). The application of this algorithm to the entire data sample is illustrated in Figure 4-4. The squared correlation associated with the composite algorithm [classification by distance from (4-3) and (4-4) followed by application of (4-1) or (4-2) as appropriate] is 0.71 for all stations. Were we to exclude station 168, which is apparently misclassified by the [yellow,color] index pair, the squared correlation would improve to 0.86, and if we also excluded station 143 it would improve to 0.91. Under any of these conditions, the algorithm is clearly accurate and robust enough to permit useful estimation of chlorophyll-a concentration distributions from ocean color indices measured remotely by the airborne MARS.

Table 4-1

OPTICALLY WEIGHTED PIGMENT CONCENTRATIONS

Sta:	chlide_a	chl_c	perid	fuco	hex	pras	zea	chl_b	chl_a	carot
28	44.44	115.77	6.11	226.76	124.29	138.56	139.74	343.16	647.42	61.56
30	54.05	125.75	7.26	110.36	147.76	161.76	132.98	371.42	689.30	49.99
31	23.08	125.74	0.00	208.64	95.81	195.57	117.24	260.92	671.66	58.43
61	172.76	265.08	37.94	152.66	359.77	174.65	112.66	272.04	1197.49	59.17
63	197.01	290.99	40.55	142.60	545.21	274.78	36.66	312.63	1243.85	61.95
65	294.13	467.61	22.50	337.65	454.03	270.90	190.02	252.70	1553.67	78.81
66	265.43	341.66	17.36	135.86	589.83	258.23	0.00	248.53	1240.93	69.40
67	289.80	346.55	15.10	118.90	674.20	282.73	0.00	390.88	1374.92	69.48
90	132.83	312.66	0.00	459.10	289.91	256.30	130.86	532.54	1426.10	70.31
92	350.12	403.54	0.00	179.53	783.36	385.96	0.00	424.24	1538.51	72.27
94	503.47	666.73	56.98	413.76	777.16	466.92	0.00	343.67	2290.58	90.87
101	99.38	171.72	2.36	204.74	236.85	203.75	168.60	525.01	1034.17	79.87
103	227.82	390.94	29.46	400.21	426.13	367.77	51.88	362.10	1449.76	67.19
105	97.92	171.51	1.18	175.81	219.39	194.44	163.86	474.02	915.77	78.59
107	84.58	243.12	64.23	251.93	229.60	293.90	0.00	339.37	999.48	72.47
113	46.01	65.42	0.00	52.17	97.92	113.35	0.00	0.00	327.10	21.55
117	210.80	282.08	0.00	787.85	136.01	177.58	7.08	244.89	1345.53	55.49
132	72.50	102.46	0.00	148.20	99.28	0.00	100.74	332.56	517.32	41.42
133	8.10	34.90	0.00	0.00	0.00	0.00	0.00	0.00	230.44	15.59
135	444.63	676.58	0.00	260.56	943.39	307.46	0.00	259.54	1918.48	85.81
136	186.00	427.09	0.00	521.12	449.44	392.60	123.49	477.70	1684.01	104.18
143	441.33	522.88	0.00	89.51	1126.60	438.55	21.18	438.82	3133.06	50.12
149	60.62	95.19	0.00	77.35	68.74	12.59	0.00	0.00	335.06	8.92
150	219.61	424.92	0.00	486.77	449.33	310.24	198.66	636.62	1759.23	106.50
151	264.16	491.67	0.00	598.32	487.92	145.06	0.00	493.35	2053.32	120.06
157	1050.04	1096.36	0.00	1196.38	676.36	271.18	0.00	778.03	3499.79	123.18
159	540.14	1113.14	0.00	1386.13	632.63	390.37	0.00	449.17	3060.25	157.82
168	466.45	863.30	0.00	992.92	388.83	198.26	0.00	312.99	2169.55	99.46
169	464.05	804.40	0.00	1008.25	785.10	333.63	0.00	629.05	2396.27	116.88
171	280.90	512.28	0.00	682.28	378.06	359.26	0.00	385.13	1759.71	84.61
174	156.27	179.62	0.00	497.16	63.21	98.81	0.00	0.00	683.90	34.23
177	129.08	383.78	0.00	632.20	159.04	286.53	0.00	269.27	1320.98	52.00

Table 4-2

Radiance Reflectance

R(wavelength) = Pi * L(wavelength) / Ed(wavelength)

STA	R(410)	R(441)	R(488)	R(520)	R(550)	R(589)	R(633)	R(671)
28	0.0259	0.0246	0.0244	0.0166	0.0131	0.0056	0.0016	0.0012
61	0.0199	0.0176	0.0175	0.0124	0.0097	0.0043	0.0013	0.0018
63	0.0215	0.0186	0.0179	0.0125	0.0097	0.0041	0.0013	0.0017
65	0.0181	0.0151	0.0154	0.0121	0.0101	0.0047	0.0014	0.0026
66	0.0197	0.0166	0.0163	0.0123	0.0099	0.0041	0.0012	0.0021
67	0.0207	0.0180	0.0171	0.0122	0.0096	0.0039	0.0011	0.0017
90	0.0232	0.0212	0.0213	0.0159	0.0128	0.0055	0.0015	0.0011
92	0.0181	0.0154	0.0145	0.0105	0.0085	0.0035	0.0010	0.0011
94	0.0195	0.0169	0.0172	0.0135	0.0113	0.0050	0.0015	0.0020
101	0.0257	0.0245	0.0242	0.0166	0.0127	0.0056	0.0017	0.0012
103	0.0203	0.0182	0.0189	0.0149	0.0126	0.0057	0.0017	0.0015
105	0.0243	0.0227	0.0232	0.0160	0.0124	0.0052	0.0015	0.0011
107	0.0242	0.0215	0.0215	0.0146	0.0110	0.0045	0.0013	0.0013
113	0.0306	0.0317	0.0279	0.0142	0.0096	0.0038	0.0010	0.0006
117	0.0272	0.0260	0.0247	0.0159	0.0124	0.0054	0.0016	0.0010
132	0.0088	0.0111	0.0137	0.0099	0.0077	0.0036	0.0011	0.0008
133	0.0124	0.0154	0.0182	0.0111	0.0081	0.0035	0.0010	0.0006
135	0.0185	0.0156	0.0155	0.0126	0.0105	0.0046	0.0014	0.0020
143	0.0202	0.0169	0.0161	0.0127	0.0103	0.0042	0.0012	0.0010
149	0.0105	0.0132	0.0158	0.0108	0.0082	0.0036	0.0011	0.0008
150	0.0169	0.0154	0.0163	0.0140	0.0122	0.0058	0.0019	0.0018
151	0.0163	0.0130	0.0138	0.0122	0.0108	0.0047	0.0013	0.0020
157	0.0096	0.0078	0.0082	0.0088	0.0092	0.0052	0.0017	0.0045
159	0.0142	0.0128	0.0142	0.0134	0.0129	0.0065	0.0020	0.0026
168	0.0187	0.0195	0.0213	0.0163	0.0132	0.0062	0.0020	0.0013
169	0.0145	0.0131	0.0158	0.0164	0.0163	0.0085	0.0026	0.0021
171	0.0177	0.0162	0.0177	0.0144	0.0120	0.0056	0.0017	0.0021
174	0.0066	0.0091	0.0123	0.0092	0.0073	0.0035	0.0010	0.0006
177	0.0106	0.0110	0.0141	0.0122	0.0106	0.0053	0.0016	0.0020

FIGURE 4-1

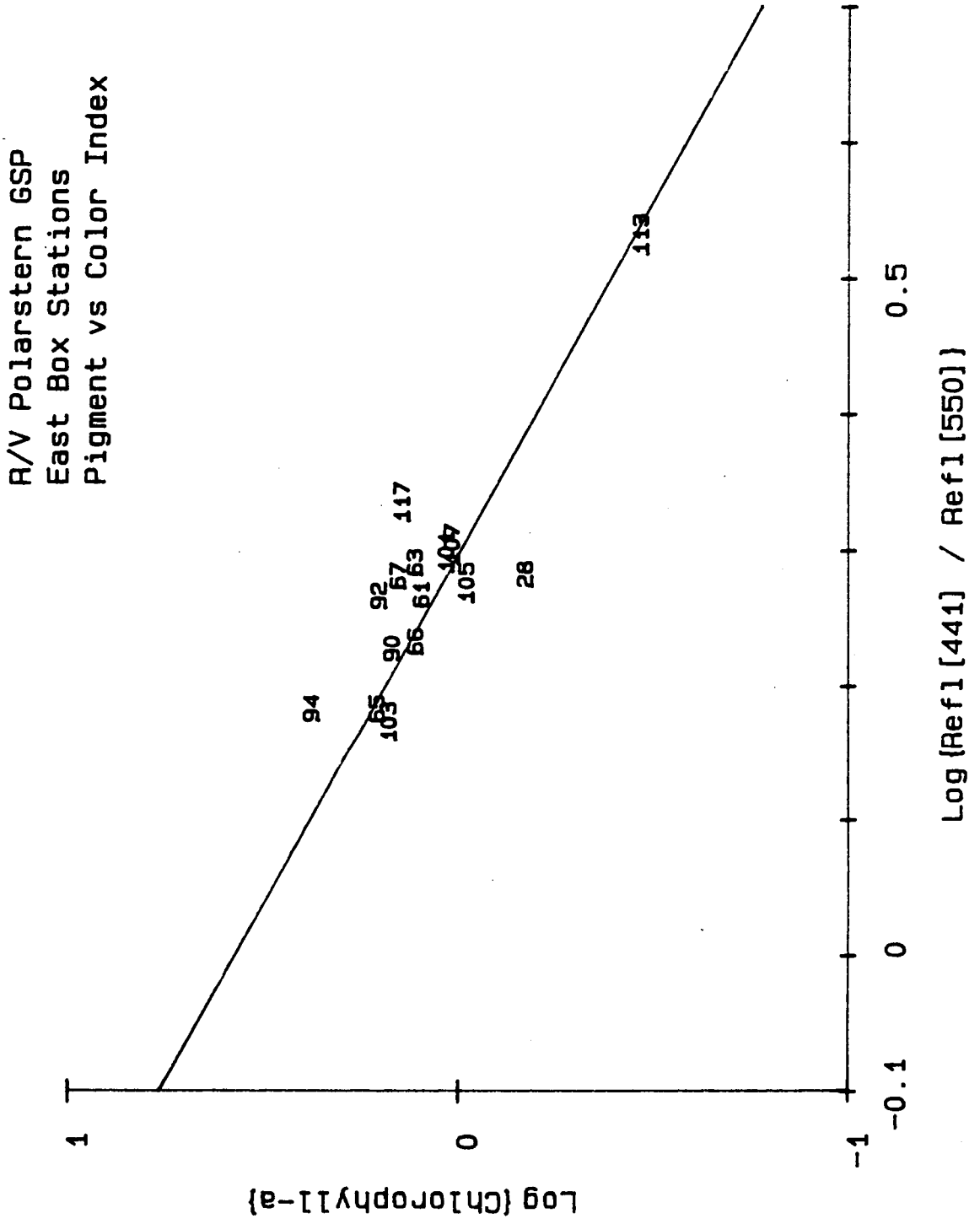
R/V Polarstern GSP
East Box Stations
Pigment vs Color Index
Log (Chlorophyll-a)
Log (Refl [441] / Refl [550])
1
0
-1
-0.1
0
0.5
94
103
65
90
66
92
61
67
63
117
107
105
28
113

FIGURE 4-2

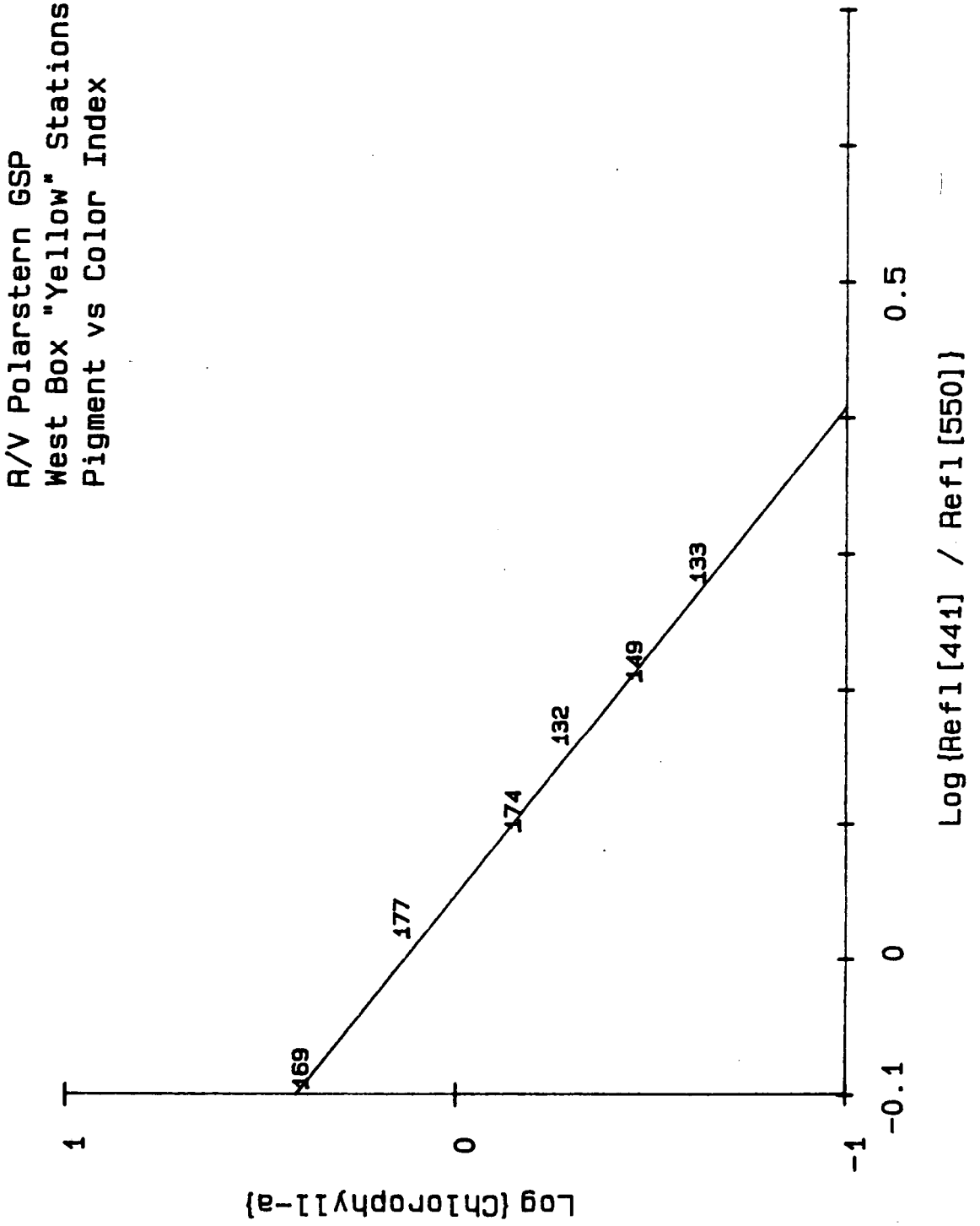
R/V Polarstern GSP
West Box "Yellow" Stations
Pigment vs Color Index
Log (Chlorophyll-a)
1
0
-1
Log (Refl [441] / Refl [550])
-0.1
0
0.5
169
177
174
132
149
133

FIGURE 4-3

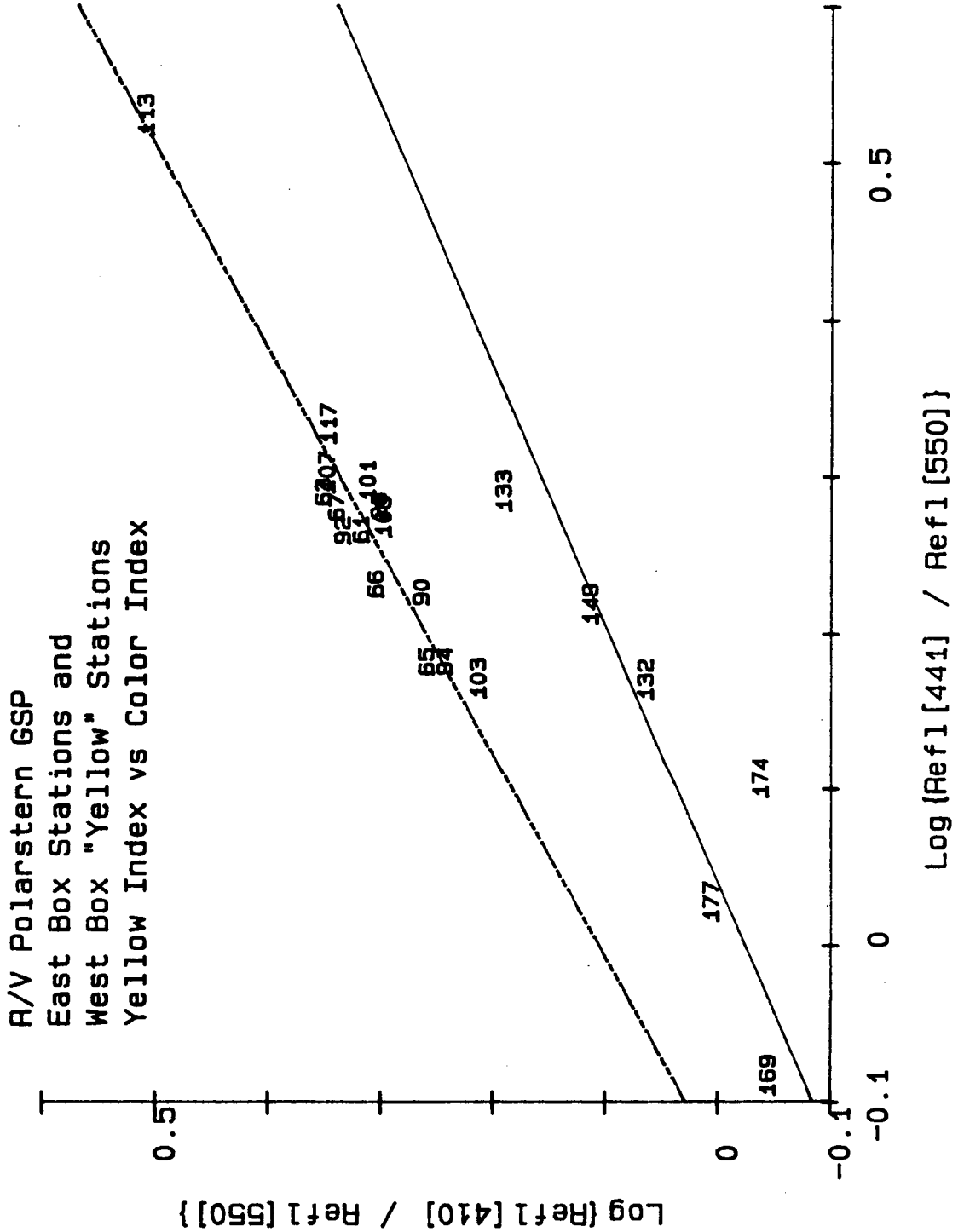
R/V Polarstern GSP
East Box Stations and
West Box "Yellow" Stations
Yellow Index vs Color Index
Log {Refl [410] / Refl [550]}
Log {Refl [441] / Refl [550]}
0.5
0
-0.1
-0.1
0
0.5
113
117
107
101
92
66
90
65
103
133
148
132
177
174
169

FIGURE 4-4

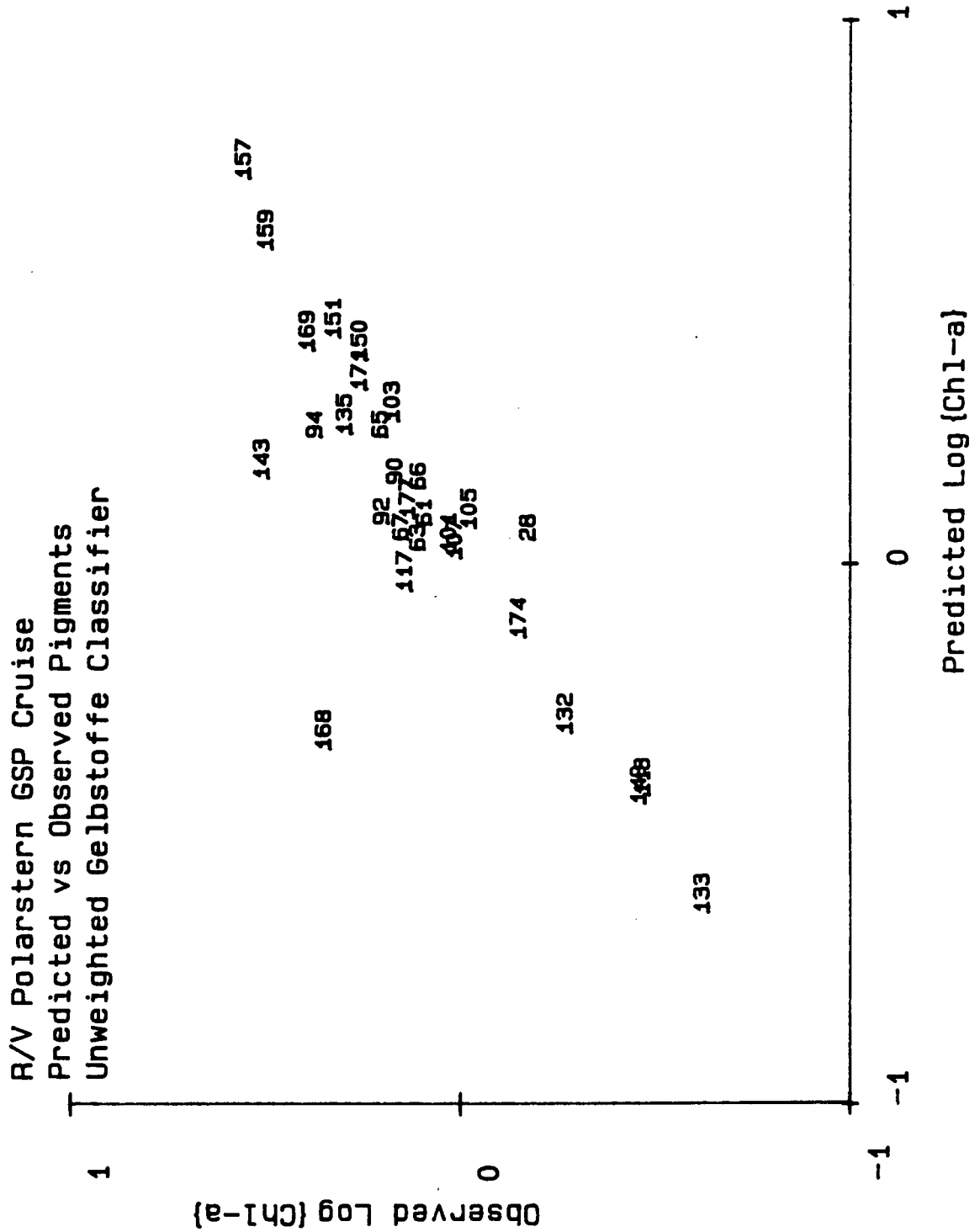
R/V Polarstern GSP Cruise
Predicted vs Observed Pigments
Unweighted Gelbstoffe Classifier
Observed Log (Chl-a)
Predicted Log (Chl-a)
1
0
-1
-1
0
1
157
159
169
151
150
135
103
94
143
90
105
28
174
132
168
133

5.0 ALGORITHM ADJUSTMENTS by COMPARING MARS RADIANCE RATIOS with REFLECTANCE RATIOS MEASURED from the RV POLARSTERN

The in-water remote sensing algorithm (Section 4) determines chlorophyll-a concentration in micro-grams per liter as a function of the color index R(440)/R(550), after selection of the appropriate regression equation by comparing the color index with a "yellow index" R(410)/R(550).

After atmospheric correction of radiances Lt(410), Lt(440), and Lt(550) [MARS channels 1, 2 and 5] by subtracting the appropriately scaled value of Lt(725) [MARS channel 10], we are able to form estimates of the water leaving radiance ratios

$$Lw(440)/Lw(550)$$

a "radiance color index", and

$$Lw(410)/Lw(550)$$

a "radiance yellow index". Were flight level irradiances measured at each wavelength, we could estimate the respective reflectance ratios as

$$R(440)/R(550) = \{Ed(550)/Ed(440)\} * \{Lw(440)/Lw(550)\}$$

and

$$R(410)/R(550) = \{Ed(550)/Ed(410)\} * \{Lw(410)/Lw(550)\}.$$

Unfortunately, the MARS did not have that capability in 1987.

An additional uncertainty was introduced by our observation that Lt(410) in channel 1 was chronically greater than radiance in any of the other channels. This condition is common to radiance spectra measured over ice, water and clouds. This spectral characteristic is not plausible under any reasonable set of assumptions, if only because incident solar flux at 410 nm is significantly less than that at either 440 or 550 nm, and skylight irradiance is also always less at 410 nm than at 440 nm. Channel 1 clearly was more sensitive at the time the MARS measurements were made over the Greenland Sea (21 May through 2 June 1987) than at the time of laboratory calibration following the mission (circa 16 June 1987). We have considered two possible explanations: 1) these channels of the instrument may be sensitive to ambient temperature, a possibility that will be explored in laboratory experiments as soon as time permits, or 2) a new Barium-Sulfate coating was applied to the interior of the sphere during on or about 15 May 1987, and if the coating aged

significantly during the first month, we would expect to see the largest reflectance loss at short wavelengths (where Barium-Sulfate is least efficient and most susceptible to aging). Unfortunately, there is no way to definitively determine the cause, and we have had to resort to a post-hoc adjustment to this channel based on the limited number of comparisons between the MARS and ground truth reflectances measured with the MER-1032 by Trees aboard the RV Polarstern.

We therefore have carefully compared MARS water leaving radiance ratios to MER in-water reflectance ratios at the 6 stations where the two measurements were nearly simultaneous. We assumed that the apparent sensitivity bias of MARS channel 1 (409 nm) [and to a lesser extent in channel 2 (439 nm)] was the dominant factor in biasing the MARS radiance ratios relative to MER reflectance ratios at the wavelengths in question. We assumed also that the station to station variation in these comparisons was dominated by temporal variability in illumination conditions, primarily due to variability in cloud cover; these variations would affect not only the local ratio of downwelling irradiances as discussed above, but could cause the actual spectral ratios of path radiance plus surface reflectance used in atmospheric corrections (Section 4 above) to depart severely from those derived from sea ice reflectance cases.

Given these uncertainties and the very limited amount of ground truth control data, we felt we could do little more than adjust the apparent sensitivities for MARS channels 1 and 2 to reconcile the two MARS radiance ratios {Lw(410)/Lw(550) and Lw(440)/Lw(550)} into "reasonable" agreement with MER reflectance ratios {R(410)/R(550) and R(440)/R(550)}. For each station, we computed the mean water leaving radiance estimates from 3 to 5 separate data runs by the Dornier over the Polarstern, and compared the corresponding radiance ratio color and yellow indices to MER reflectance ratio color and yellow indices. We then arbitrarily adjusted the calibration gain values for channels 1 and 2 to yield grand mean (over all 6 stations) ratios of radiance:reflectance yellow and color indices respectively to approximately 1.0, with the further constraint that these ratios at individual stations should be no less than 0.75 and no greater than 1.50. This exercise produced the best (admittedly subjective) agreement for the 6 intercomparison stations when channel 1 gain was reduced by the scale factor 0.83 and when channel 2 was reduced by the scale factor 0.95.

Using these post hoc 0.83 and 0.95 gain reduction factors for MARS channels 1 and 2 respectively, the average in-water reflectance ratios (averaged over MER readings in the top 1 m at each station) and corresponding MARS water leaving radiance ratios, and ratios between each, are listed in Table 5-1.

Table 5-1

Comparison Between MARS Water Leaving Radiance Ratios
and In-Water MER Reflectance Ratios
at Six RV Polarstern Stations in the Greenland Sea

Sta:	R(410):R(550)	Lw(410):Lw(550)	Lw:R Index Ratio
92	2.129	2.135	1.003
133	1.531	1.245	0.813
143	1.961	1.504	0.767
151	1.509	2.048	1.357
159	1.101	1.138	1.034
169	0.890	1.280	1.438
		MEAN:	1.069

Sta:	R(440):R(550)	Lw(440):Lw(550)	Lw:R Index Ratio
92	1.812	1.787	0.986
133	1.901	1.425	0.750
143	1.641	1.327	0.809
151	1.204	1.730	1.437
159	0.992	1.123	1.132
169	0.804	1.108	1.378
		MEAN:	1.082

6.0 MARS TRACKLINE and R/V POLARSTERN STATION LOCATIONS

The attached maps illustrate the tracklines followed by the Dornier aircraft during MARS data acquisition. The geographical positions were extracted from the MARS data files, following merger of the INS navigation data as interpolated to the time of each MARS data record.

Note that the aircraft made turns at the beginning and/or end of many of the tracklines. We have not edited these track segments from the chlorophyll trackline plots presented in Section 8 below.

Short data tracklines over the Polarstern may also contain multiple tracklines (see e.g. tracklines A and B on 29 May). The plots in Section 8 concatenate these into a single curve (to indicate data content, variability, and quality).

To facilitate future comparisons between MARS data and in situ observations, geographic positions of stations occupied by Polarstern within two days of each flight are plotted on each trackline map.

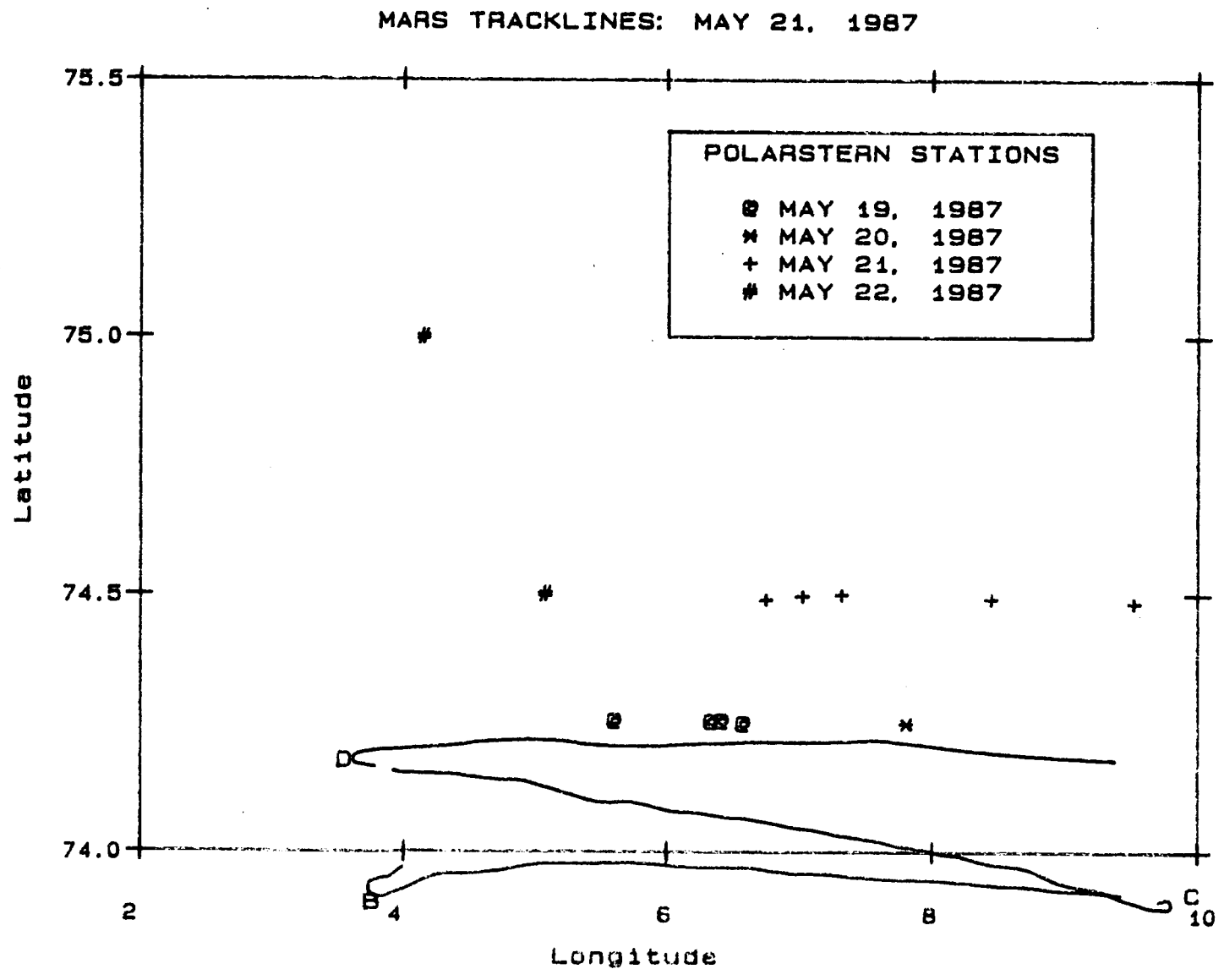
MARS TRACKLINES: MAY 21, 1987
POLARSTERN STATIONS
@ MAY 19, 1987
* MAY 20, 1987
+ MAY 21, 1987
# MAY 22, 1987
75.5
75.0
74.5
74.0
Latitude
2
4
6
8
10
Longitude
B
C

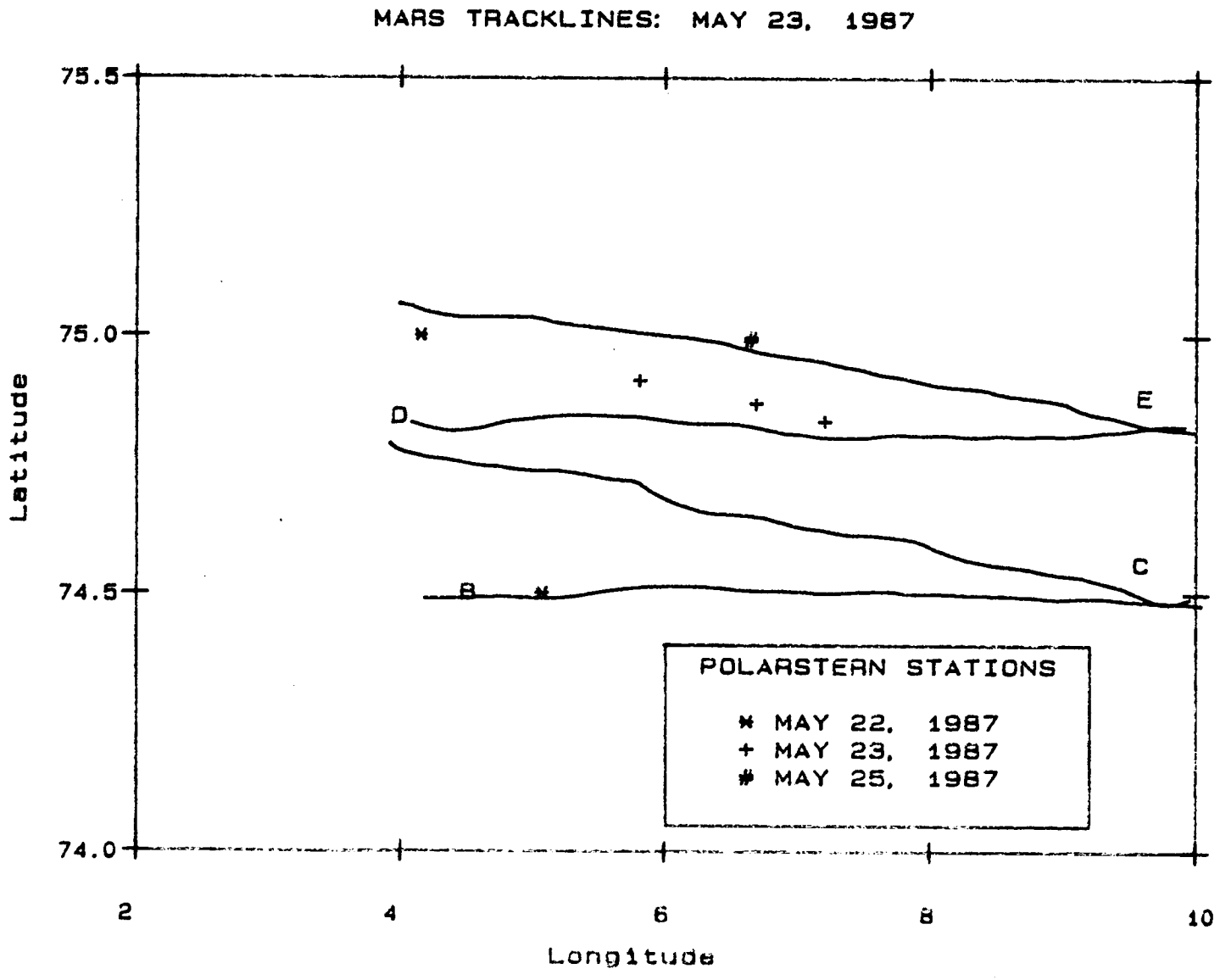
MARS TRACKLINES: MAY 23, 1987
75.5
75.0
74.5
74.0
Latitude
2
4
6
8
10
Longitude
D
E
C
B
POLARSTERN STATIONS
* MAY 22, 1987
+ MAY 23, 1987
# MAY 25, 1987

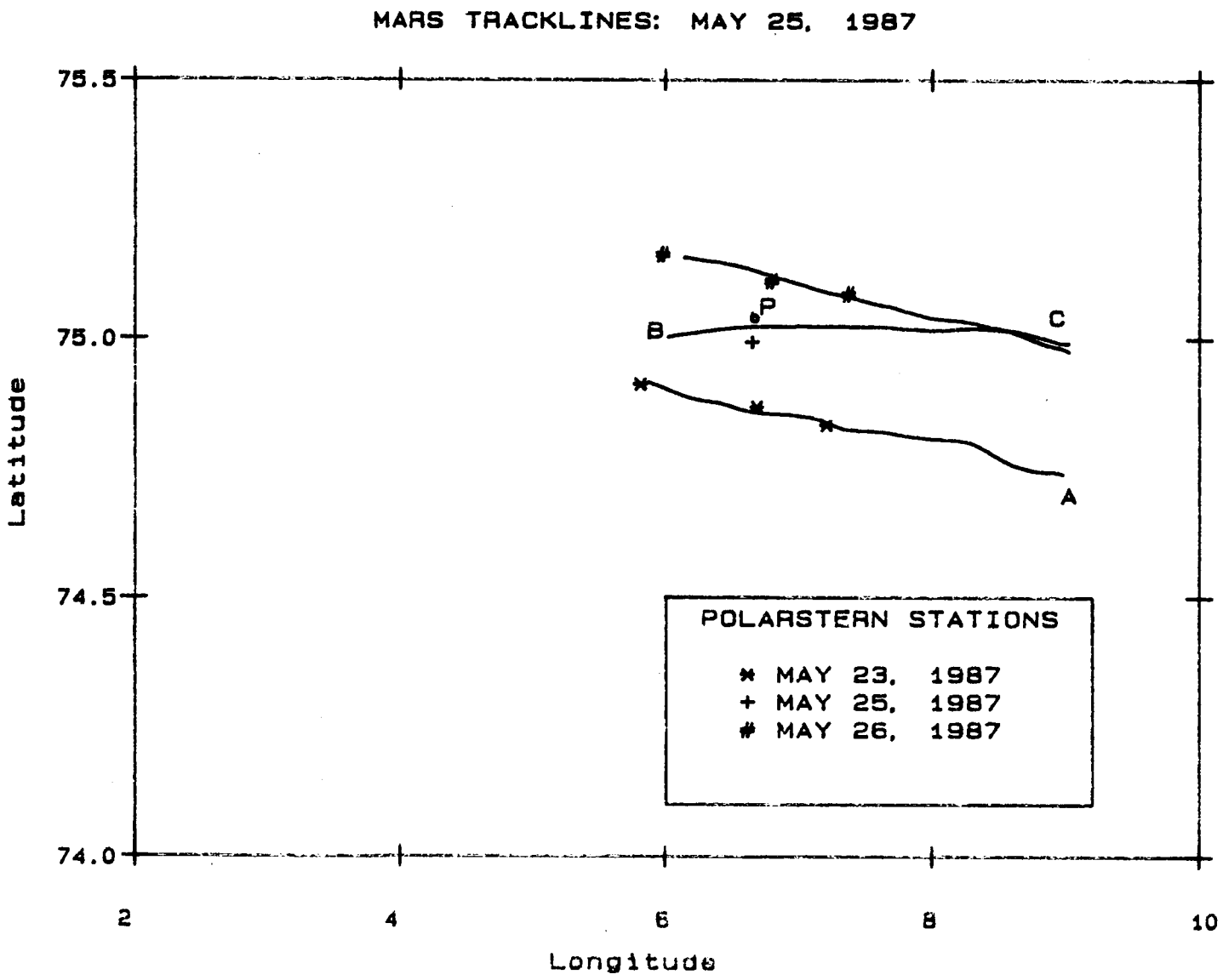
MARS TRACKLINES: MAY 25, 1987
75.5
75.0
74.5
74.0
Latitude
2
4
6
8
10
Longitude
P
B
C
A
POLARSTERN STATIONS
* MAY 23, 1987
+ MAY 25, 1987
# MAY 26, 1987

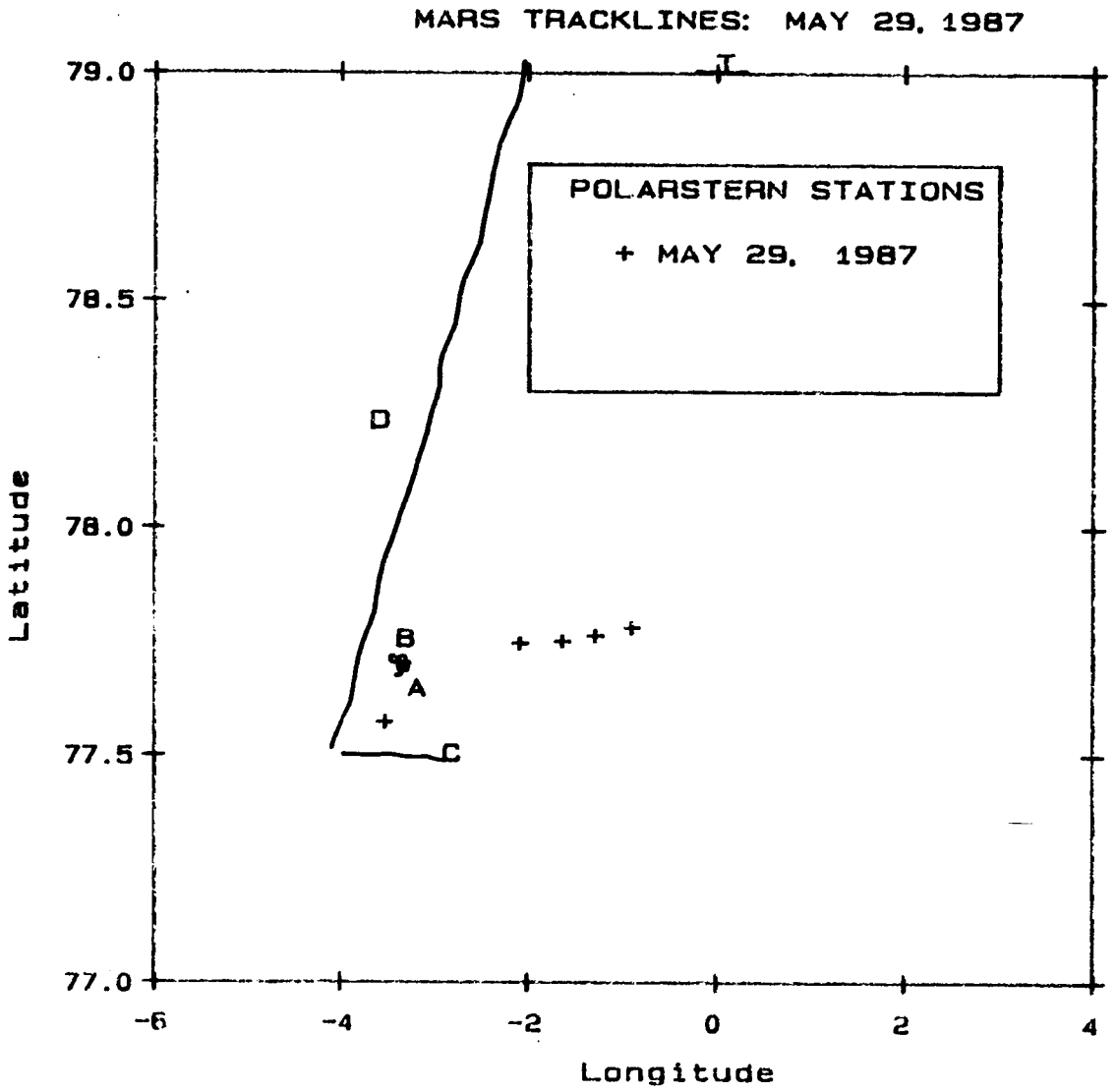
MARS TRACKLINES: MAY 29, 1987
POLARSTERN STATIONS
+ MAY 29, 1987
79.0
78.5
78.0
77.5
77.0
-6
-4
-2
0
2
4
Latitude
Longitude
D
B
A
C

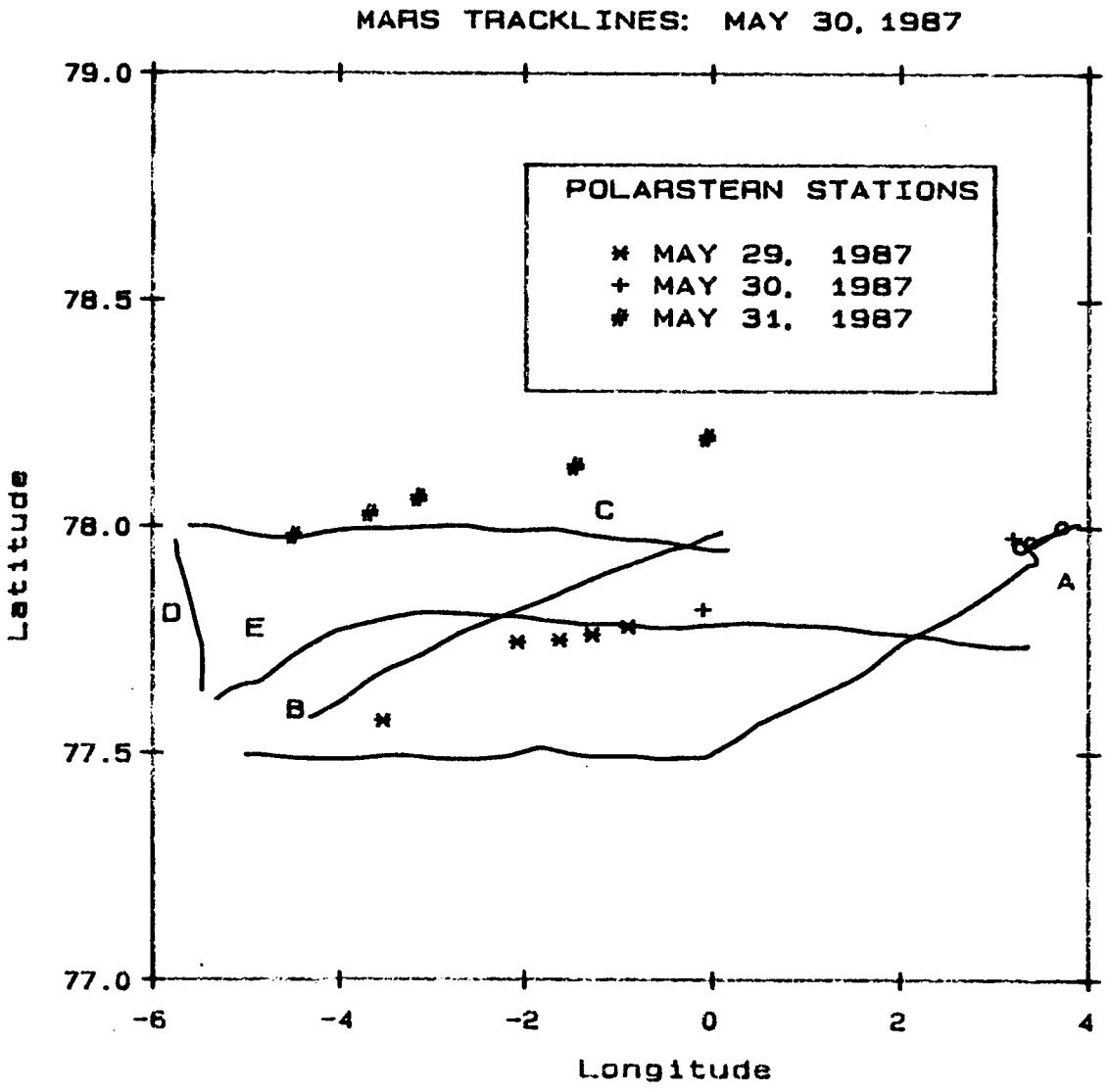
MARS TRACKLINES: MAY 30, 1987
POLARSTERN STATIONS
* MAY 29, 1987
+ MAY 30, 1987
# MAY 31, 1987
79.0
78.5
78.0
77.5
77.0
Latitude
-6
-4
-2
0
2
4
Longitude
A
B
C
D
E

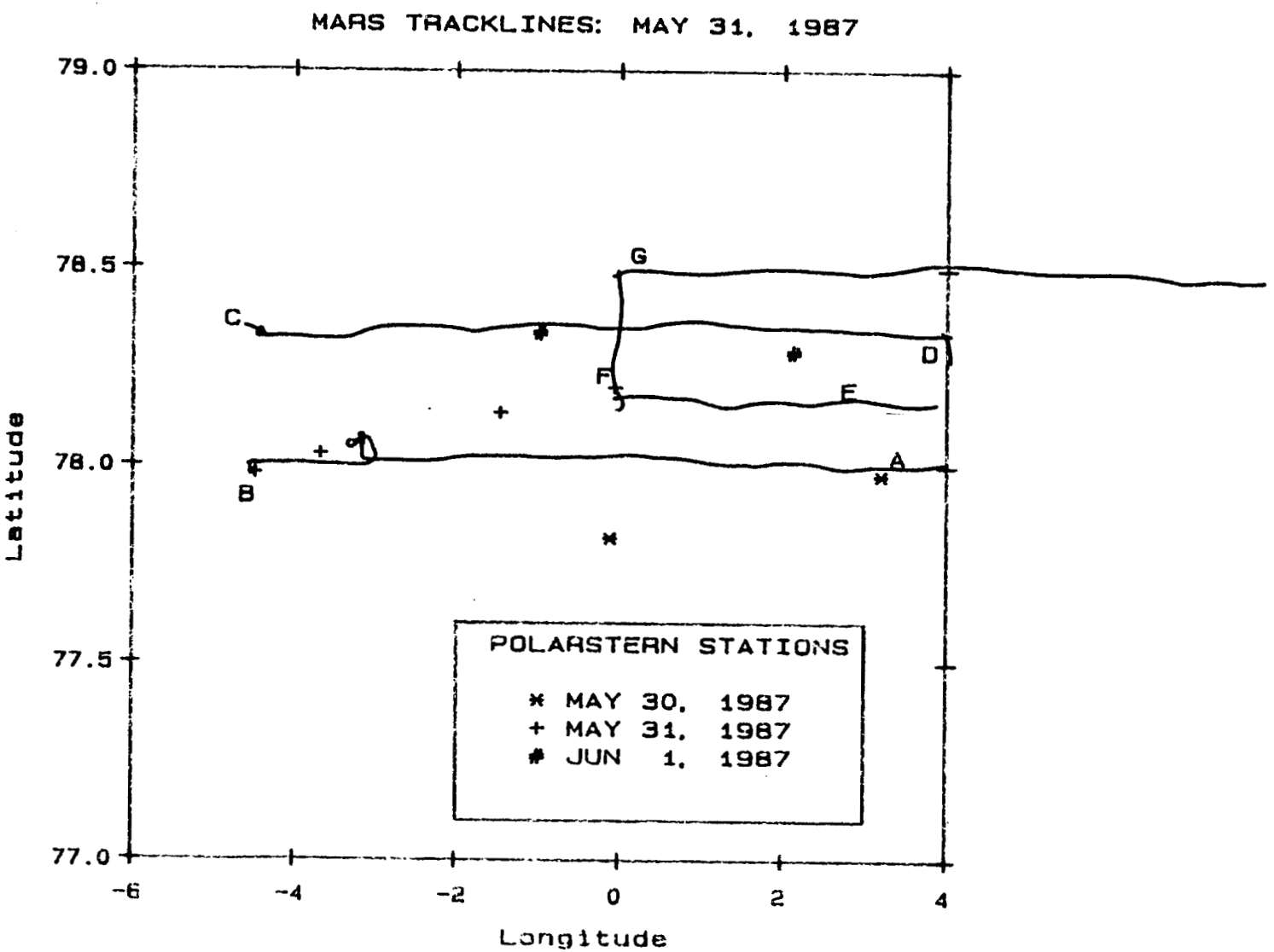
MARS TRACKLINES: MAY 31, 1987
79.0
78.5
78.0
77.5
77.0
Latitude
-6
-4
-2
0
2
4
Longitude
A
B
C
D
E
F
G
POLARSTERN STATIONS
* MAY 30, 1987
+ MAY 31, 1987
# JUN 1, 1987

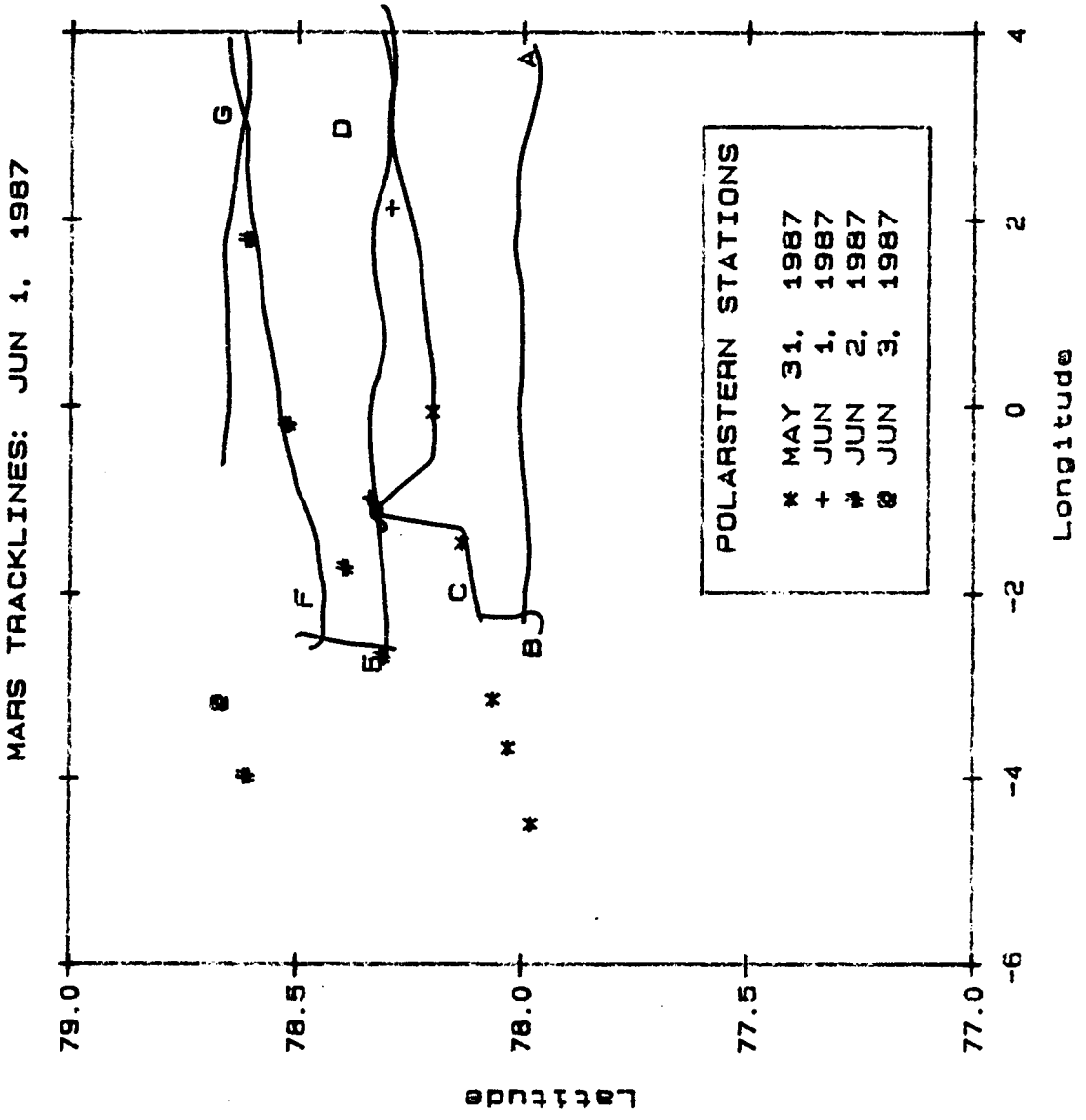
MARS TRACKLINES: JUN 1, 1987
POLARSTERN STATIONS
* MAY 31, 1987
+ JUN 1, 1987
# JUN 2, 1987
@ JUN 3, 1987
A
B
C
D
F
G
79.0
78.5
78.0
77.5
77.0
Latitude
4
2
0
-2
-4
-6
Longitude

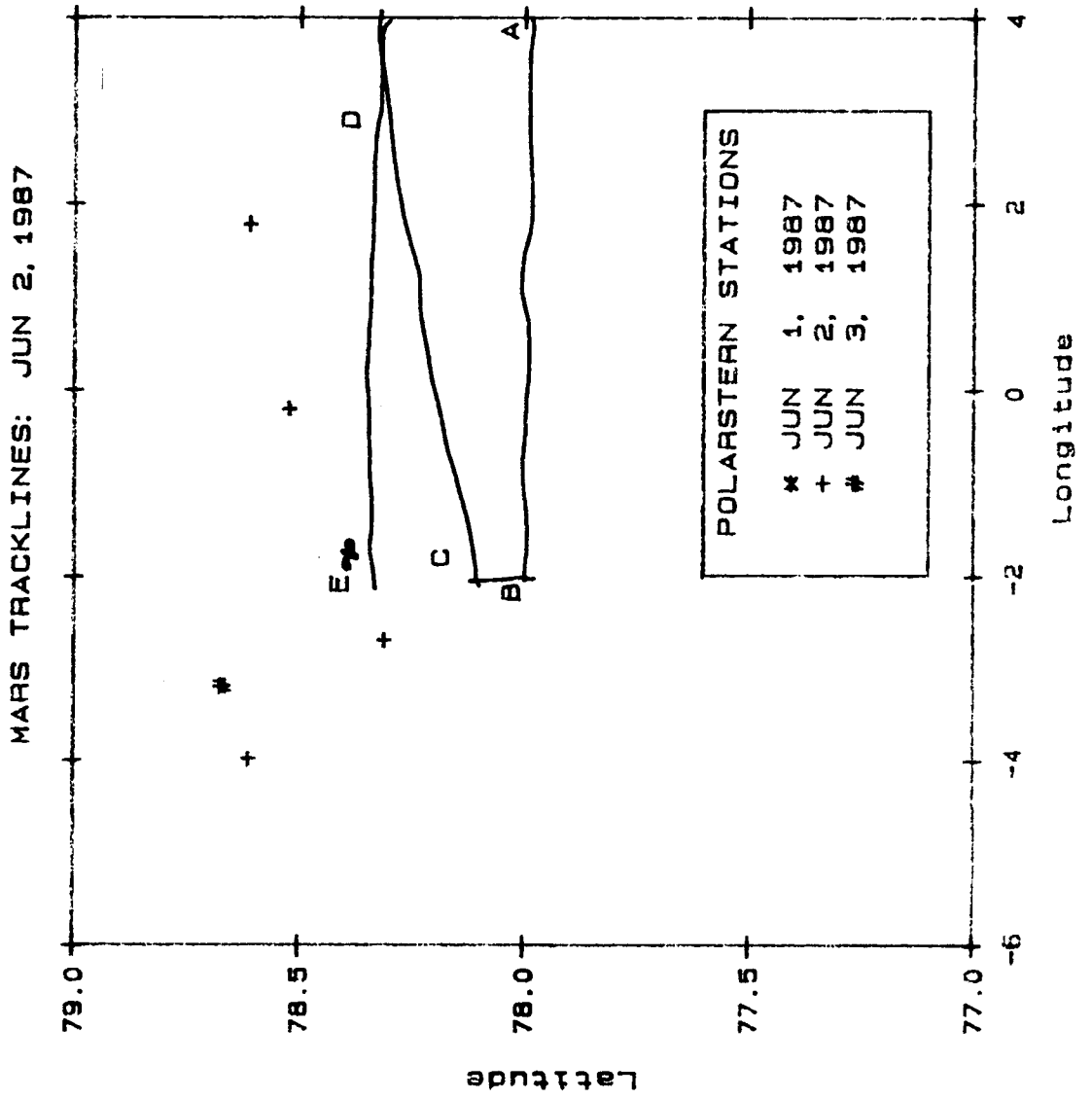
MARS TRACKLINES: JUN 2, 1987
POLARSTERN STATIONS
* JUN 1, 1987
+ JUN 2, 1987
# JUN 3, 1987
A
B
C
D
E
79.0
78.5
78.0
77.5
77.0
Latitude
4
2
0
-2
-4
-6
Longitude

7.0 TWO-DIMENSIONAL CHLOROPHYLL DISTRIBUTIONS ("Stick-plot" Descriptions of Selected MARS Tracklines)

The following maps display chlorophyll-a concentrations calculated from MARS radiance ratios as "sticks" perpendicular to a straight-line approximation of each trackline. To avoid clutter, and yet present a sense of two-dimensional variability in chlorophyll-a over the area covered by each flight, we have omitted a few of the tracklines (compare with Section 6).

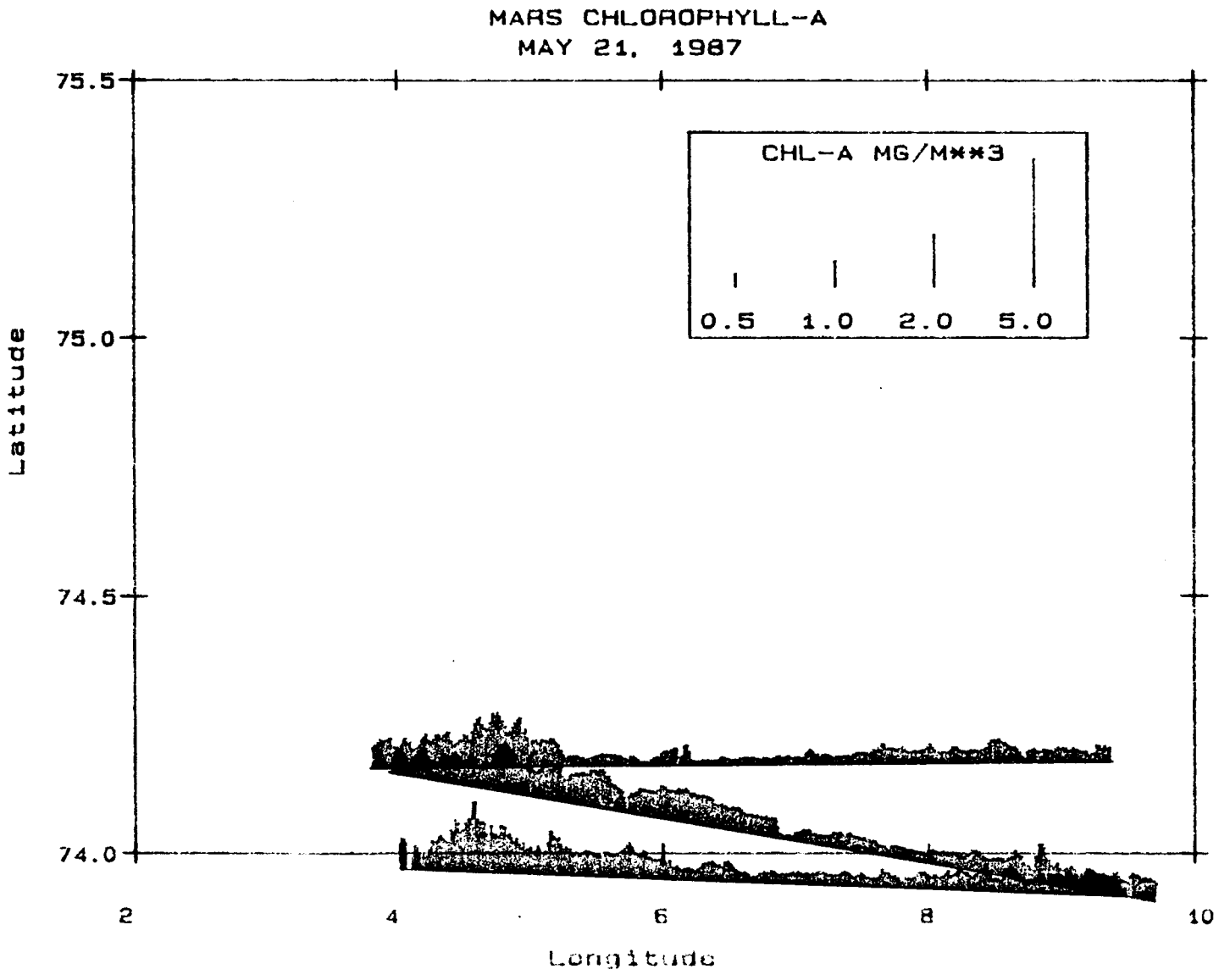
MARS CHLOROPHYLL-A
MAY 21, 1987
CHL-A MG/M**3
0.5
1.0
2.0
5.0
75.5
75.0
74.5
74.0
Latitude
2
4
6
8
10
Longitude

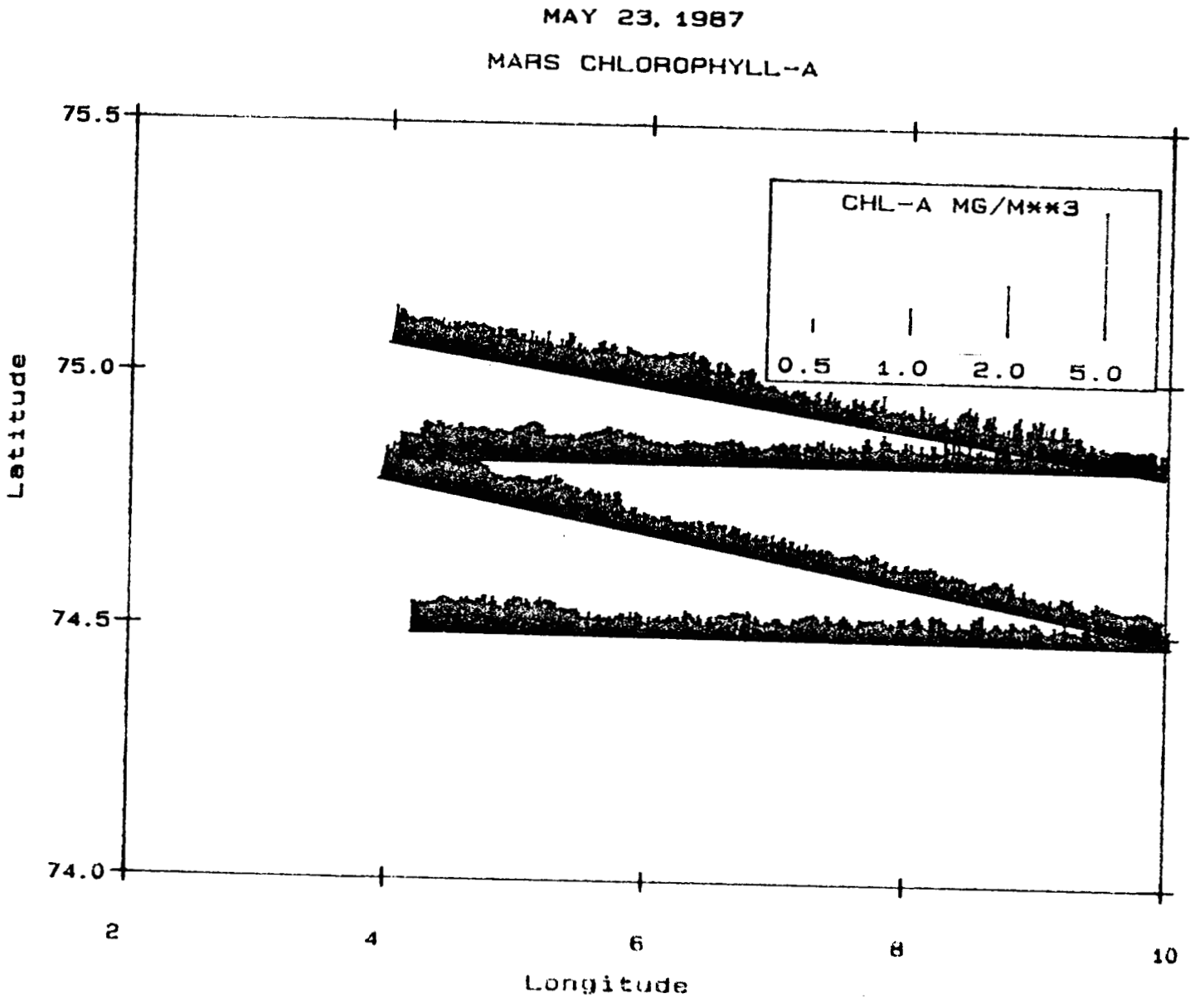
MAY 23, 1987
MARS CHLOROPHYLL-A
CHL-A MG/M**3
0.5
1.0
2.0
5.0
75.5
75.0
74.5
74.0
Latitude
2
4
6
8
10
Longitude

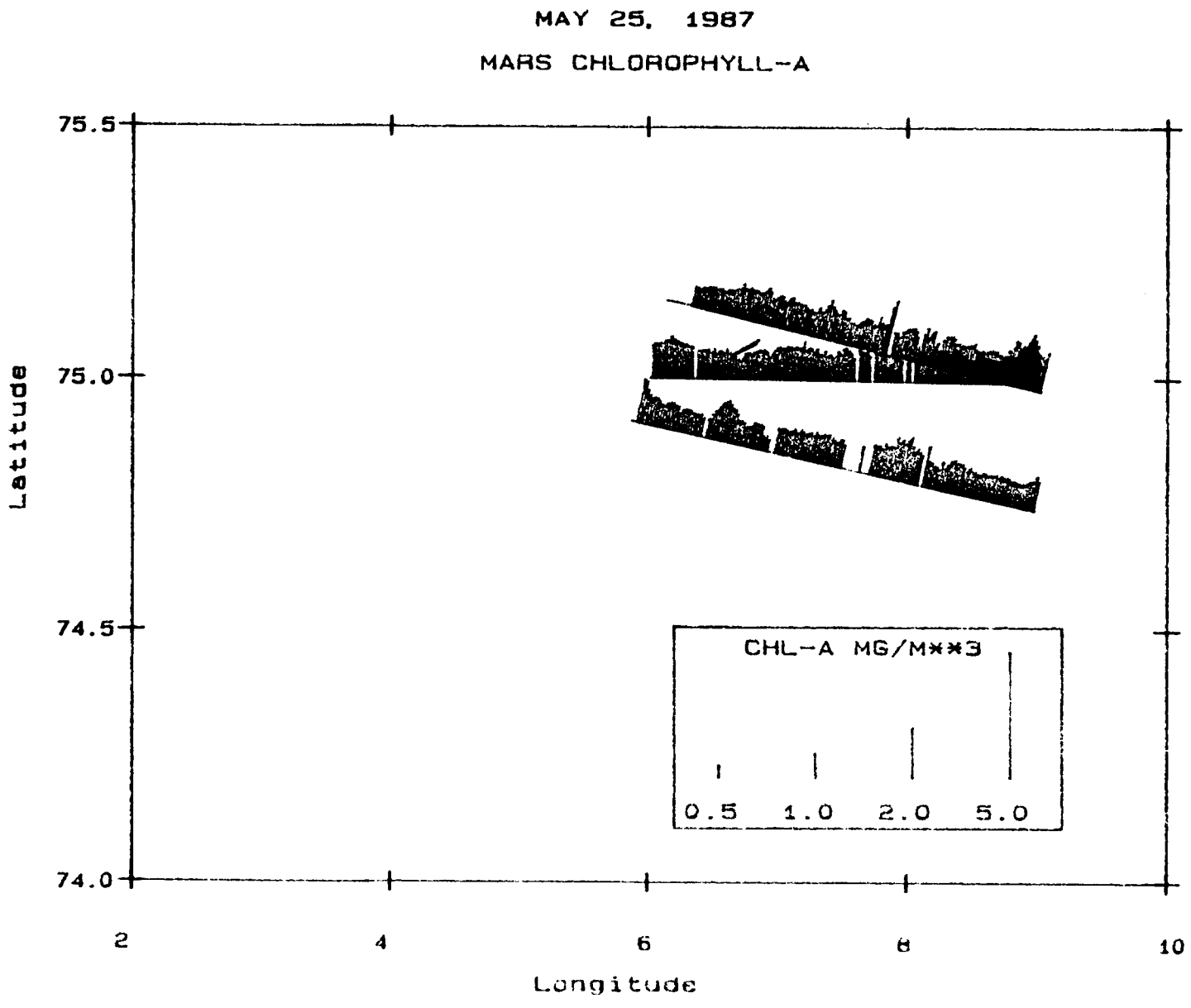
MAY 25, 1987
MARS CHLOROPHYLL-A
75.5
75.0
74.5
74.0
Latitude
2
4
6
8
10
Longitude
CHL-A MG/M**3
0.5
1.0
2.0
5.0

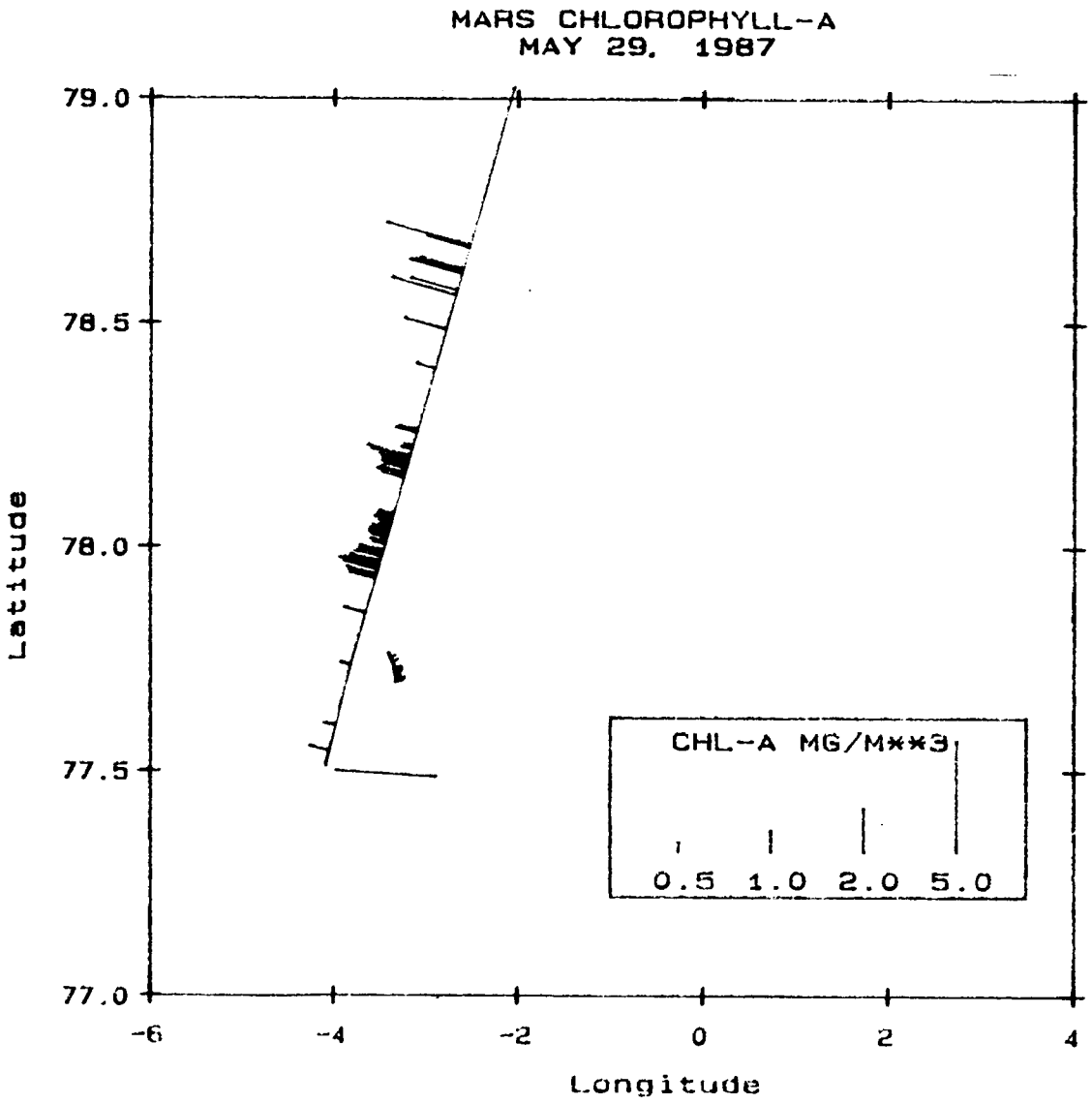
MARS CHLOROPHYLL-A
MAY 29, 1987
79.0
78.5
78.0
77.5
77.0
Latitude
-6
-4
-2
0
2
4
Longitude
CHL-A MG/M**3
0.5 1.0 2.0 5.0

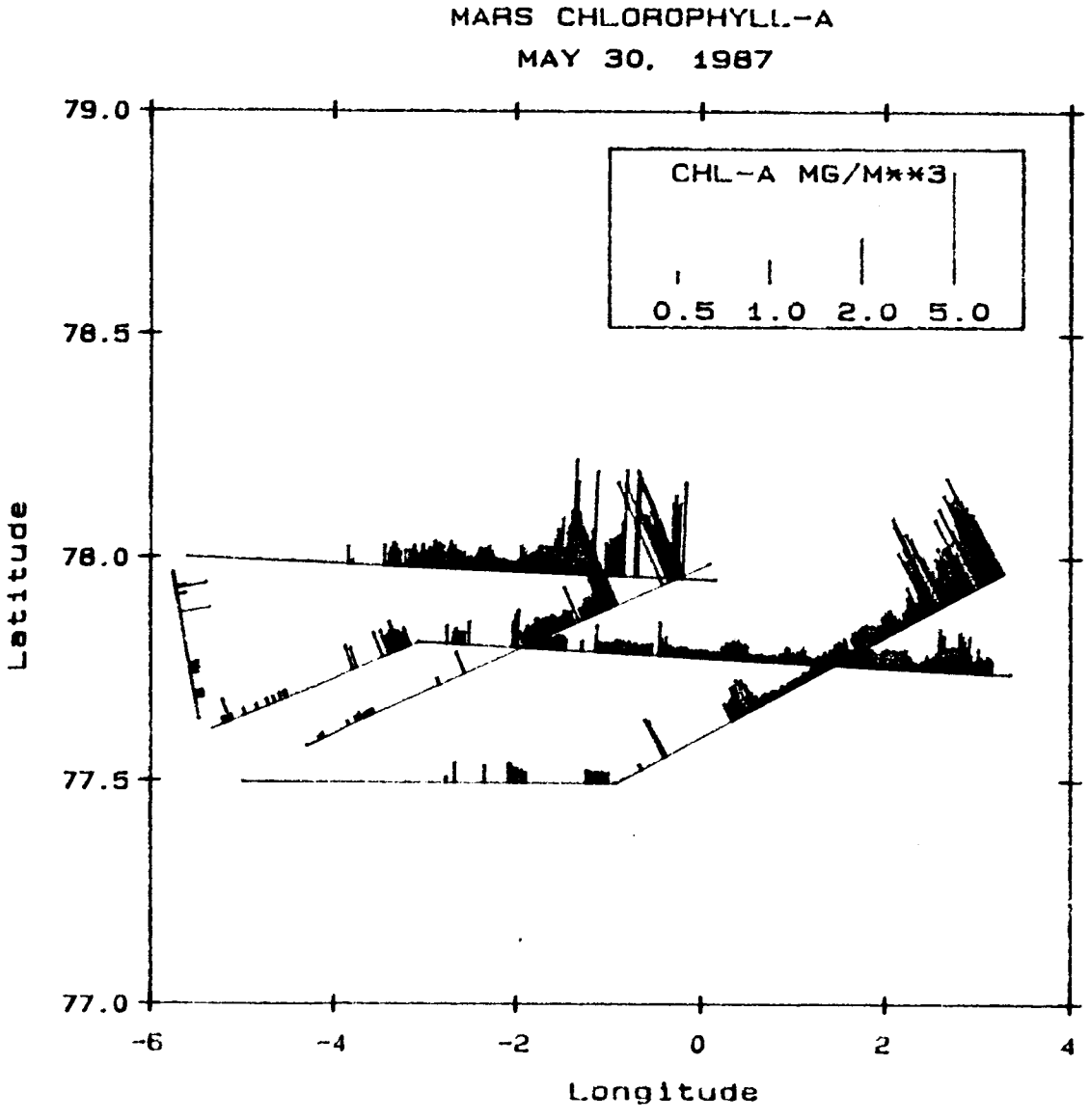
MARS CHLOROPHYLL-A
MAY 30, 1987
CHL-A MG/M**3
0.5 1.0 2.0 5.0
79.0
78.5
78.0
77.5
77.0
Latitude
-6
-4
-2
0
2
4
Longitude

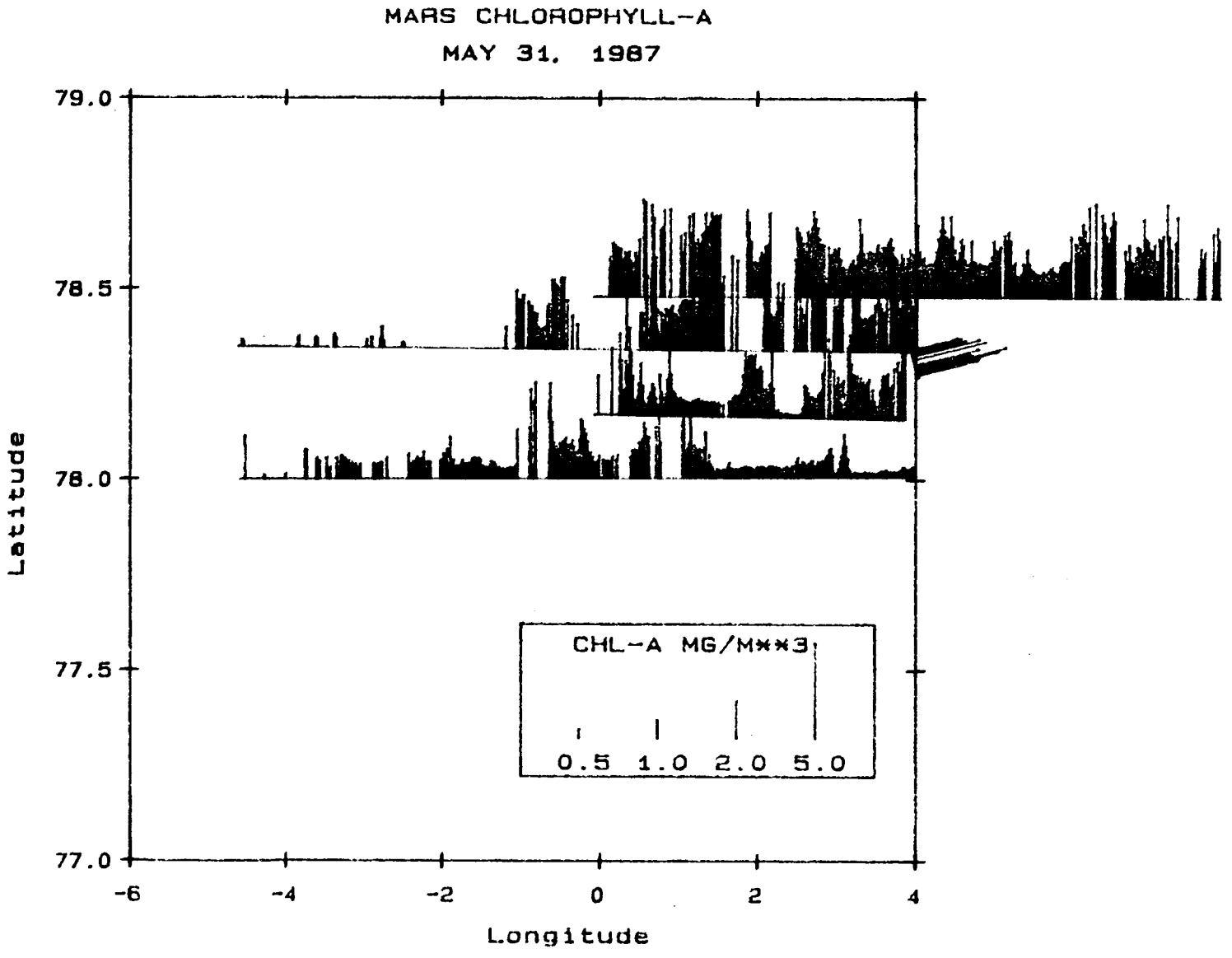
MARS CHLOROPHYLL-A
MAY 31, 1987
79.0
78.5
78.0
77.5
77.0
Latitude
-6
-4
-2
0
2
4
Longitude
CHL-A MG/M**3
0.5 1.0 2.0 5.0

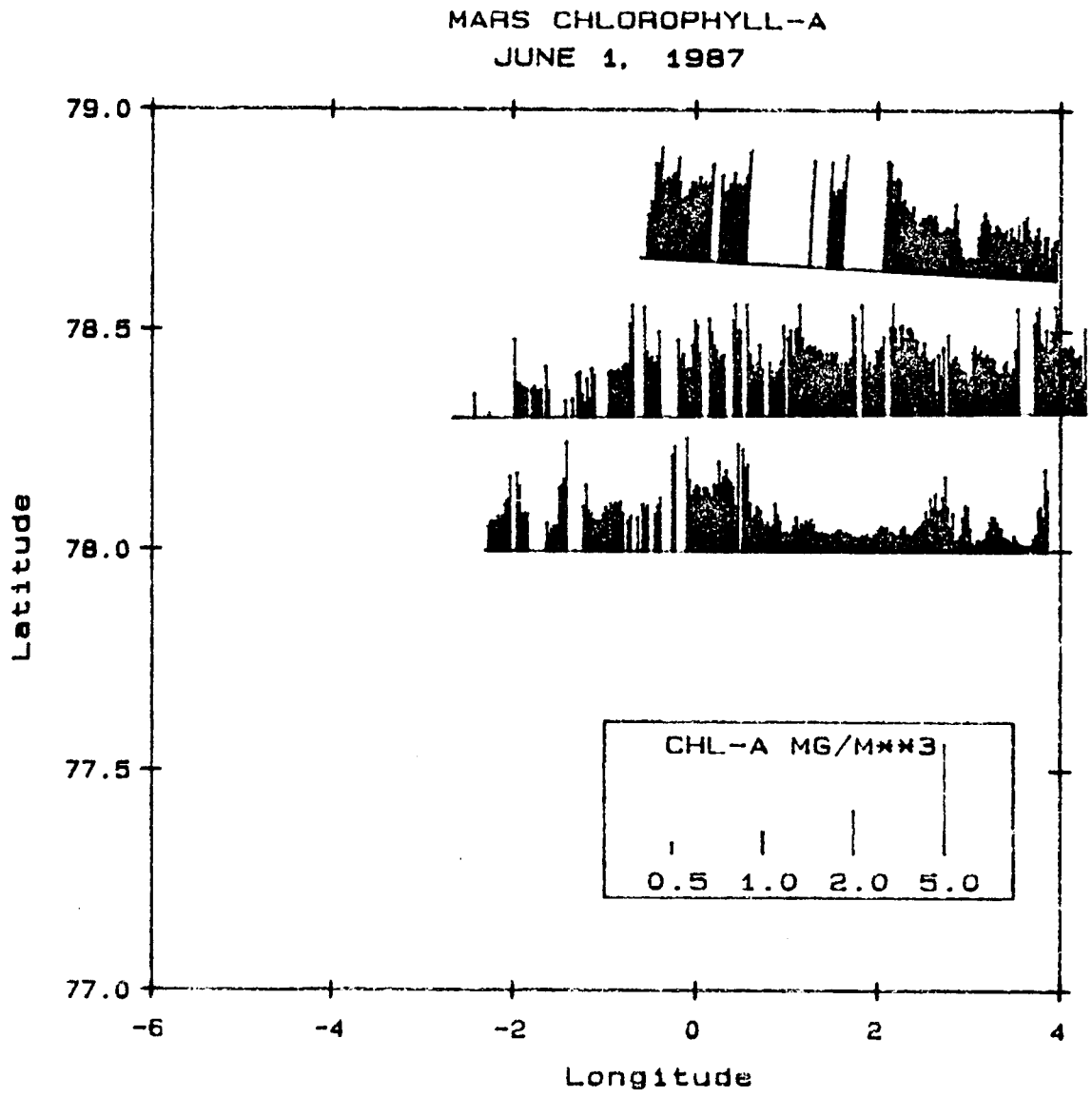
MARS CHLOROPHYLL-A
JUNE 1, 1987
79.0
78.5
78.0
77.5
77.0
Latitude
-6
-4
-2
0
2
4
Longitude
CHL-A MG/M**3
0.5 1.0 2.0 5.0

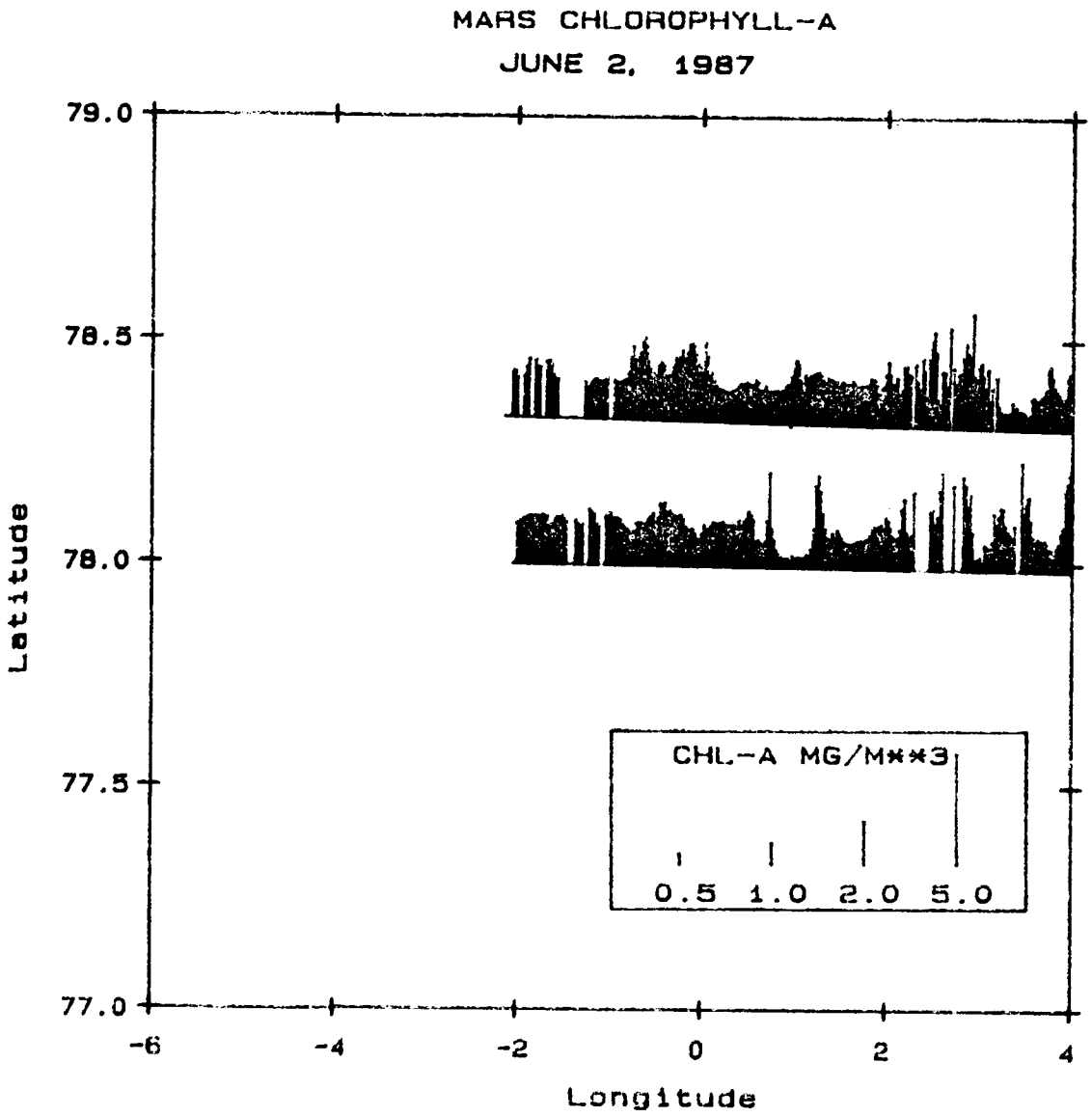
MARS CHLOROPHYLL-A
JUNE 2, 1987
79.0
78.5
78.0
77.5
77.0
Latitude
-6
-4
-2
0
2
4
Longitude
CHL-A MG/M**3
0.5 1.0 2.0 5.0

8.0 CHLOROPHYLL-A VARIABILITY ALONG MARS TRACKLINES (6-Point Averages)

The following graphs depict chlorophyll-a variability along each of the MARS tracklines. The abcissa scale in each case is relative distance from 0 to 100%, with the western-most endpoint always to the left (0%). Turns at the beginning, end, or intermediate points within tracklines have not been edited from, or otherwise noted, in these curves. Refer to the corresponding trackline maps in Section 6 to view the geographic trackline pattern associated with each data curve.

The data in each curve indicate the coverage and extent of data contained in the corresponding chlorophyll-a data file. The curves are smoothed by averaging over 6 records alongtrack, and thus represent approximately 12-second averages, which corresponds to an oval spatial footprint approximately 160m cross-track by 1 km along-track. The chlorophyll estimates are recorded for each valid data record (excluding clouds, ice reflectance, and obviously bad data points) in the associated ASCII file on magnetic tape.

MARS Pigment (6 pt averages), 21 May 87

TRACKLINE B

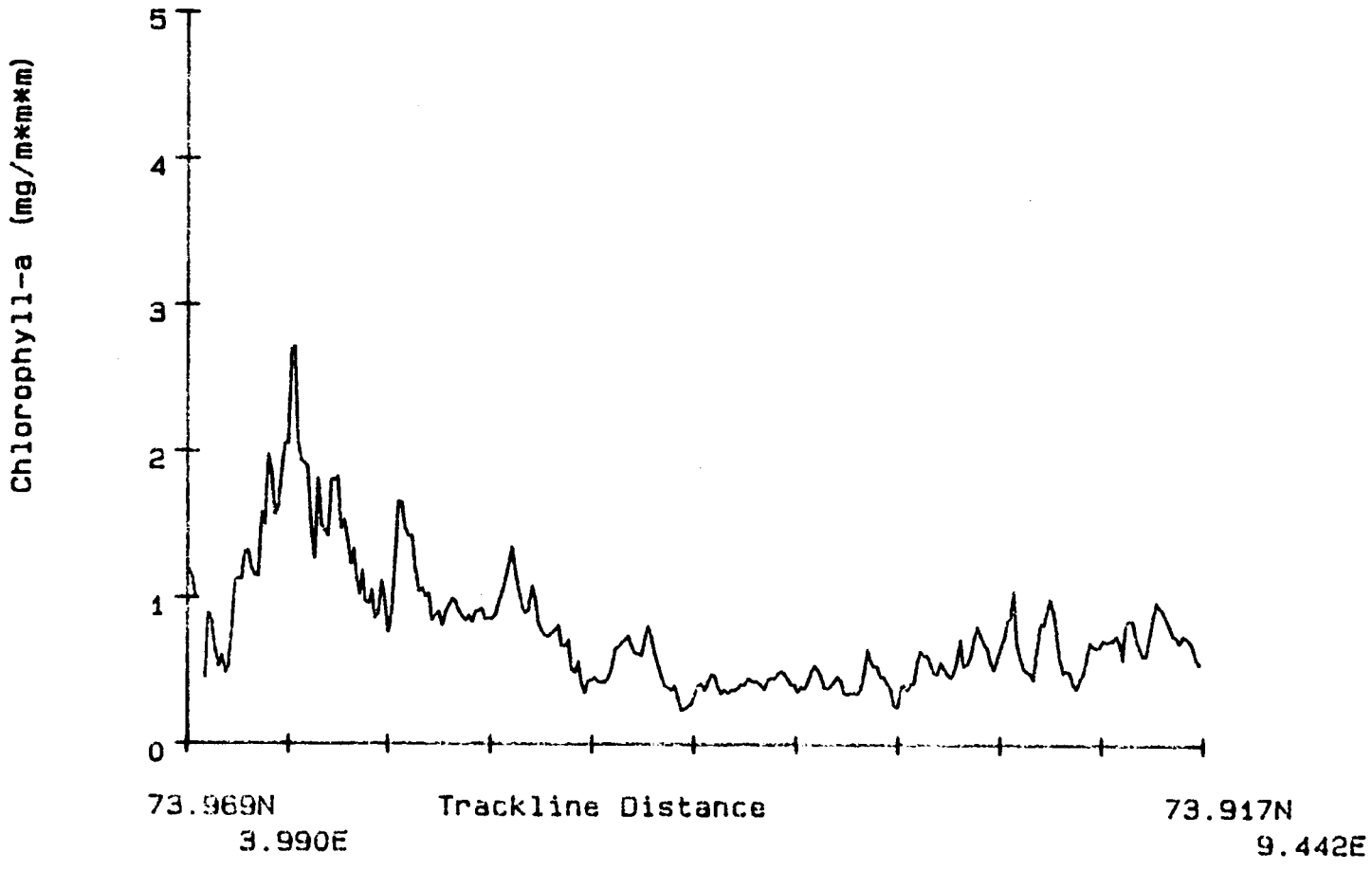

MARS Pigment (6 pt averages), 21 May 87

TRACKLINE C

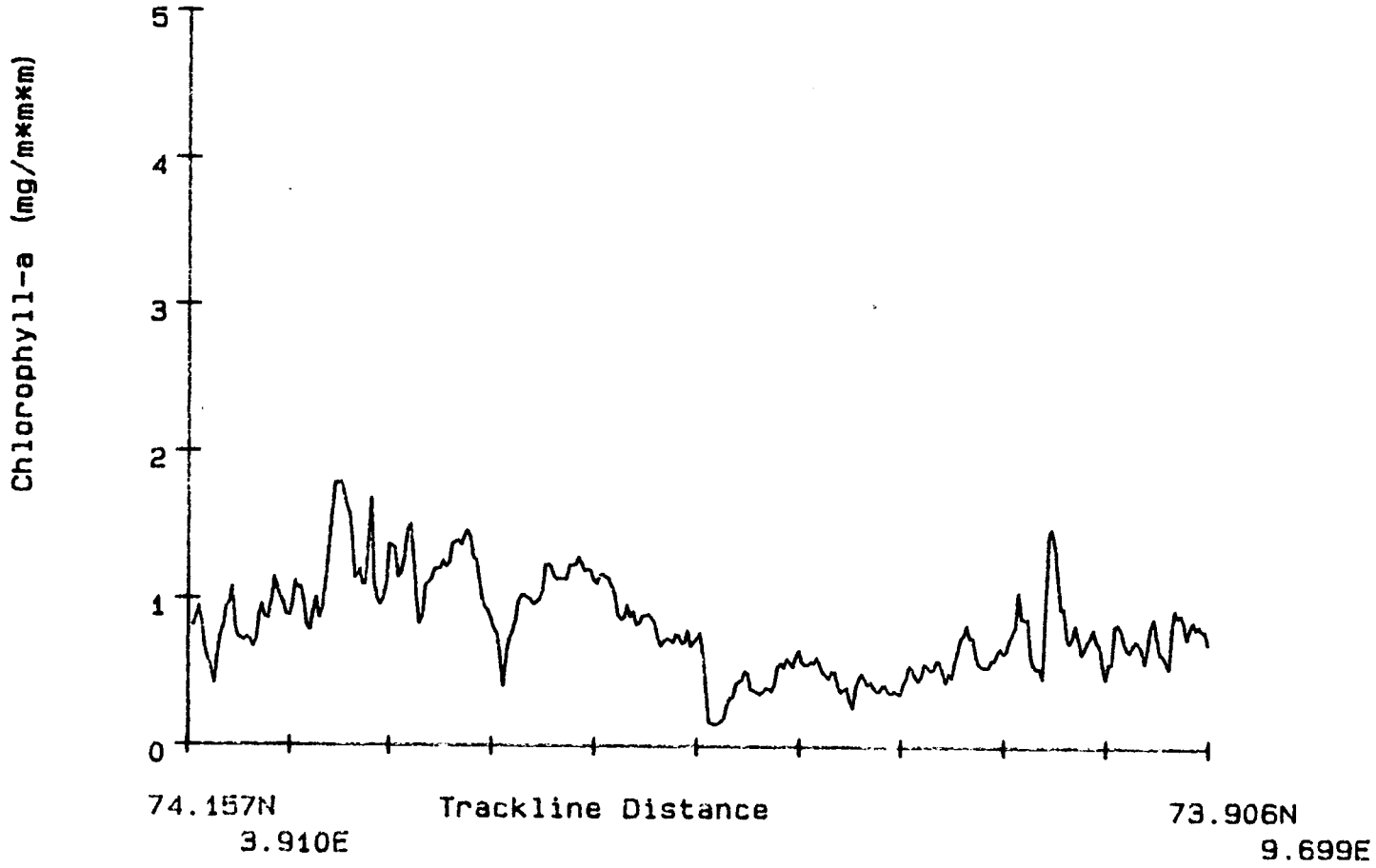

MARS Pigment (6 pt averages), 21 May 87

TRACKLINE D

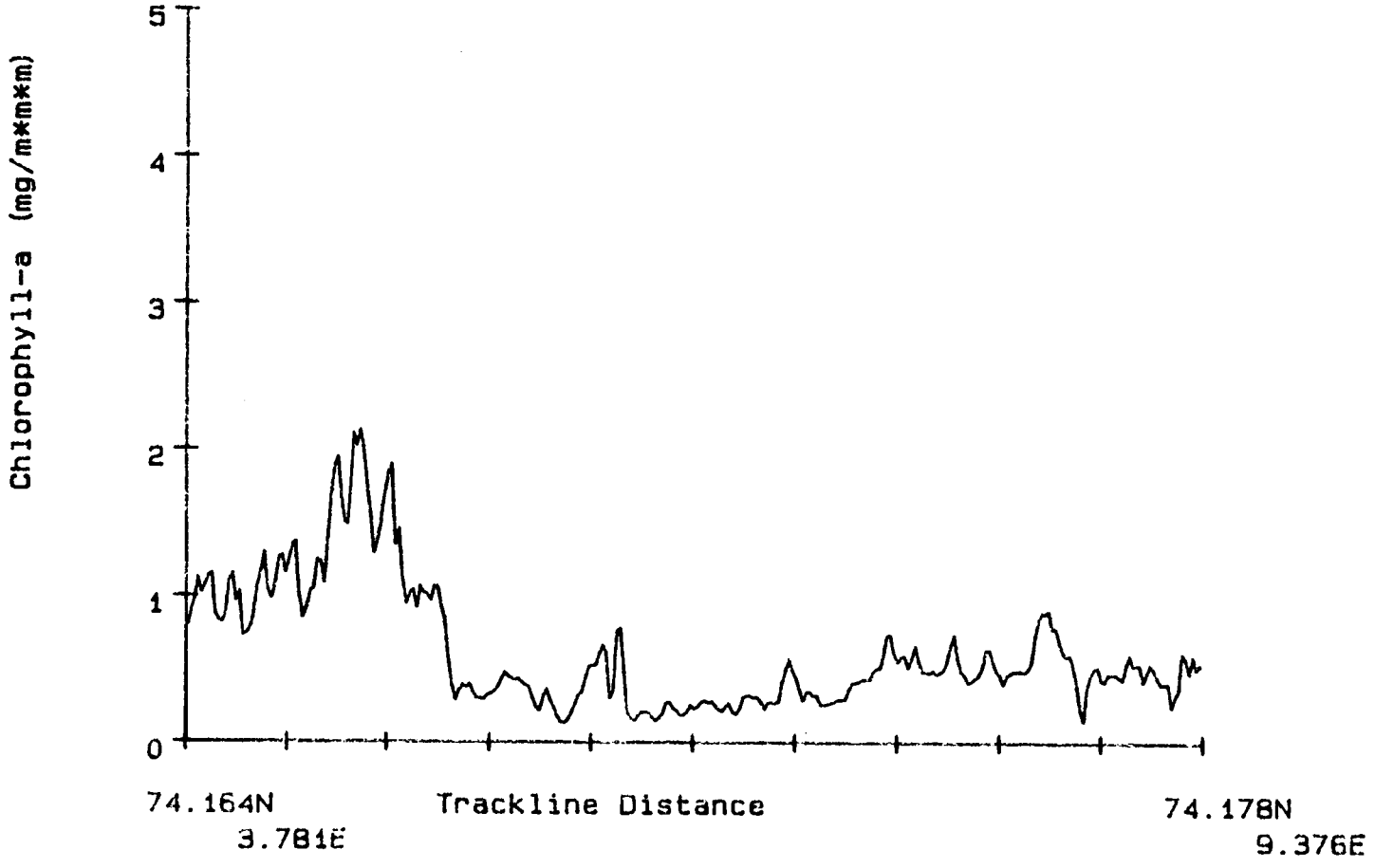

MARS Pigment (6 pt averages), 23 May 87

TRACKLINE A

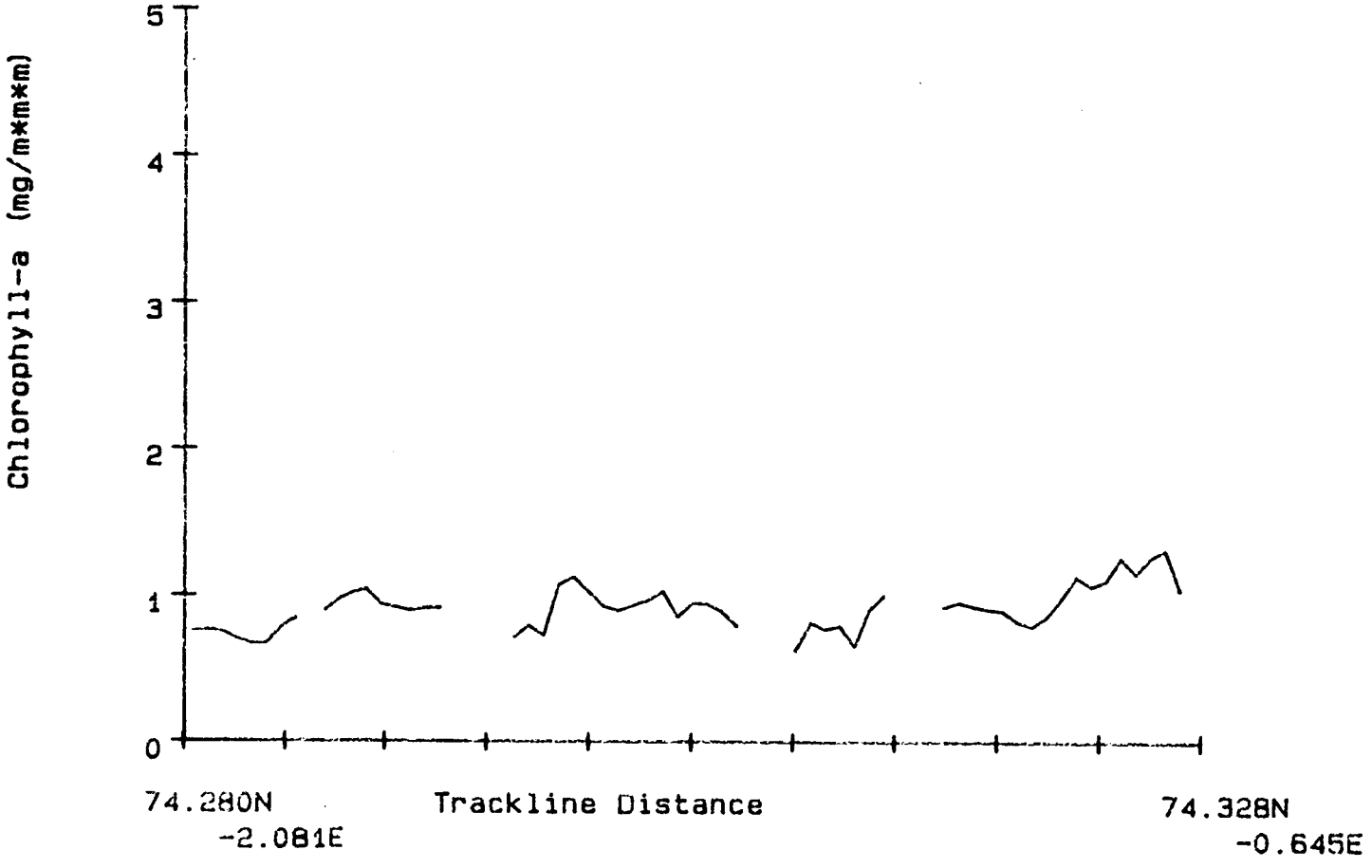

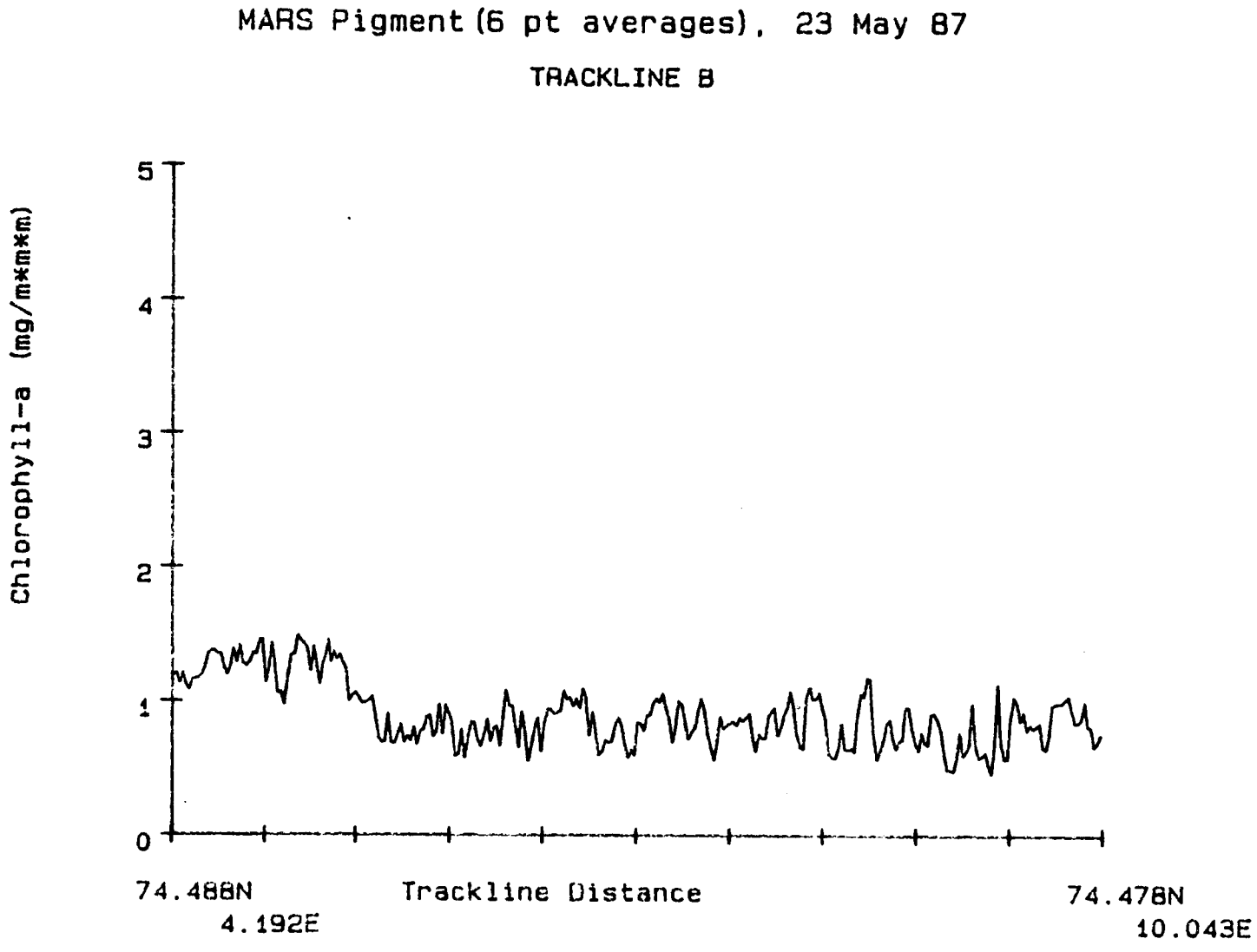
MARS Pigment (6 pt averages), 23 May 87
TRACKLINE B
Chlorophyll-a (mg/m*m*m)
5
4
3
2
1
0
74.488N
4.192E
Trackline Distance
74.478N
10.043E

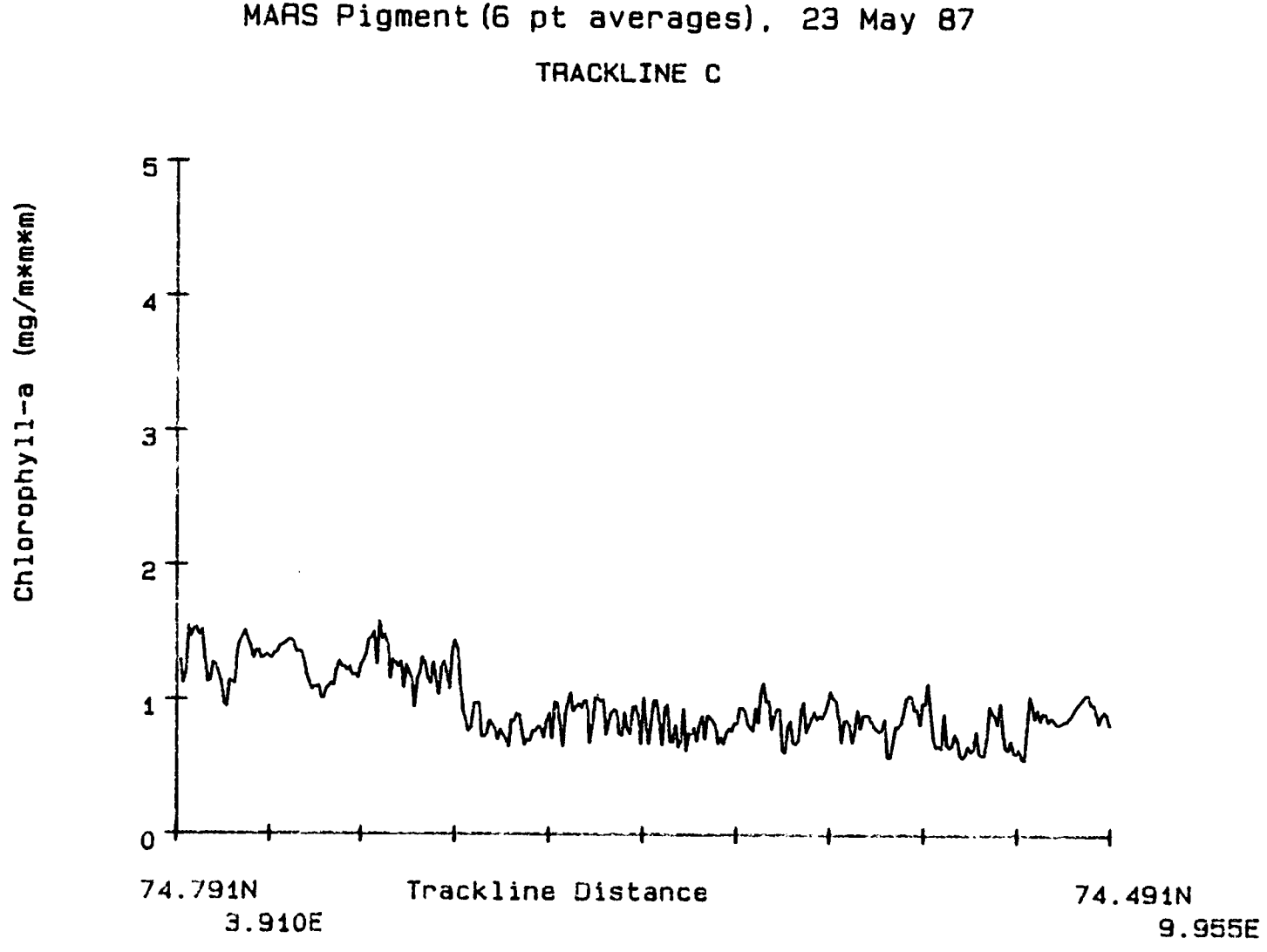
MARS Pigment (6 pt averages), 23 May 87
TRACKLINE C
Chlorophyll-a (mg/m*m*m)
5
4
3
2
1
0
74.791N
3.910E
Trackline Distance
74.491N
9.955E

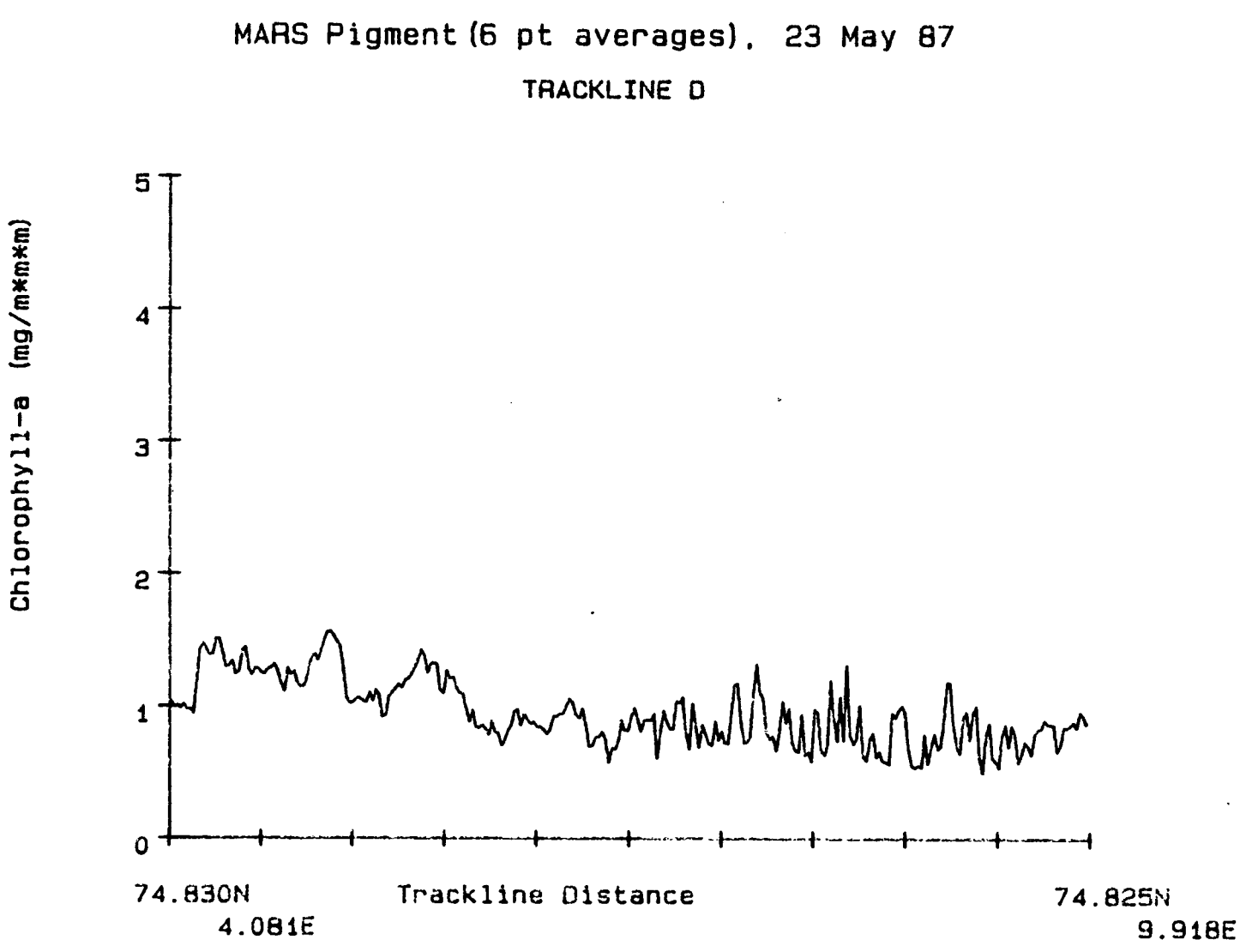
MARS Pigment (6 pt averages), 23 May 87
TRACKLINE D
Chlorophyll-a (mg/m*m*m)
5
4
3
2
1
0
74.830N
4.081E
Trackline Distance
74.825N
9.918E

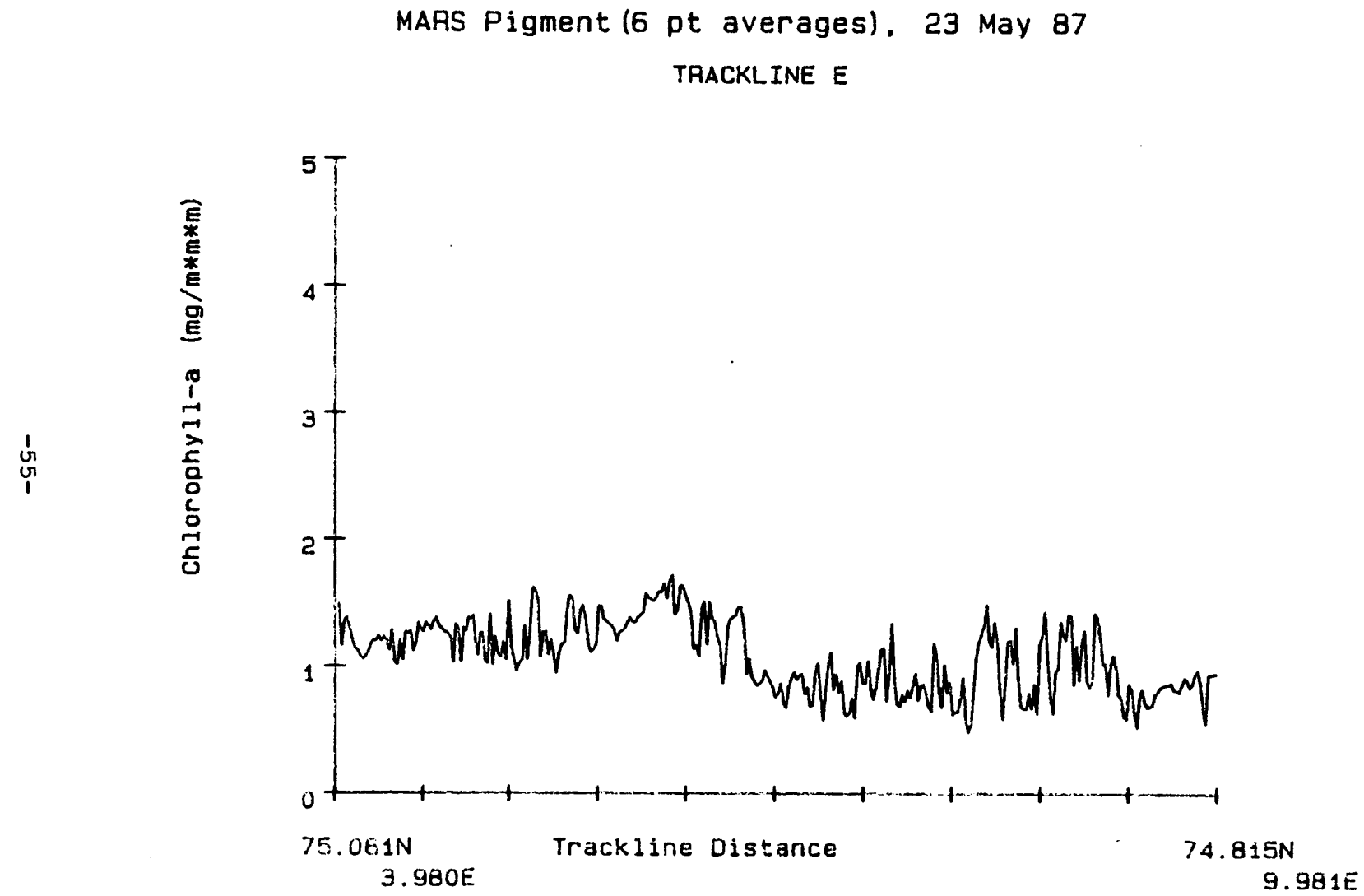
MARS Pigment (6 pt averages), 23 May 87
TRACKLINE E
Chlorophyll-a (mg/m*m*m)
5
4
3
2
1
0
75.061N
3.980E
Trackline Distance
74.815N
9.981E

MARS Pigment (6 pt averages), 25 May 87

TRACKLINE A

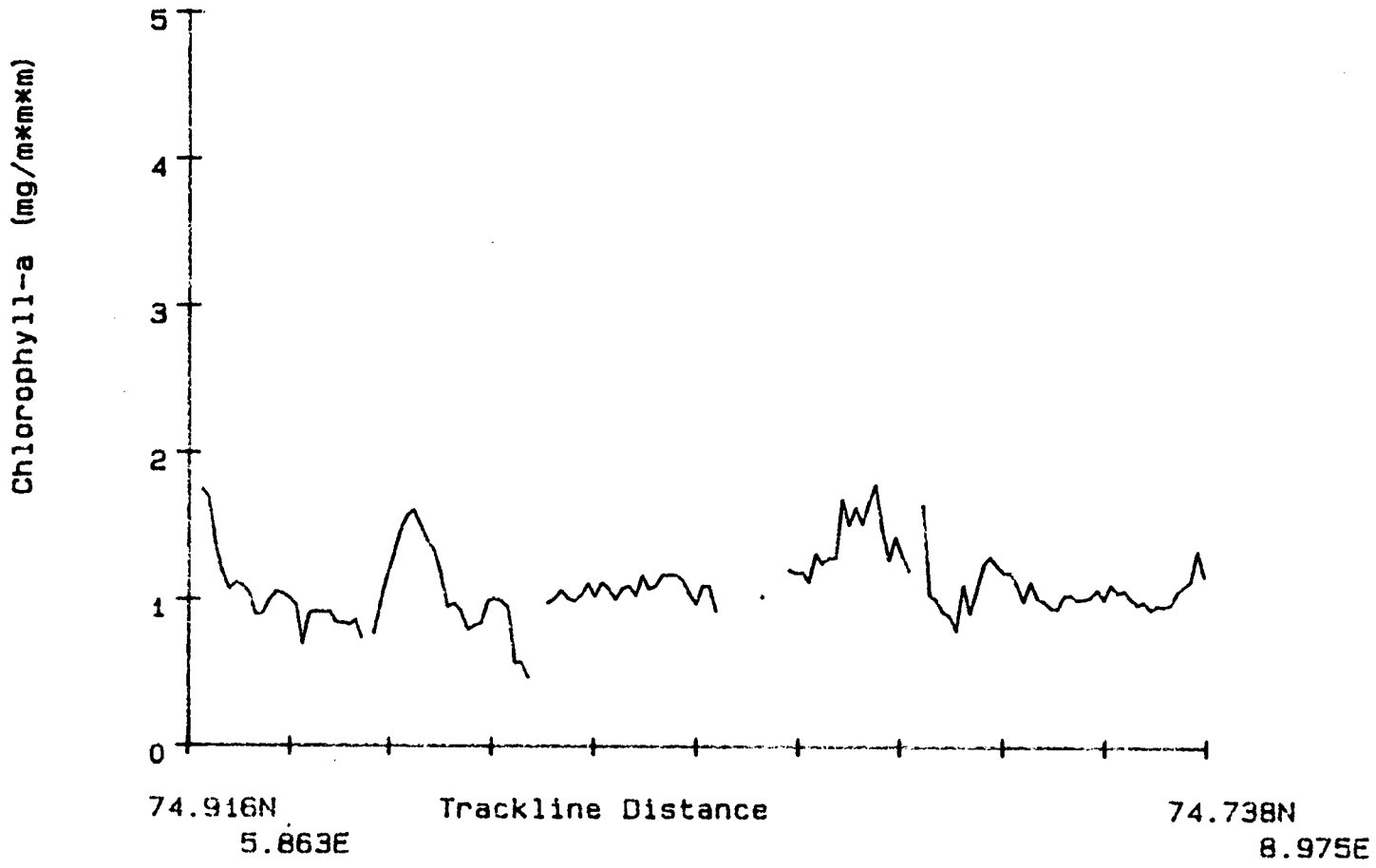

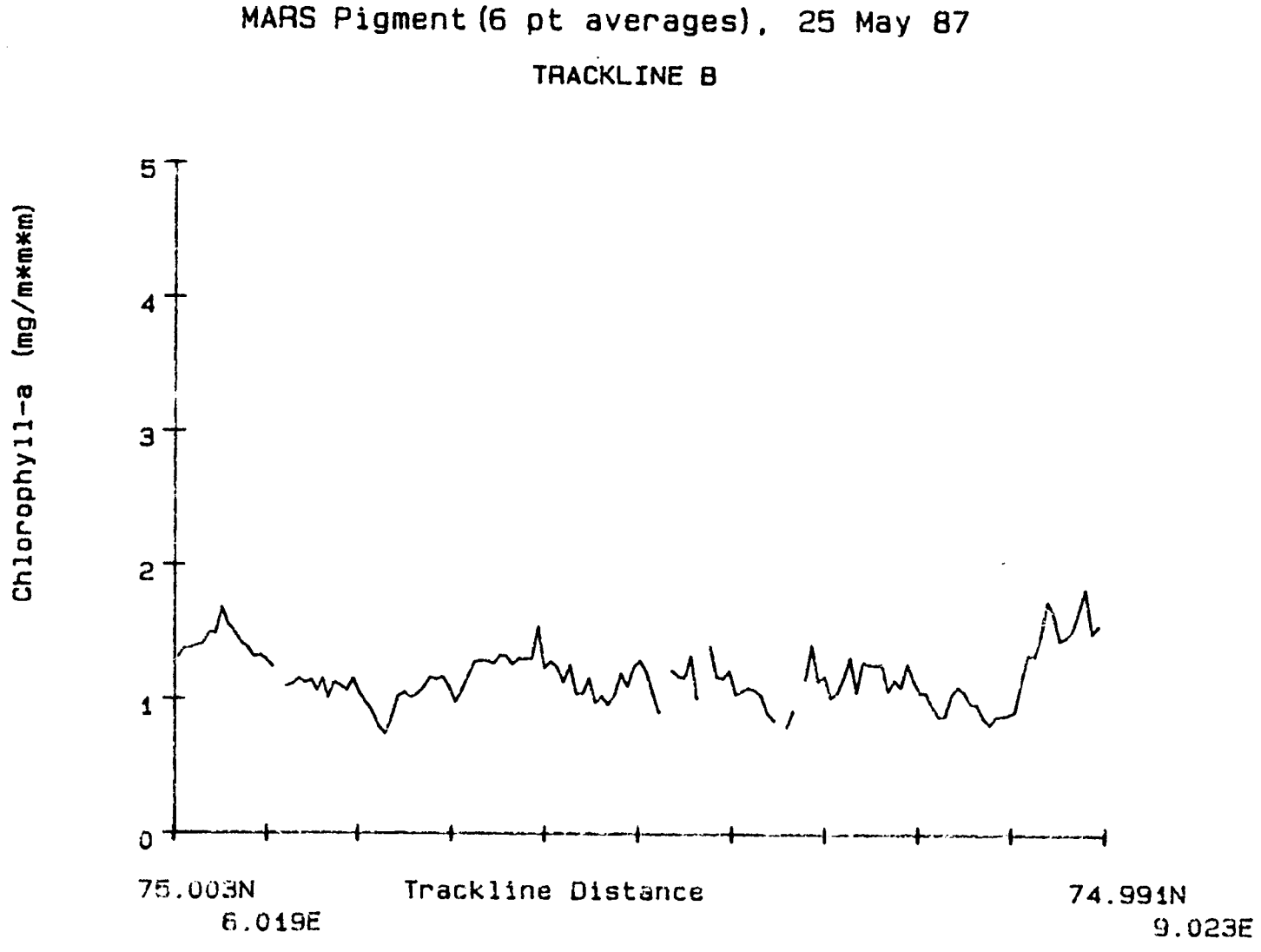
MARS Pigment (6 pt averages), 25 May 87
TRACKLINE B
Chlorophyll-a (mg/m*m*m)
5
4
3
2
1
0
75.003N
6.019E
Trackline Distance
74.991N
9.023E

MARS Pigment (6 pt averages), 25 May 87

TRACKLINE C

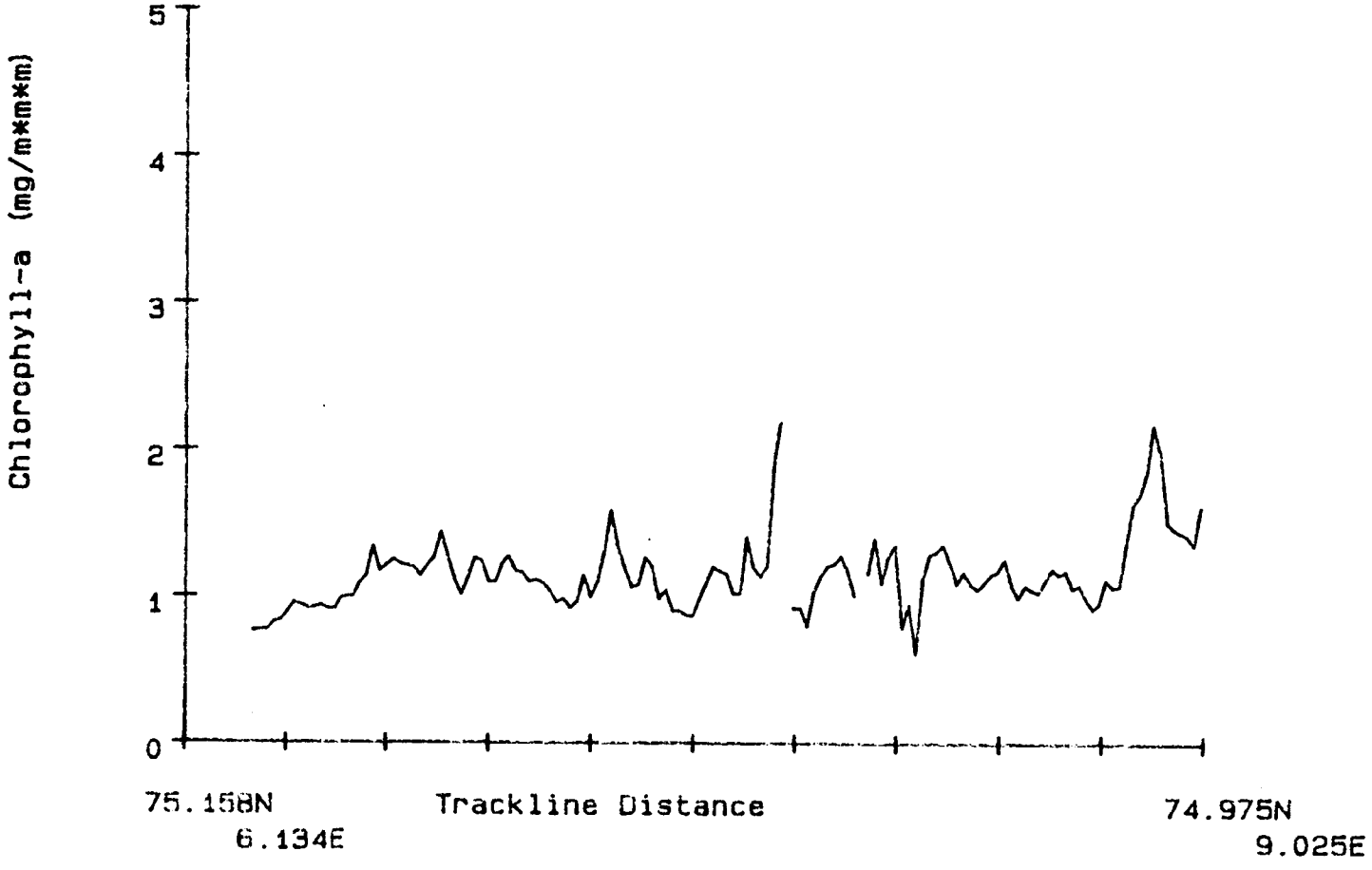

MARS Pigment (6 pt averages), 25 May 87

TRACKLINE P

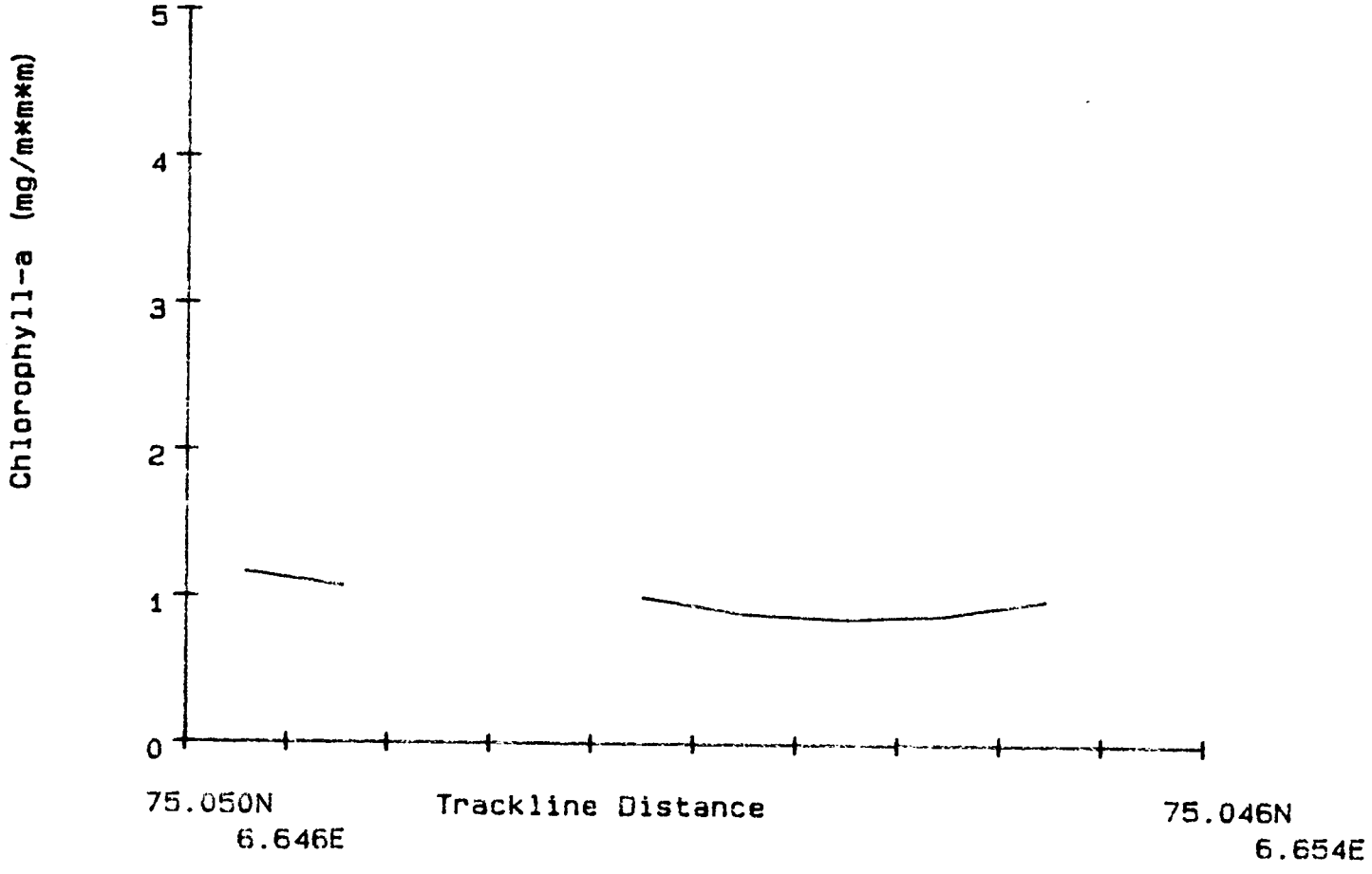

MARS Pigment (6 pt averages), 29 May 87

TRACKLINE D

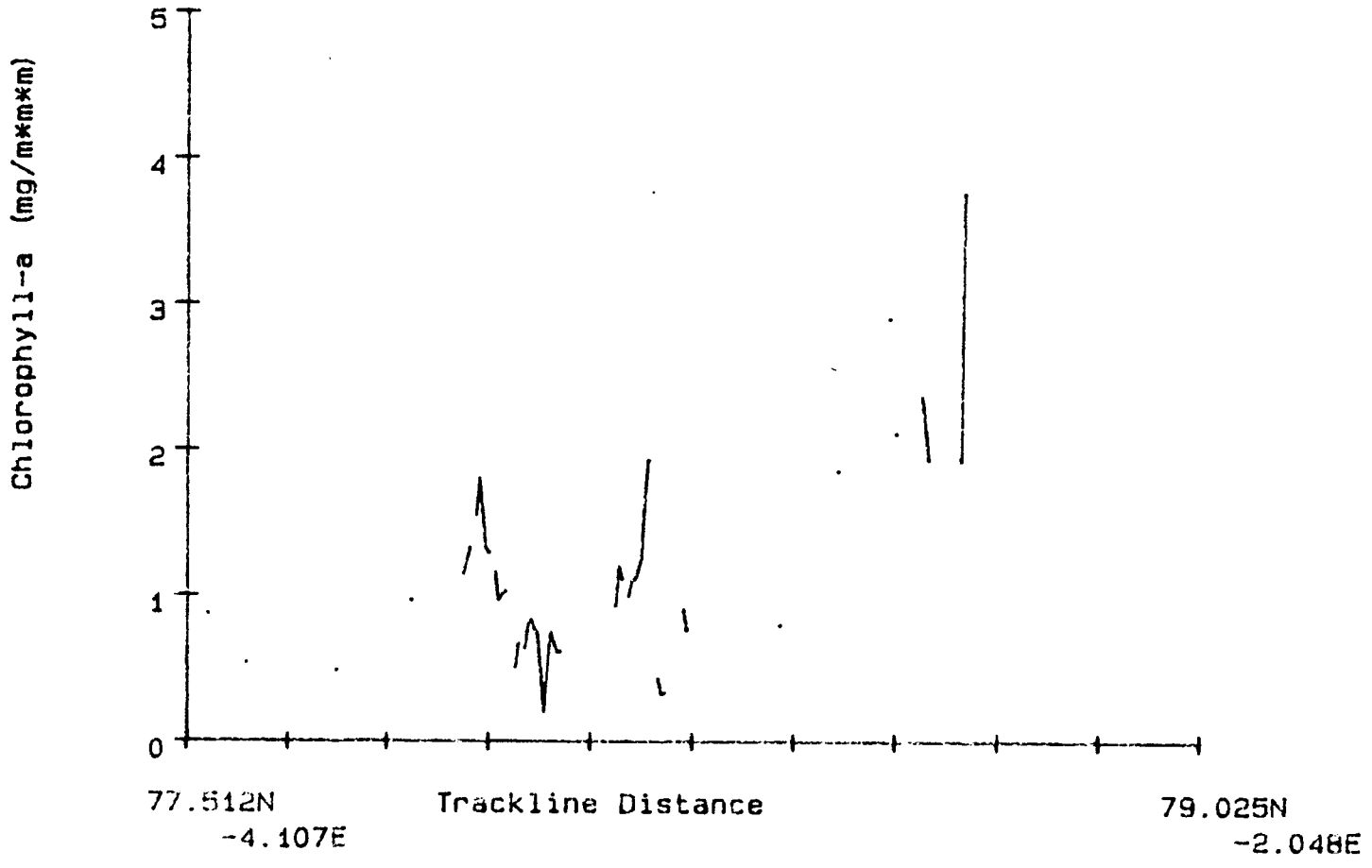

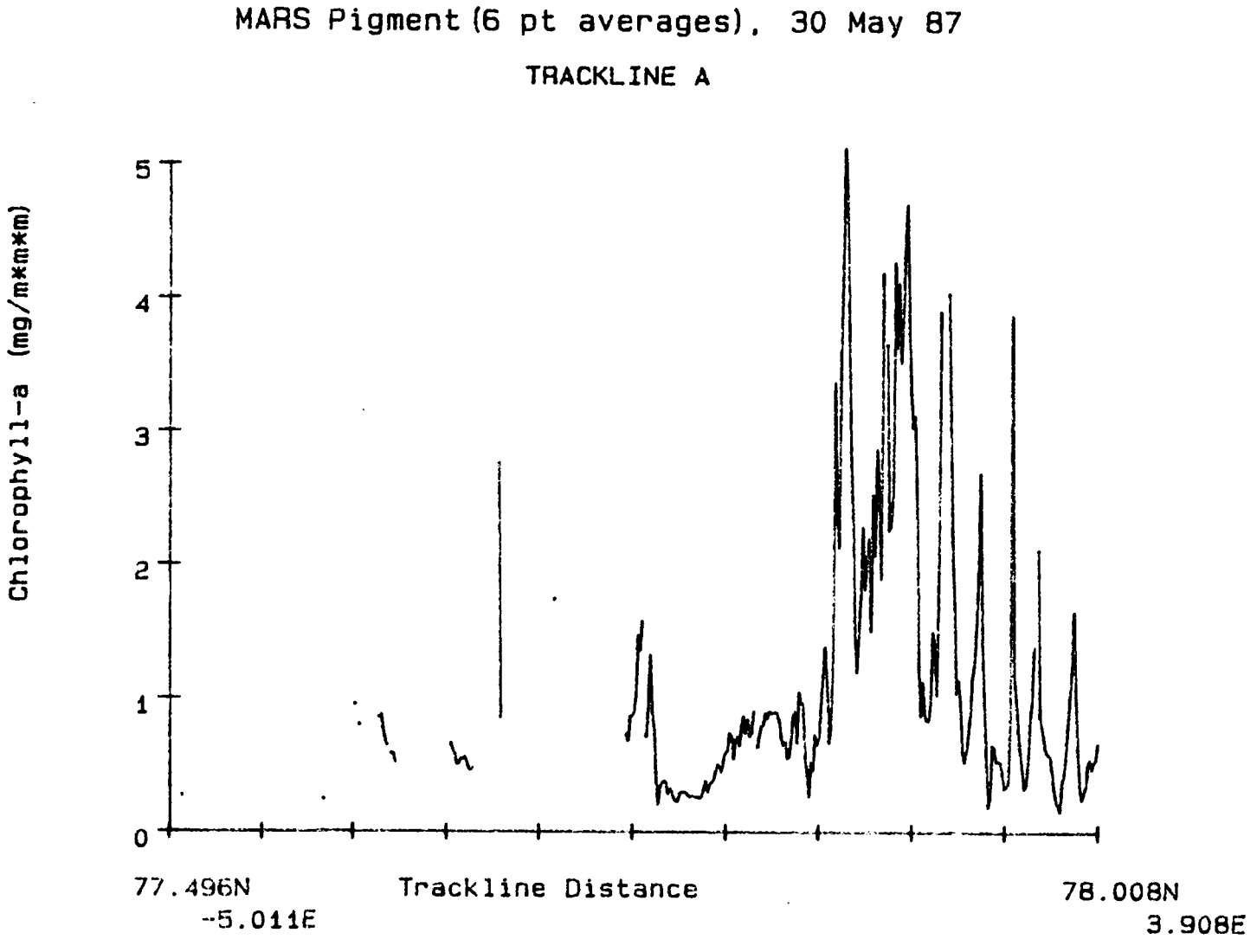
MARS Pigment (6 pt averages), 30 May 87
TRACKLINE A
Chlorophyll-a (mg/m*m*m)
5
4
3
2
1
0
77.496N
-5.011E
Trackline Distance
78.008N
3.908E

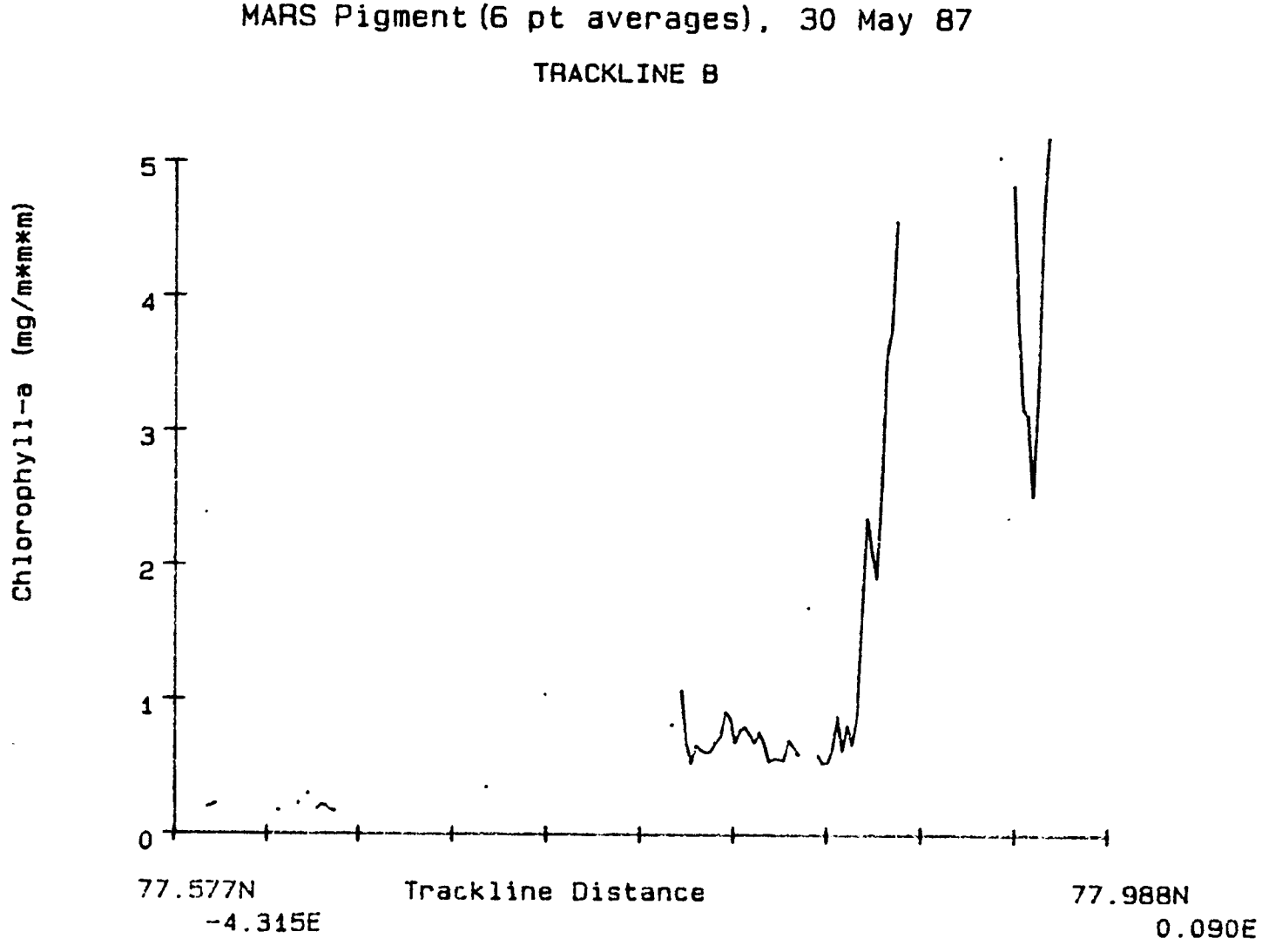
MARS Pigment (6 pt averages), 30 May 87
TRACKLINE B
Chlorophyll-a (mg/m*m*m)
5
4
3
2
1
0
77.577N
-4.315E
Trackline Distance
77.988N
0.090E

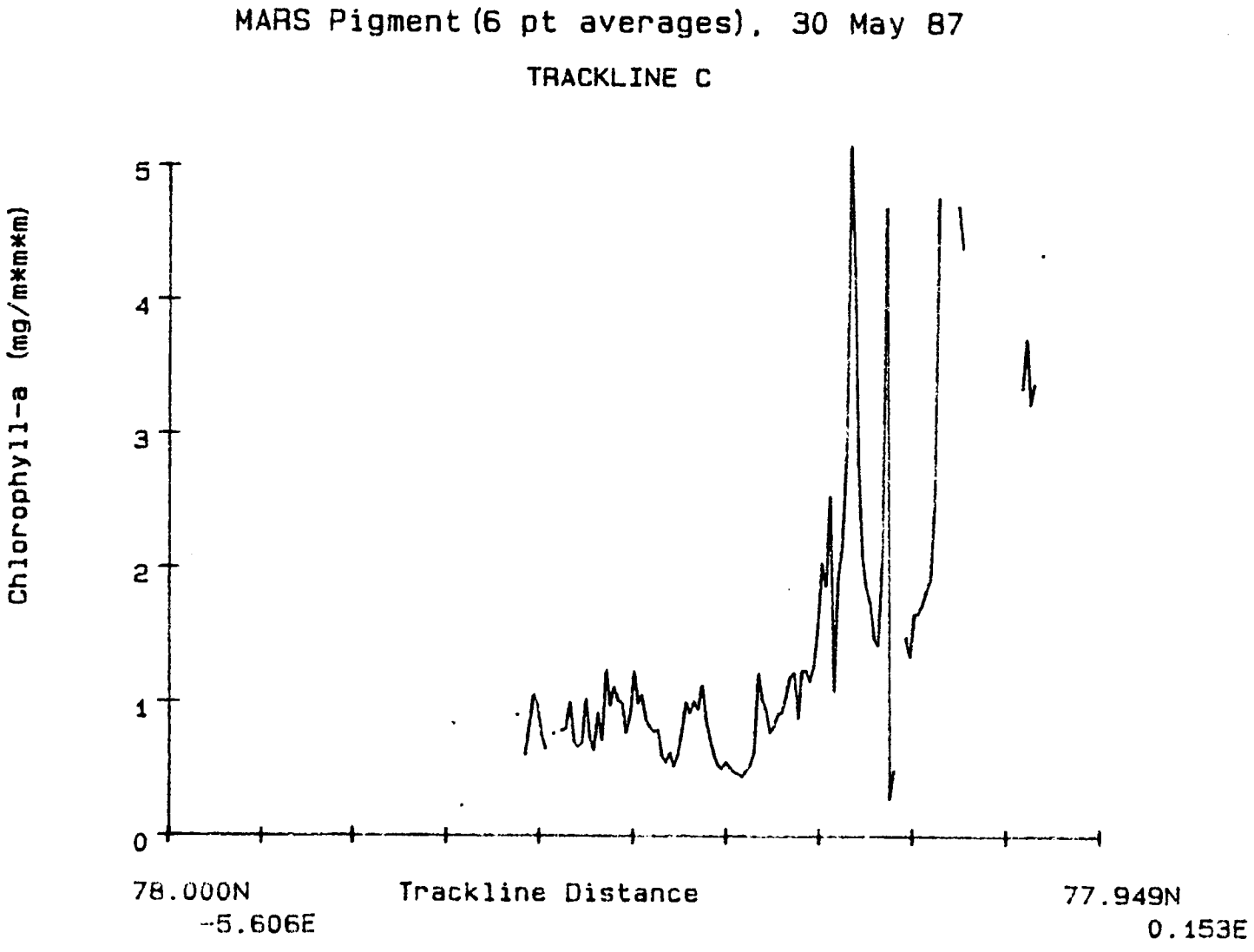
MARS Pigment (6 pt averages), 30 May 87
TRACKLINE C
Chlorophyll-a (mg/m*m*m)
5
4
3
2
1
0
78.000N
-5.606E
Trackline Distance
77.949N
0.153E

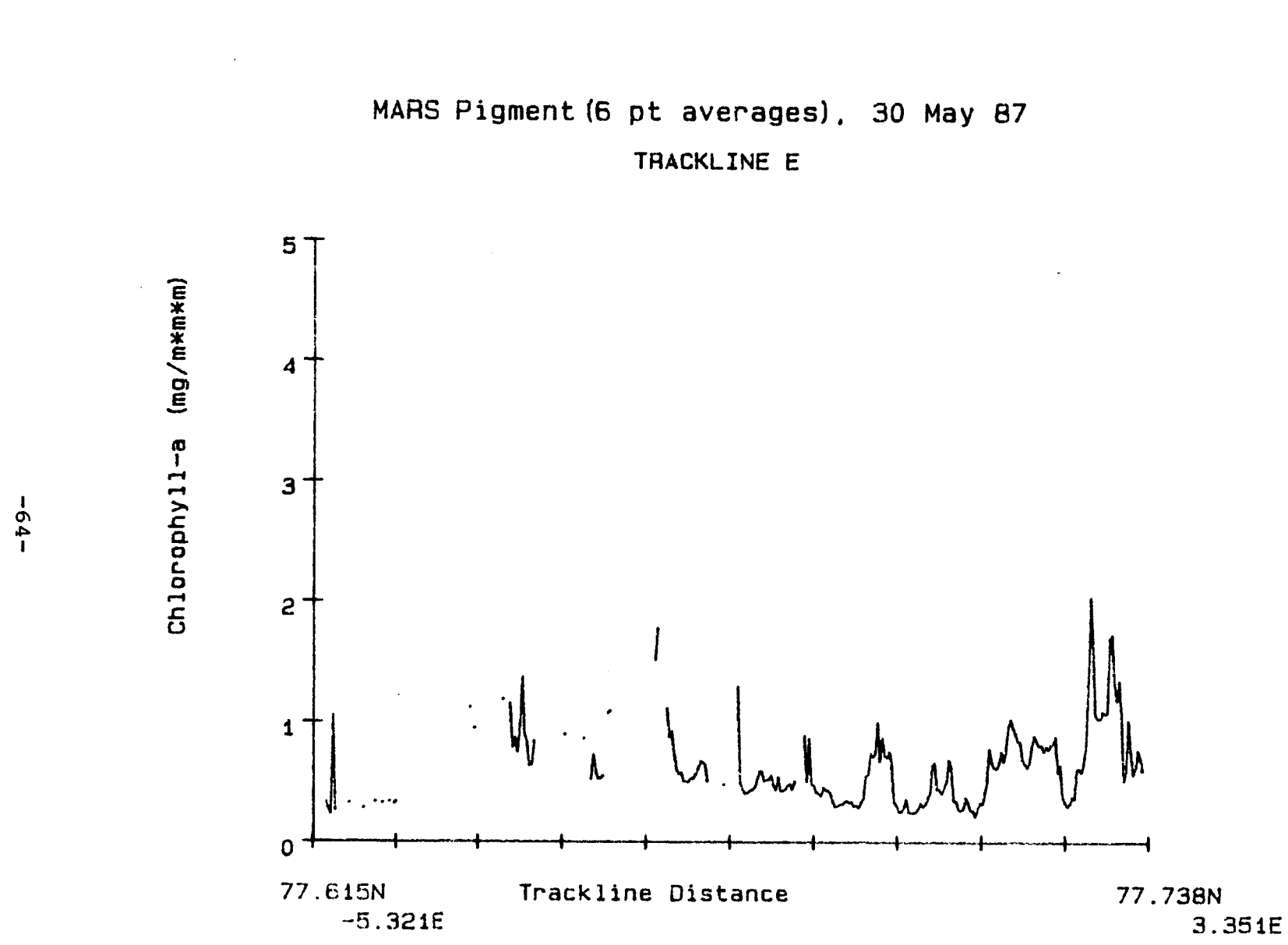
MARS Pigment (6 pt averages), 30 May 87
TRACKLINE E
Chlorophyll-a (mg/m*m*m)
5
4
3
2
1
0
77.615N
-5.321E
Trackline Distance
77.738N
3.351E

MARS Pigment (6 pt averages), 31 May 87

TRACKLINE A

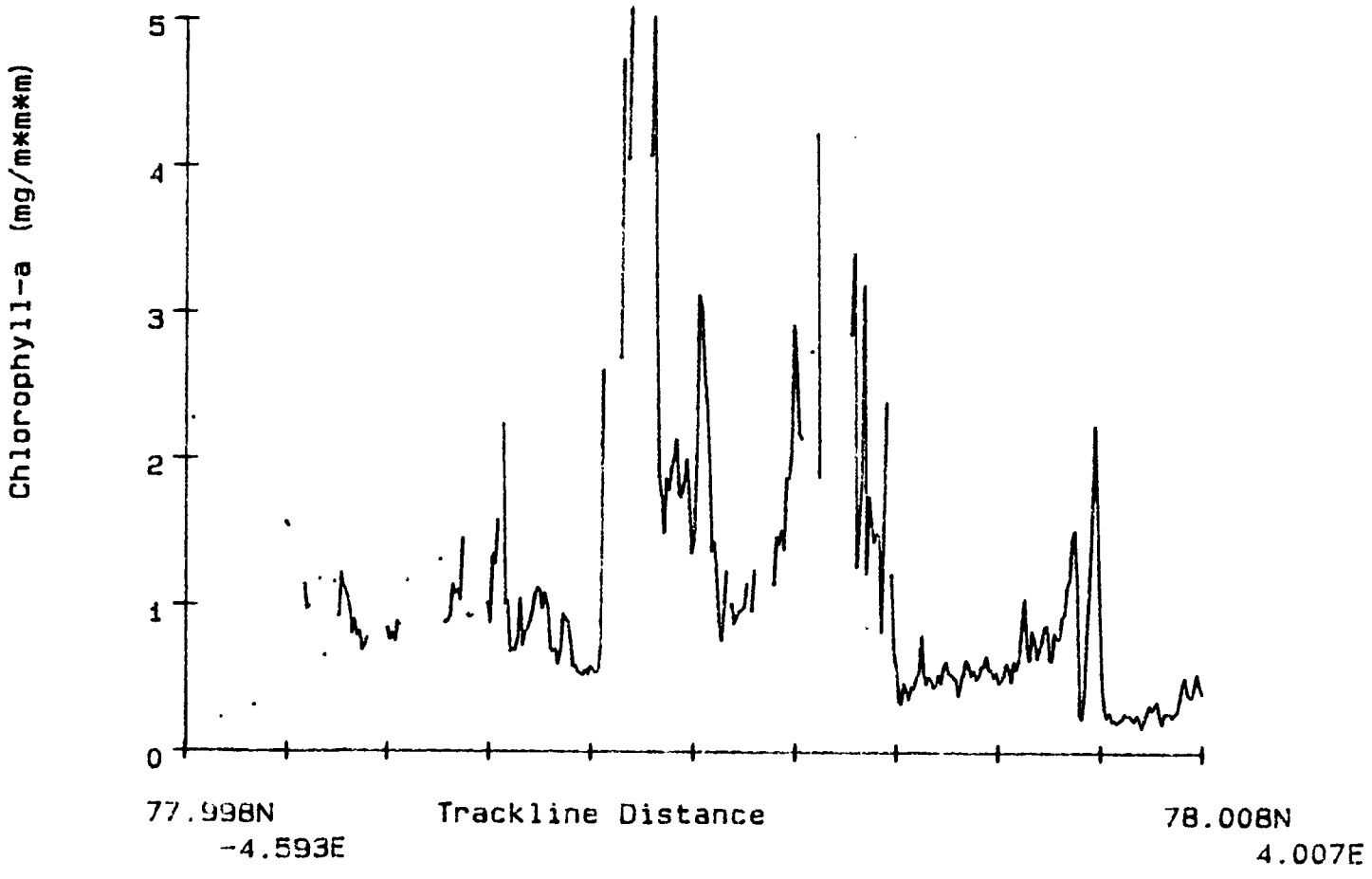

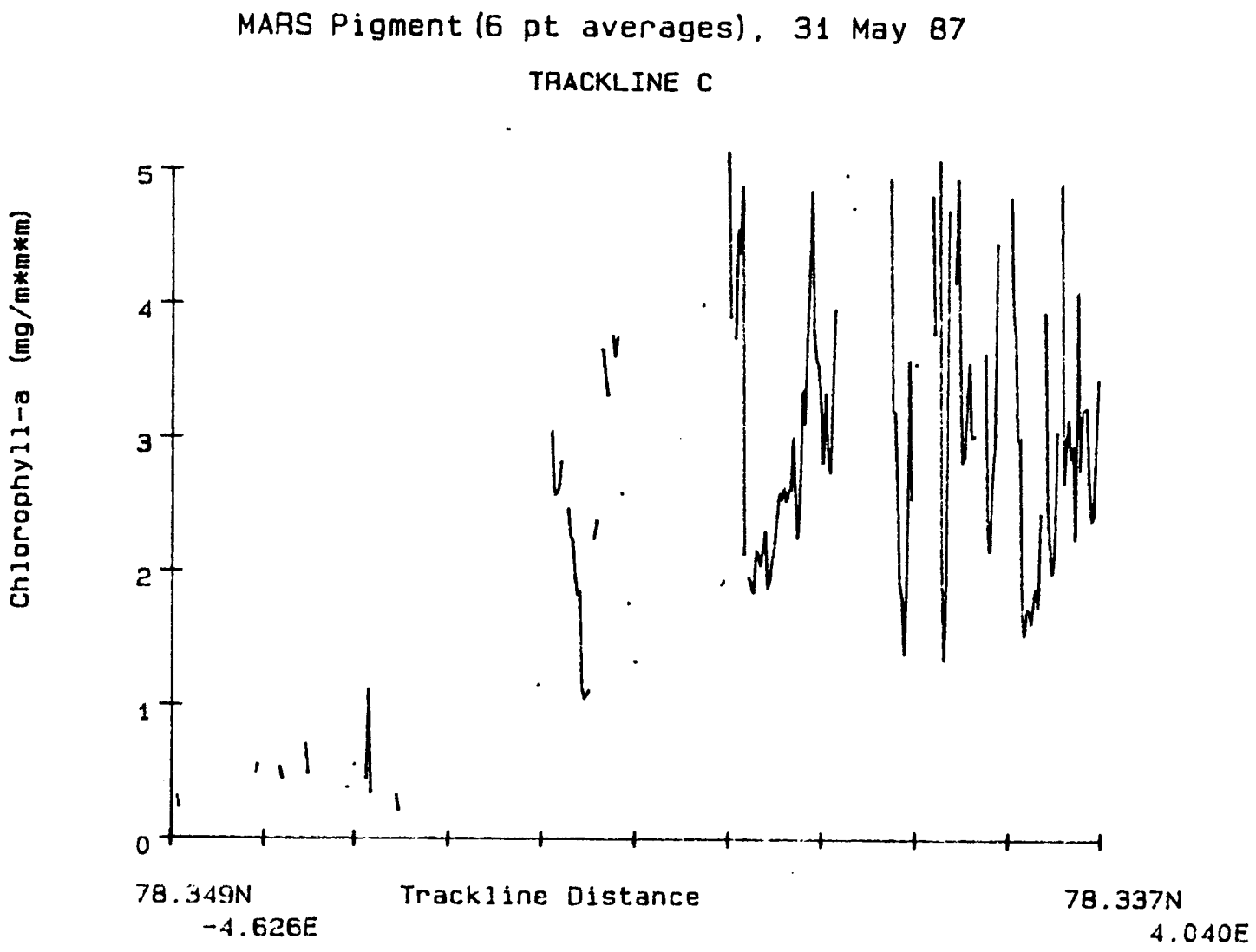
MARS Pigment (6 pt averages), 31 May 87
TRACKLINE C
Chlorophyll-a (mg/m*m*m)
5
4
3
2
1
0
78.349N
-4.626E
Trackline Distance
78.337N
4.040E

MARS Pigment (6 pt averages), 31 May 87

TRACKLINE D

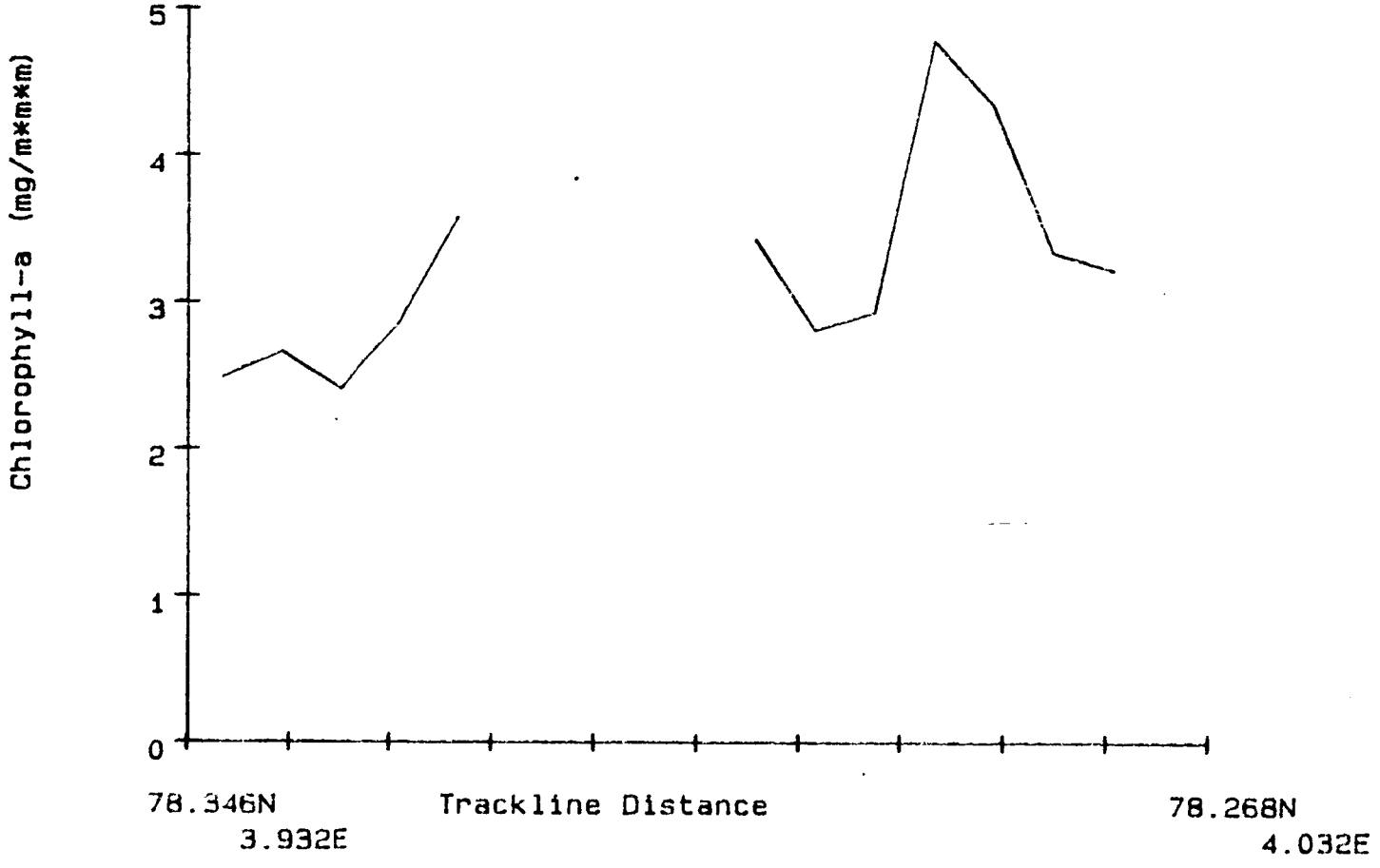

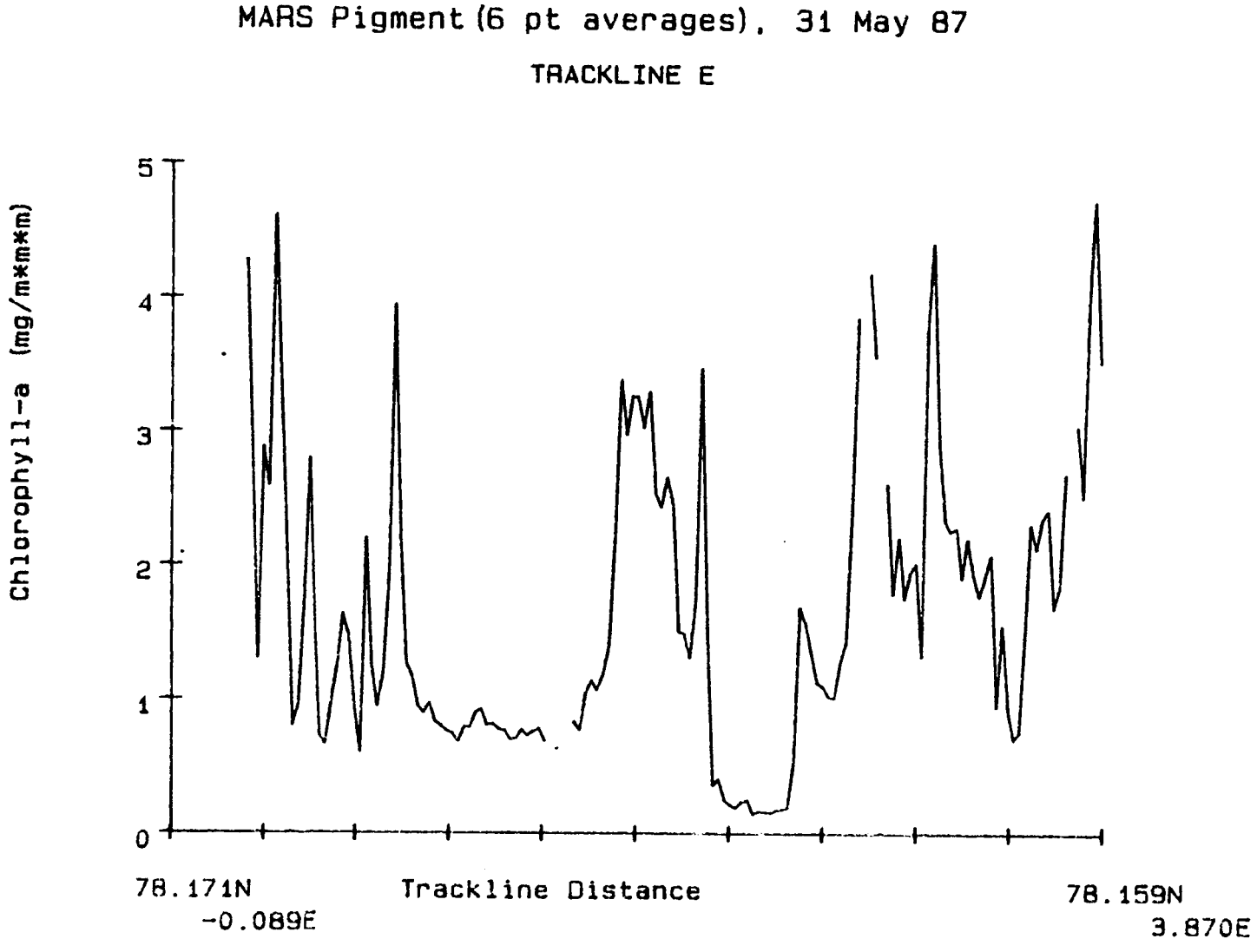
MARS Pigment (6 pt averages), 31 May 87
TRACKLINE E
Chlorophyll-a (mg/m*m*m)
5
4
3
2
1
0
78.171N
-0.089E
Trackline Distance
78.159N
3.870E

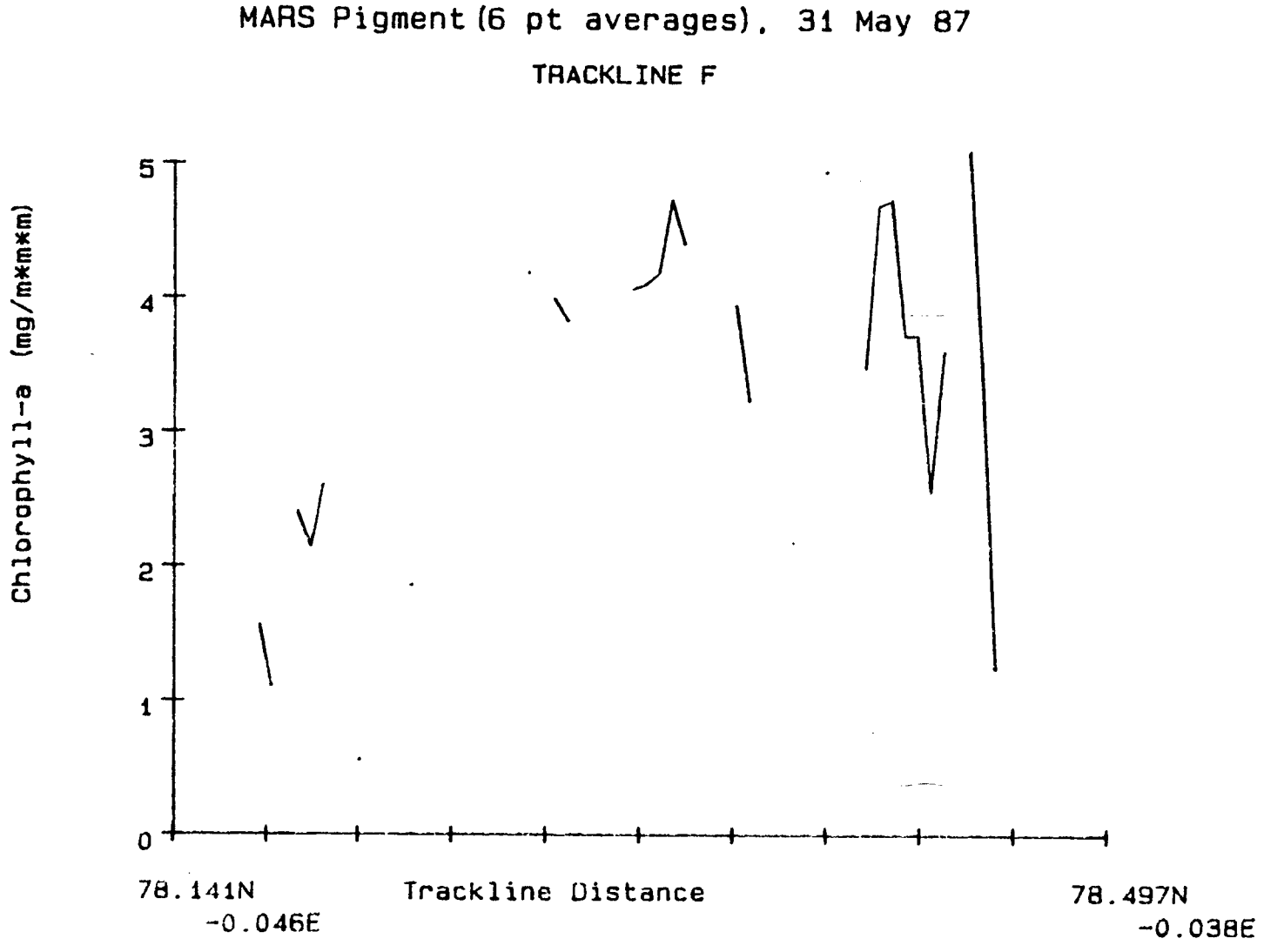
MARS Pigment (6 pt averages), 31 May 87
TRACKLINE F
Chlorophyll-a (mg/m*m*m)
5
4
3
2
1
0
78.141N
-0.046E
Trackline Distance
78.497N
-0.038E

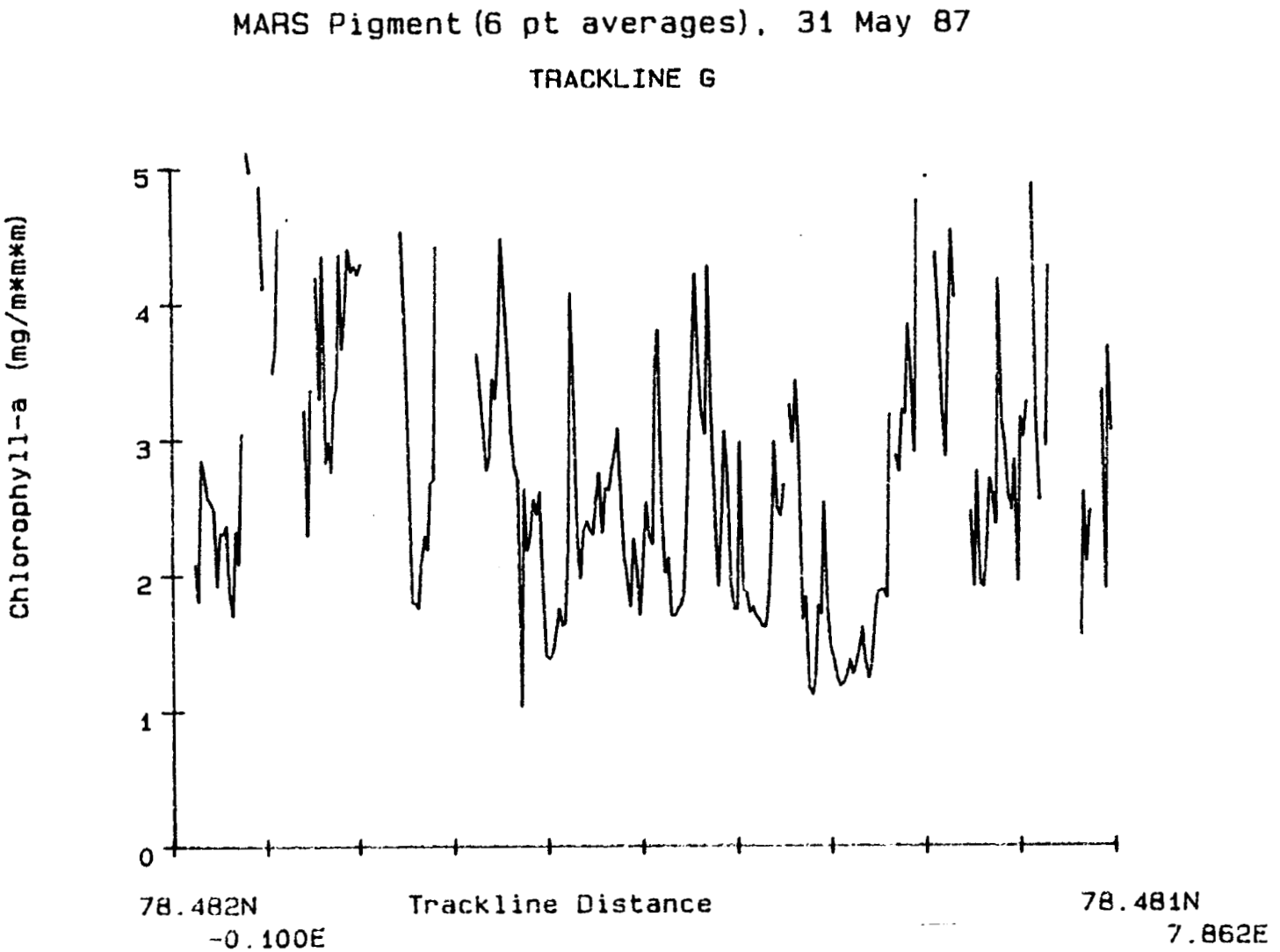
MARS Pigment (6 pt averages), 31 May 87
TRACKLINE G
Chlorophyll-a (mg/m*m*m)
5
4
3
2
1
0
78.482N
-0.100E
Trackline Distance
78.481N
7.862E

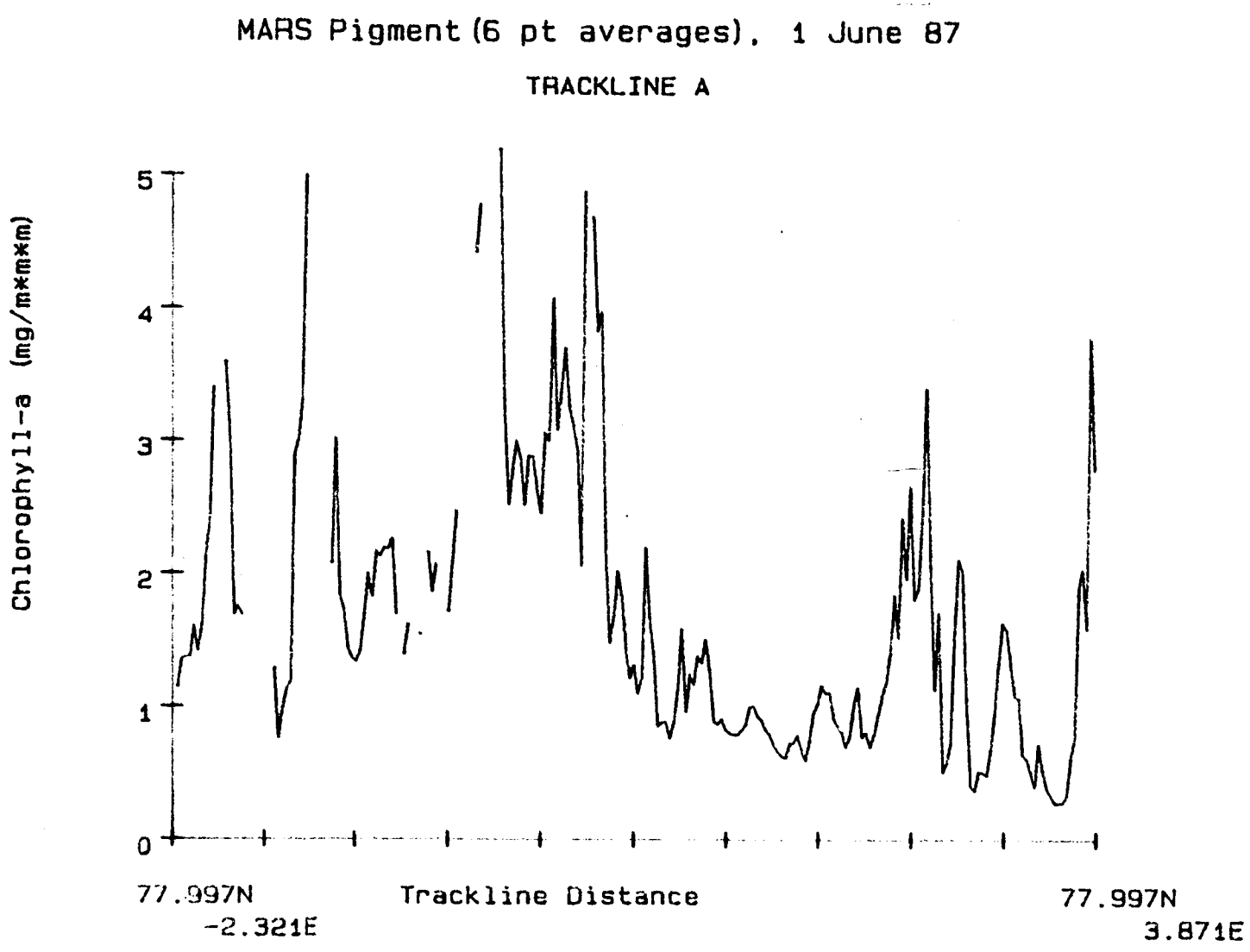
MARS Pigment (6 pt averages), 1 June 87
TRACKLINE A
Chlorophyll-a (mg/m*m*m)
5
4
3
2
1
0
77.997N
-2.321E
Trackline Distance
77.997N
3.871E

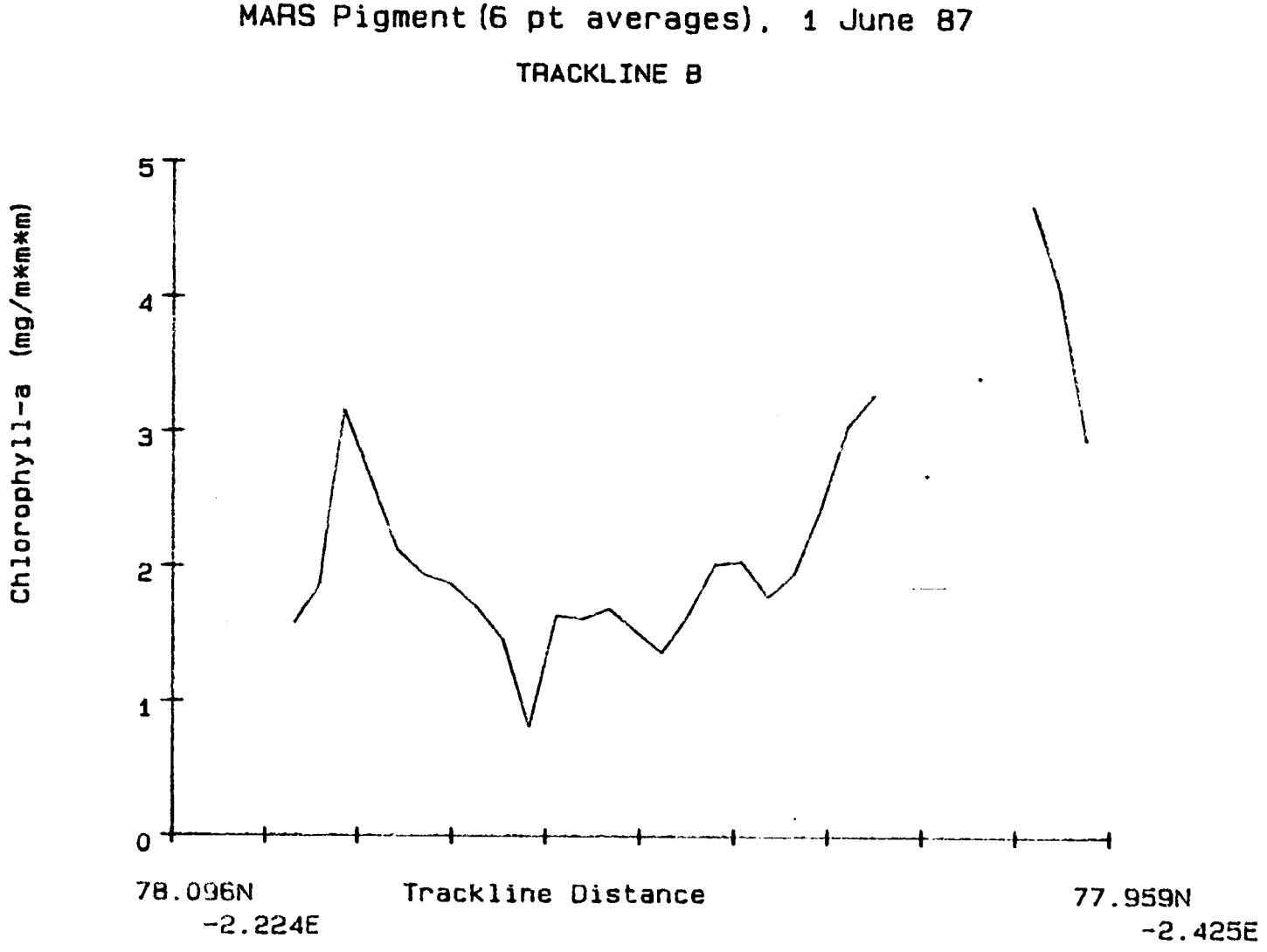
MARS Pigment (6 pt averages), 1 June 87
TRACKLINE B
Chlorophyll-a (mg/m*m*m)
5
4
3
2
1
0
78.096N
-2.224E
Trackline Distance
77.959N
-2.425E

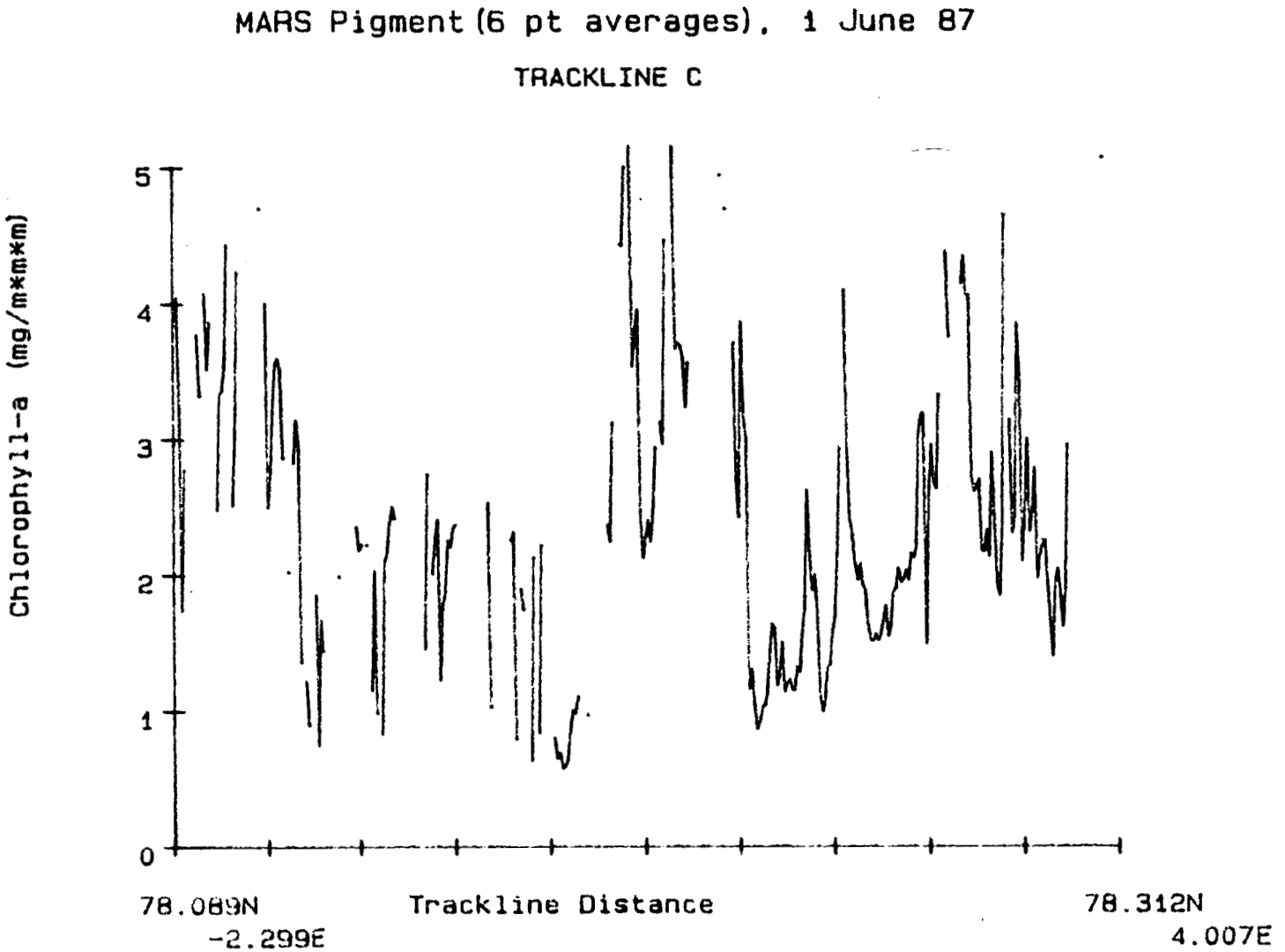
MARS Pigment (6 pt averages), 1 June 87
TRACKLINE C
Chlorophyll-a (mg/m*m*m)
5
4
3
2
1
0
78.089N
-2.299E
Trackline Distance
78.312N
4.007E

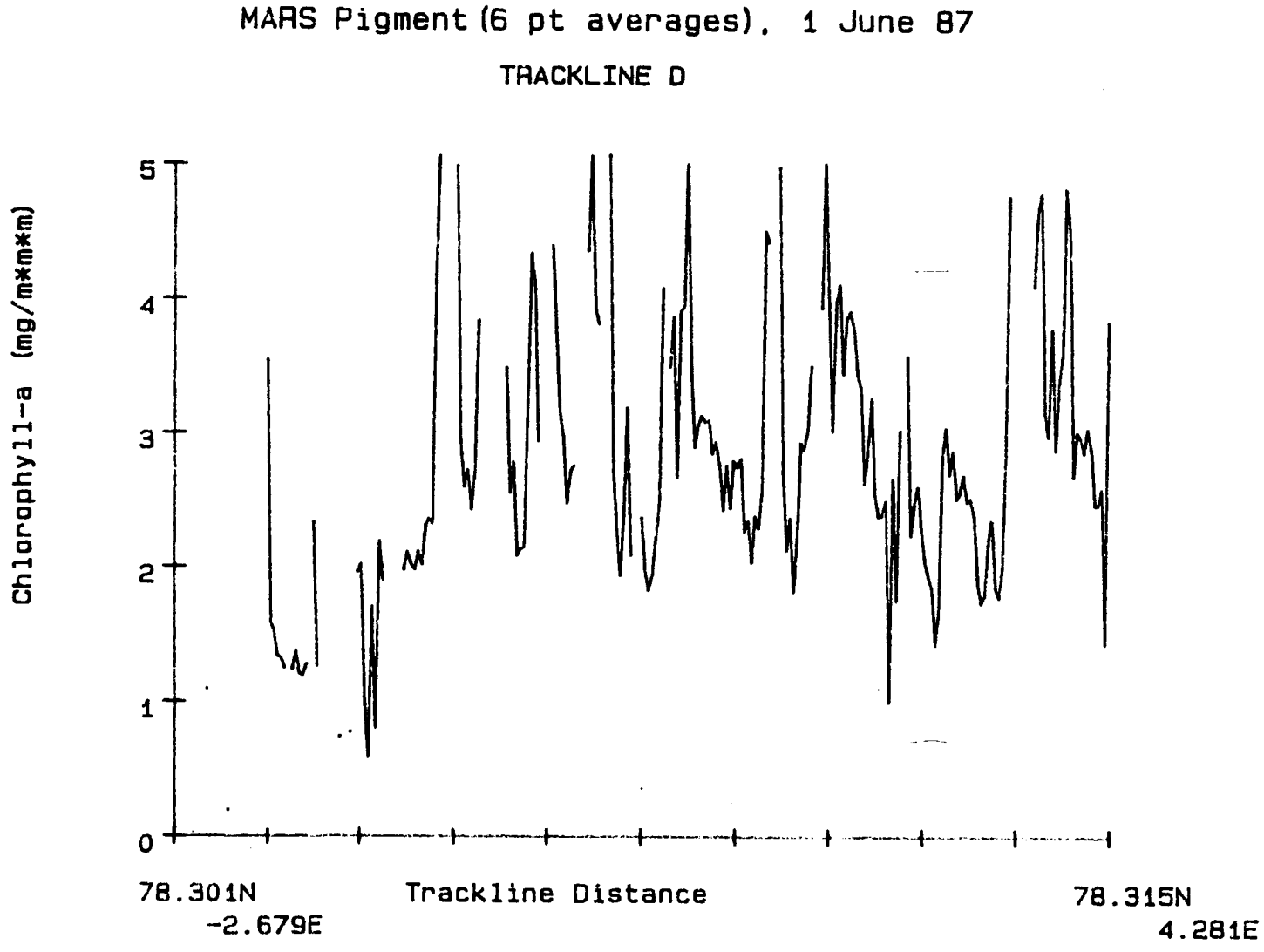
MARS Pigment (6 pt averages), 1 June 87
TRACKLINE D
Chlorophyll-a (mg/m*m*m)
5
4
3
2
1
0
78.301N
-2.679E
Trackline Distance
78.315N
4.281E

MARS Pigment (6 pt averages), 1 June 87

TRACKLINE F

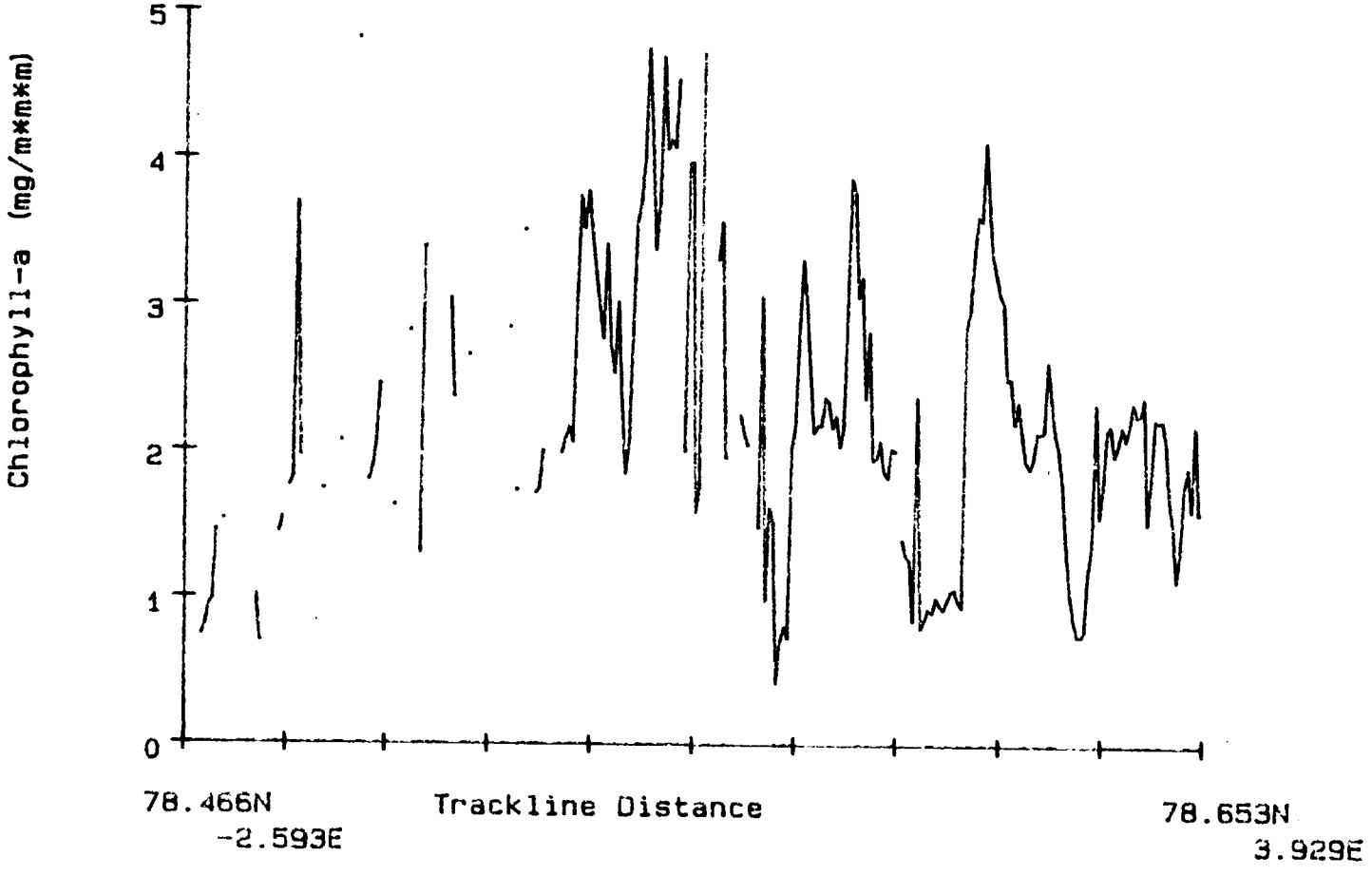

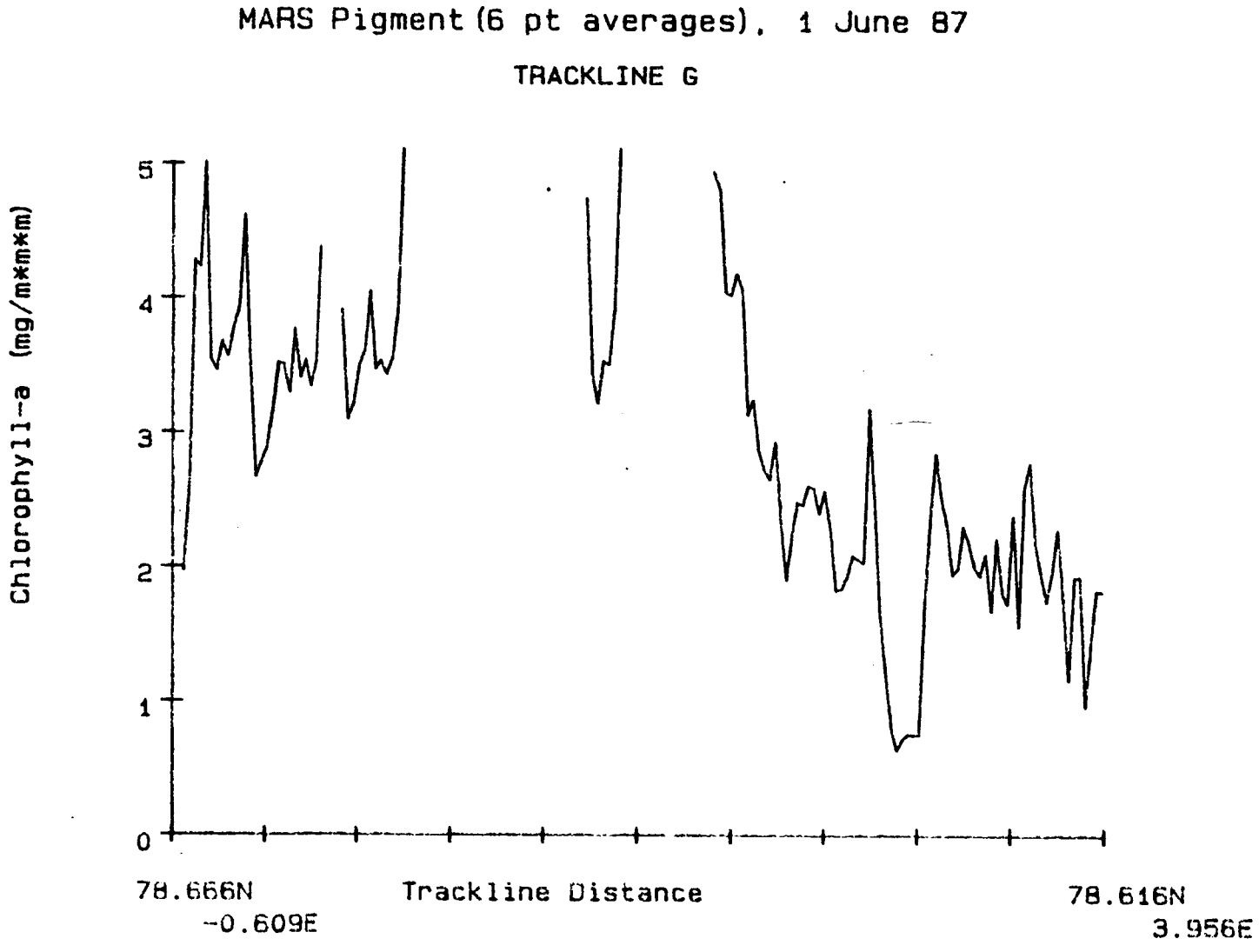
MARS Pigment (6 pt averages), 1 June 87
TRACKLINE G
Chlorophyll-a (mg/m*m*m)
5
4
3
2
1
0
78.666N
-0.609E
Trackline Distance
78.616N
3.956E

MARS Pigment (6 pt averages), 2 June 87

TRACKLINE A

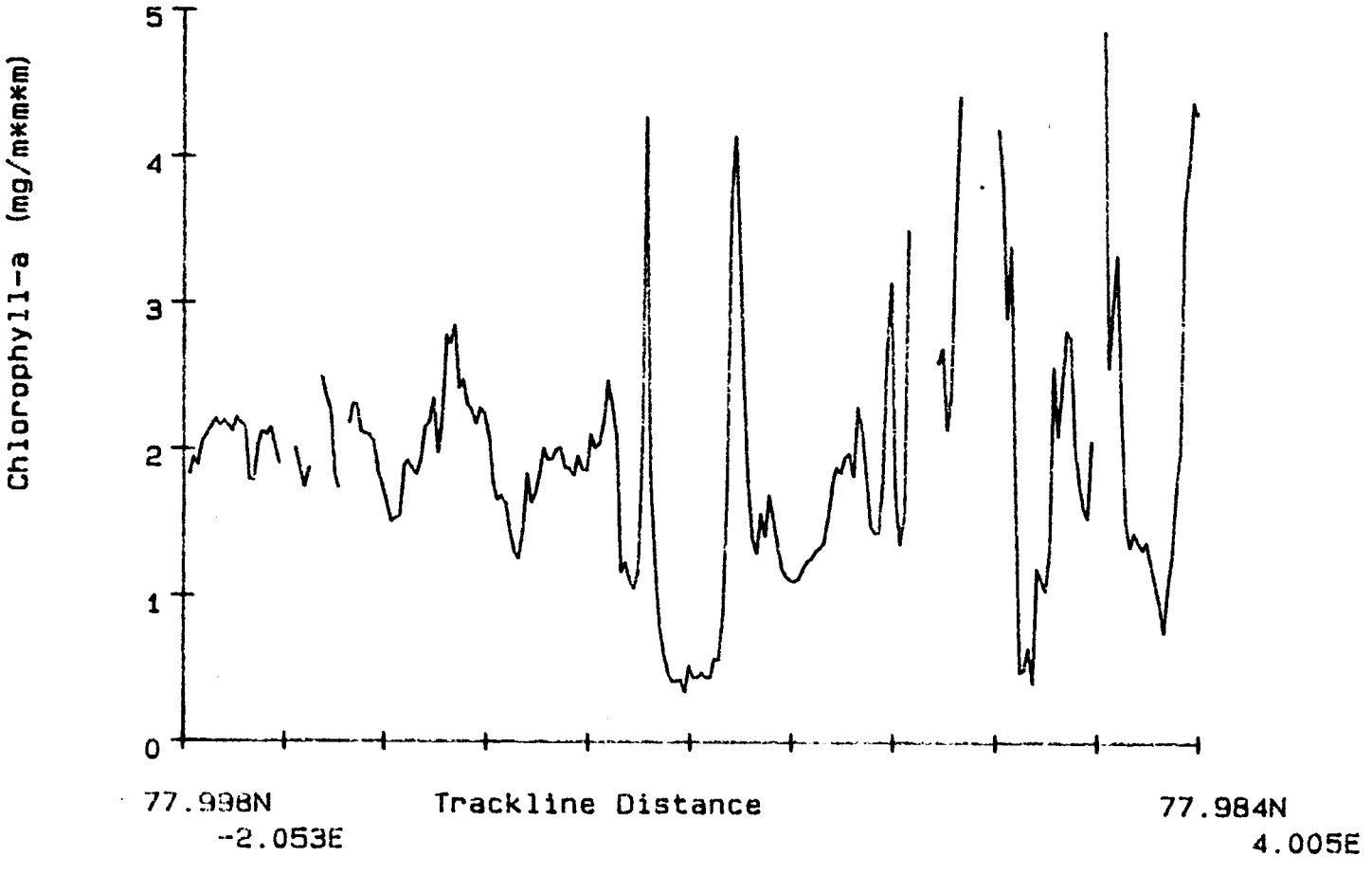

MARS Pigment (6 pt averages), 2 June 87

TRACKLINE 8

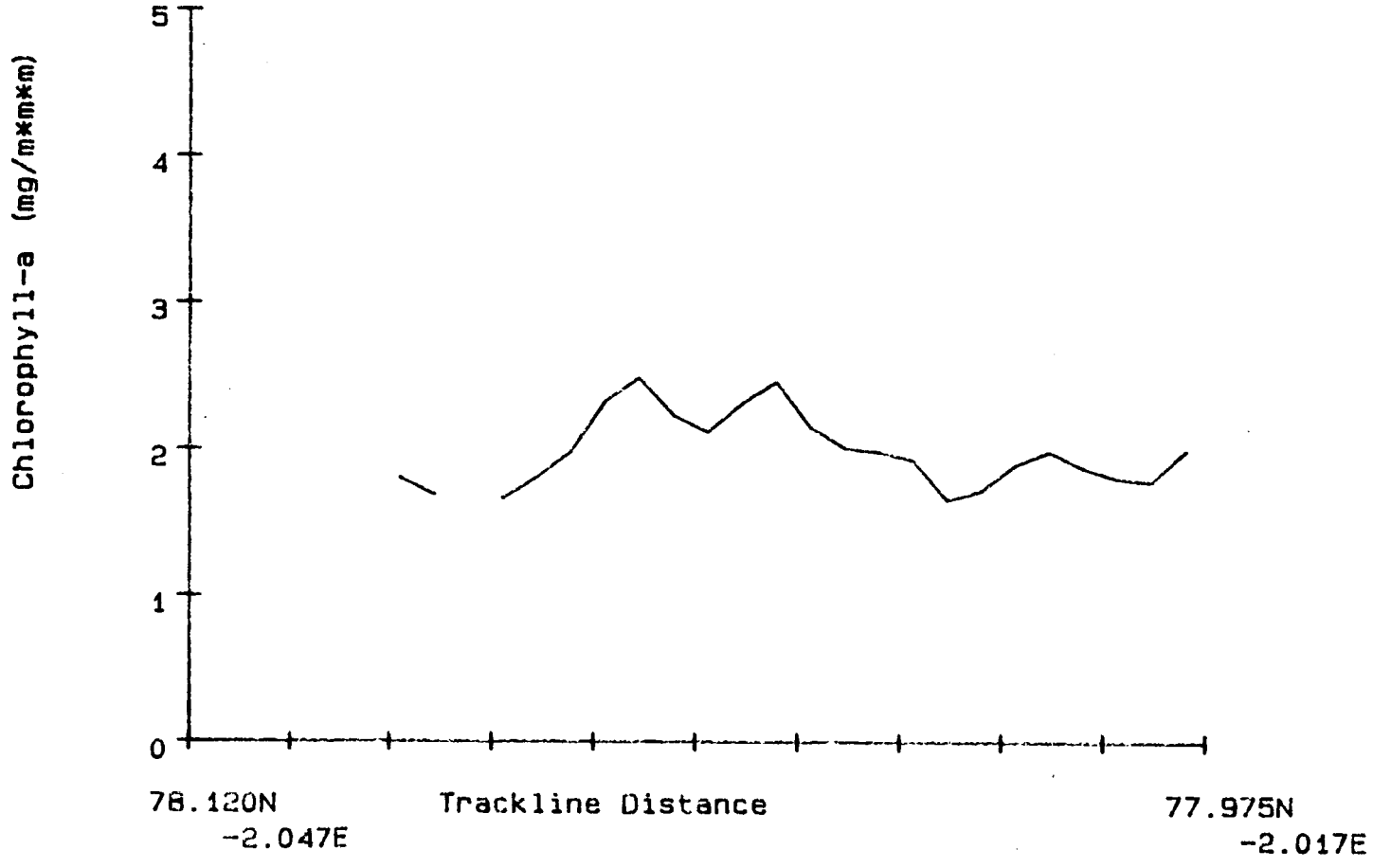

MARS Pigment (6 pt averages), 2 June 87

TRACKLINE C

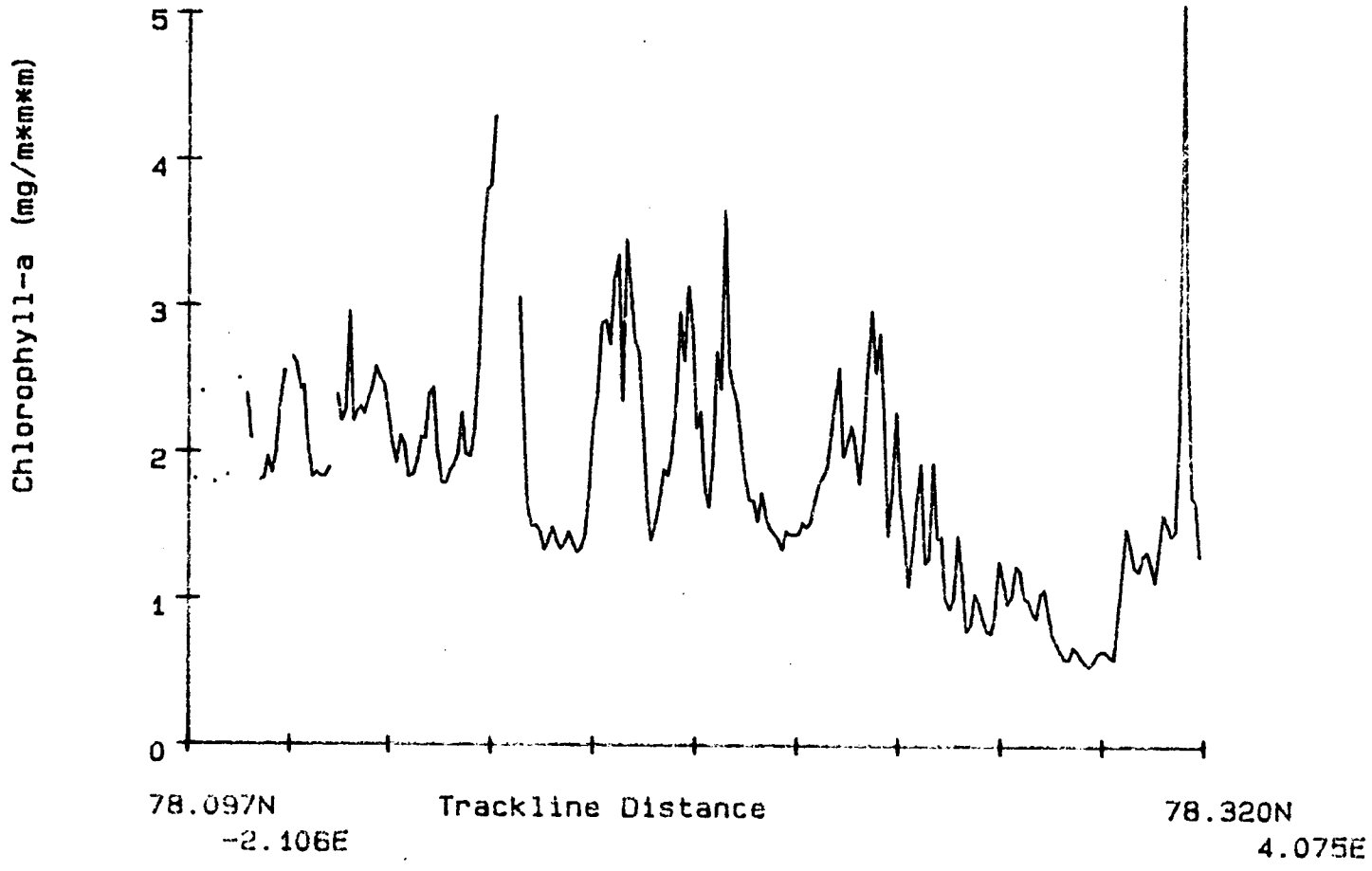

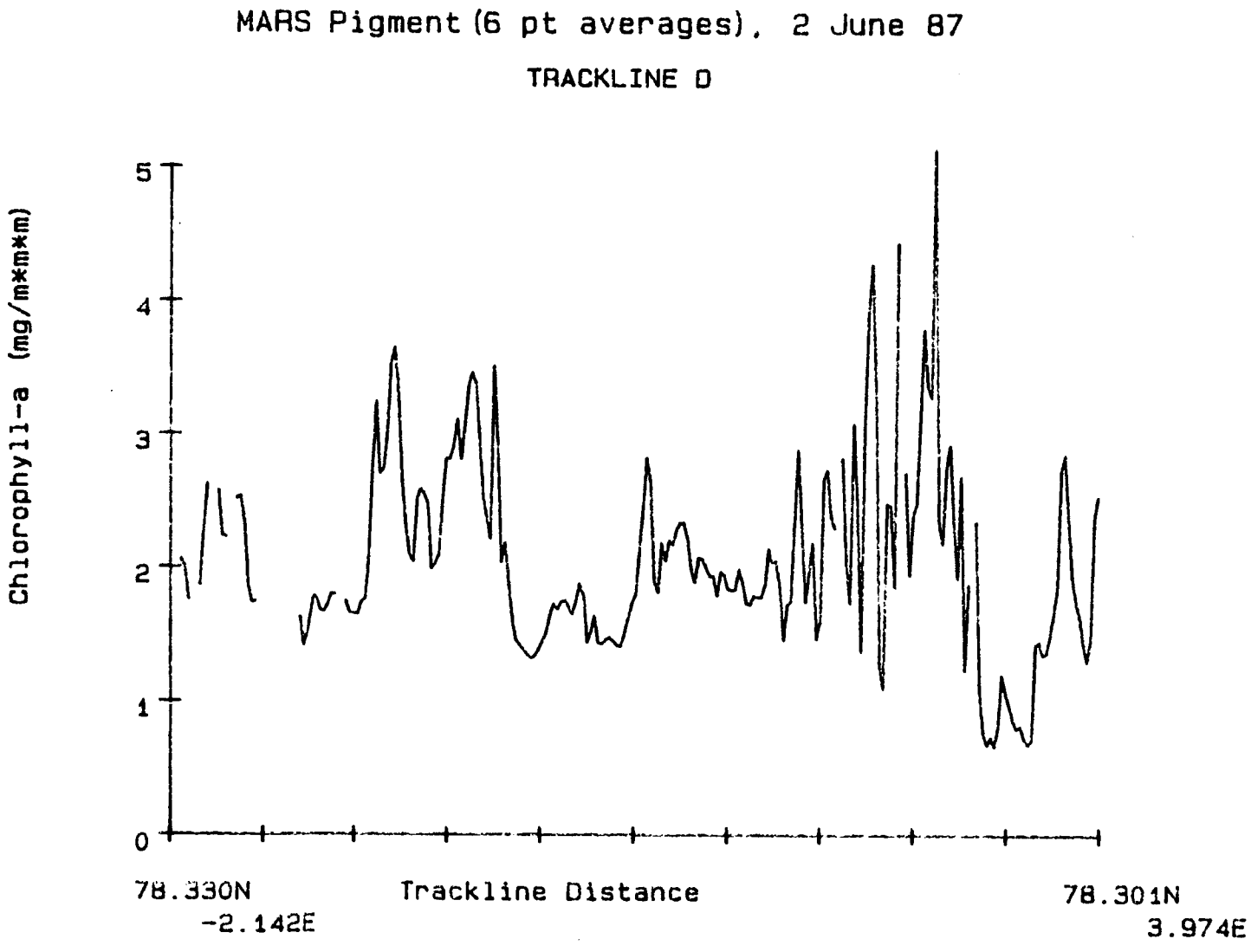
MARS Pigment (6 pt averages), 2 June 87
TRACKLINE D
Chlorophyll-a (mg/m*m*m)
5
4
3
2
1
0
78.330N
-2.142E
Trackline Distance
78.301N
3.974E

MARS Pigment (6 pt averages), 2 June 87

TRACKLINE E

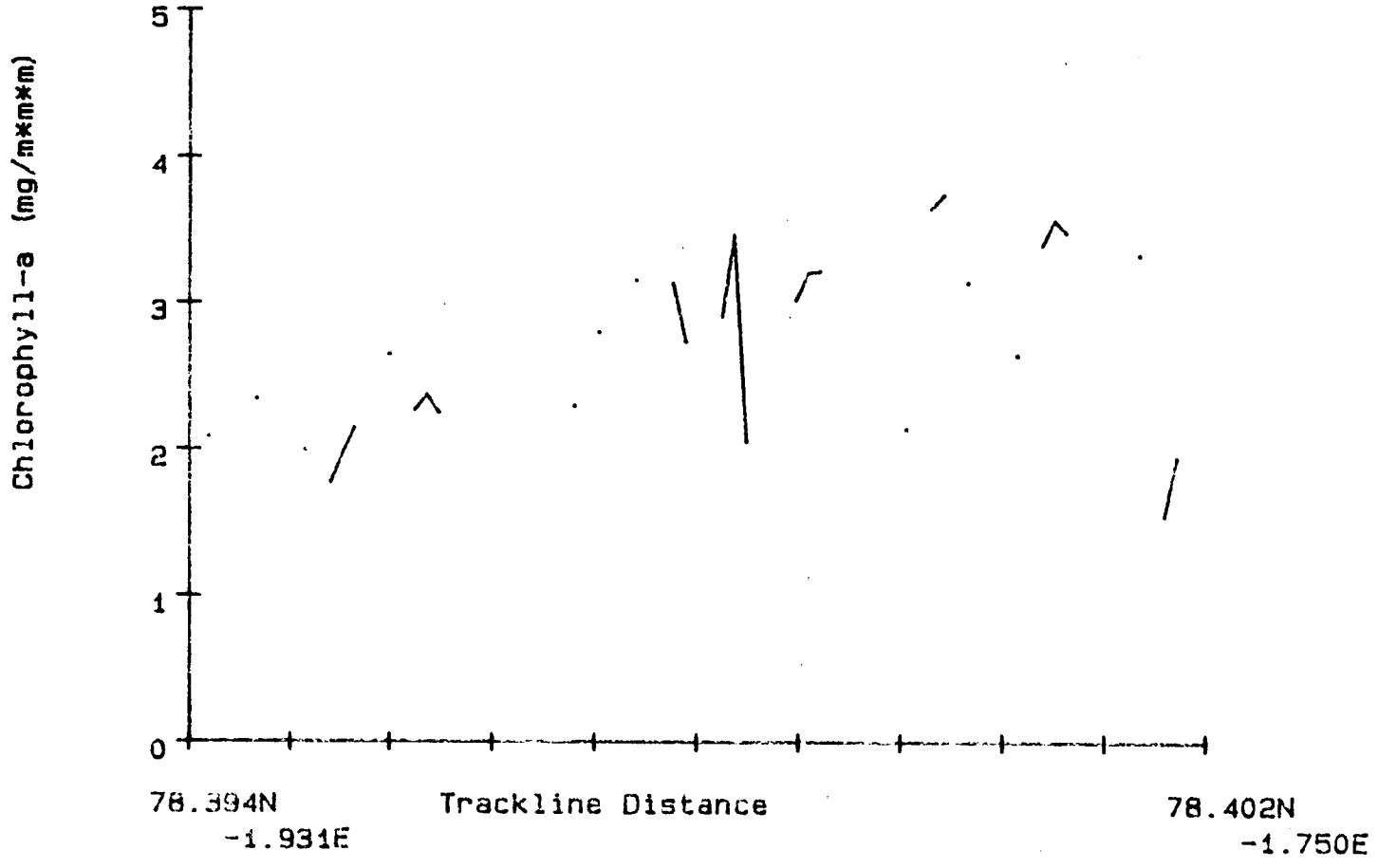

APPENDIX A: High-Performance Liquid Chromotography (HPLC) Measurements of Phytoplankton Pigment Distributions in the Greenland Sea (13 May - 19 June 1987)

TECHNICAL MEMORANDUM
OcOp-88t-003

10 March 1988

High-Performance Liquid Chromatography (HPLC) Measurements of Phytoplankton Pigment Distributions in the Greenland Sea

13 May - 9 June 1987

Charles C. Trees
Institute of Marine Resources
Scripps Institution of Oceanography
University of California, San Diego
La Jolla, CA 92093 USA

1.0 INTRODUCTION

Particulates, especially phytoplankton, significantly affect ocean optical properties by absorbing and scattering light and it is the various suite of pigments (chlorophylls, carotenoids phycobilins) present within the phytoplankton that contribute most to the attenuation of light. In coastal areas, where dissolved organic material and inorganic particulate concentrations are high, pigments have a reduced influence on the optical properties. The general absorption by the major algal pigments and the major windows of clarity in the water spectrum are shown in Figure 1. Chlorophylls (*a*, *b* and *c*) and some carotenoids (xanthophyll and carotene) have absorption maxima between 425-450 nm and from 525-575 nm for other carotenoids (fucoxanthin and peridinin) and phycoerthrins (red and blue-green algal). Between 525-650 nm another blue-green algal pigment, phycocyanin, has a maximum absorption peak. The spectra for the chlorophyll degradation products (chlorophyllides, phaeophorbides and phaeophytins) which are not shown in Figure 1 have similar absorption maxima as their associated chlorophylls.

Until the application of high-performance liquid chromatography (HPLC) to phytoplankton pigment analysis, it was difficult to quantitatively measure these various pigment compounds. HPLC is the state of the art method for the separation and quantification of photosynthetic pigments and recent investigations (Gieskes and Kray, 1983; Bidigare *et al.*, 1986; Trees *et al.*, 1986) have demonstrated that HPLC methods can be routinely used for phytoplankton pigment analysis. The use of HPLC minimizes the interferences caused by overlapping absorption and fluorescence bands of the various pigments, since the pigments are physically separated on the column and individually quantified by absorption and/or fluorescence detectors (Trees *et al.*, 1985).

HPLC derived pigments distributions were measured in the upper 75

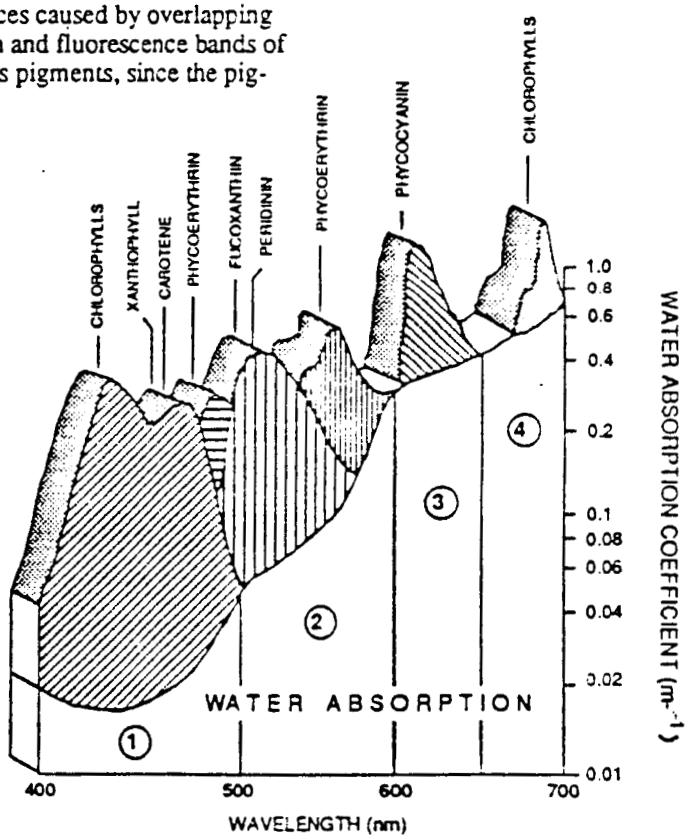

Figure 1. Relative pigment absorption and windows of water clariety (Yentsch, 1983).

meters by the Visibility Laboratory during a cruise on the RV Polarstern (13 May - 9 June 1987) in the Greenland Sea. Optical variability (OcOp-88t-004) was determined by deploying a spectral radiometer. During transects between stations, some discrete water samples were drawn from the shipboard sea chest for HPLC analysis. A generalized cruise track is shown in Figure 2 with station locations being summarized in Table 1.

2.0 HPLC METHODS AND INSTRUMENTATION

Water samples for pigment analyses were drawn from Niskin bottles which were spaced throughout the water column based on fluorescence profiles. At least one bottle was tripped within the phytoplankton biomass maximum. Samples were then filtered through 0.4 µm Nuclepore polyester membrane filters and extracted in an organic solvent for analysis on board the ship. The extraction solvent used was a 40:60% solution of dimethyl sulfoxide (DMSO) and 90% acetone. The advantage of this solvent is its enhanced pigment extraction efficiencies for cyanobacteria and green algae.

The HPLC system shown in Figure 3 consisted of a Spectra Physics Extended Range Pump (SP-8700XR) and Organizer Module-Dynamic Mixer (SP-8750) equipped with a reverse-phase Radial-PAK C^{18} column (10 µm particle size, Waters Associates) and 500 µl sample loop. To facilitate the separation of the dephytolated pigments (chlorophyllide *a*, phaeophorbide *a* and chlorophyll *c*) samples were mixed prior to injection with an ion-pairing solution of tetrabutylammonium acetate and ammonium acetate (Mantoura and Llewellyn, 1983). Pigments were separated on the column using a two solvent system [A-(80:10:10; methanol:ion-pairing solution:distilled water) and B-(100% methanol)]. Solvent A was pumped for three minutes followed by a linear gradient elution to 100% B in 9 minutes and then held at 100% B for 8 more minutes. At a flow rate of 10 ml min^{-1} the separation of the various pigments required 20 minutes. As the various chlorophylls and carotenoids were eluted off the column their peaks were measured using absorption a Waters Associates Model 440 Single

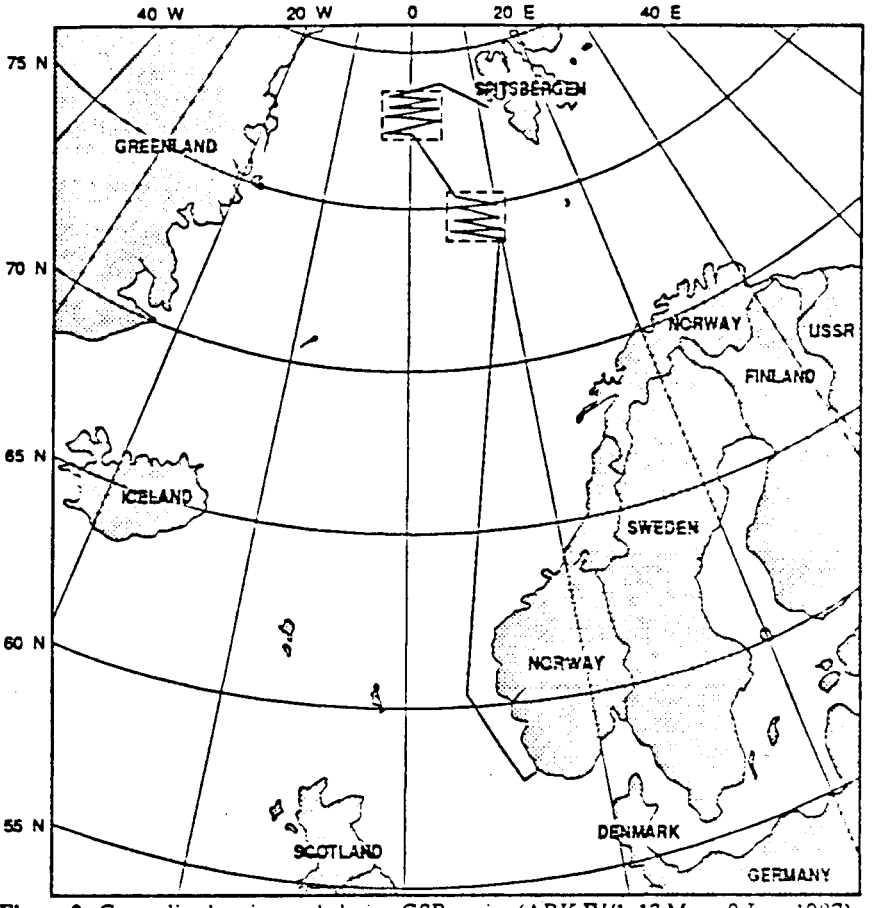

Figure 2. Generalized cruise track during GSP cruise (ARK IV/1, 13 May - 9 June 1987).

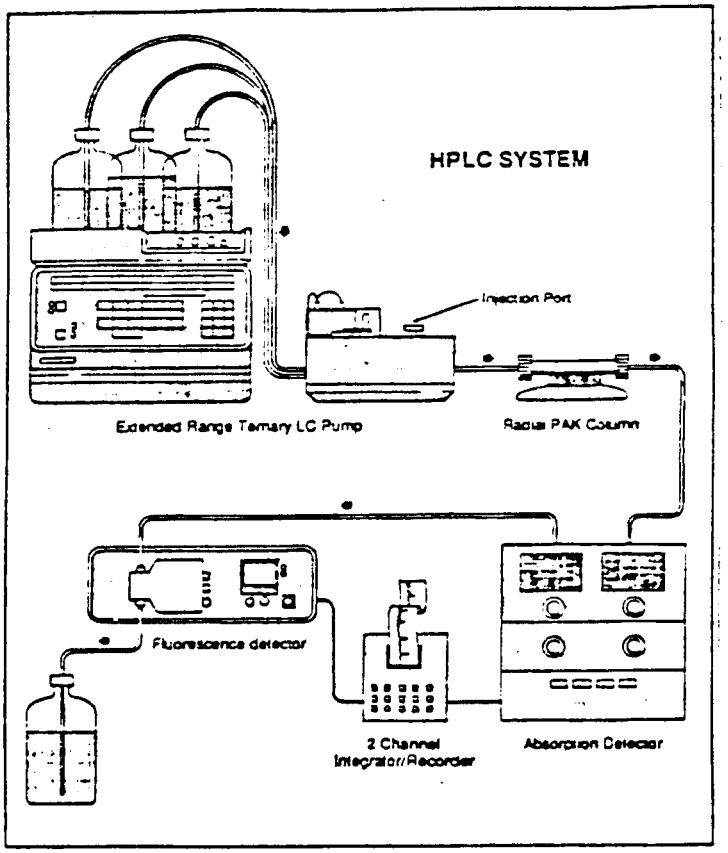

Figure 3. Simplified schematic of the high-performance liquid

Channel Absorbance Detector equipped with a 436 nm filter assembly. A sample chromatogram using this method is shown in Figure 4. The output from the absorption detector was recorded on a Spectra Physics Two Channel Computing Integrator (SP-4270) and pigment concentrations were calculated from calibration tables (concentration per peak height or area) which were prepared from pigment standards.

3.0 DATA

The HPLC derived pigment concentrations for the cruise is listed in Appendix A. Nine pigment compounds were identified and quantified from the chromatograms.

4.0 REFERENCES

Bidigare, R.R., T. Frank, C. Zastrow and J.M. Brooks. 1986. *Deep Sea Res.* 33, 923-937.

Gieskes, W.W. and G.W. Kraay. 1983. Mar. Biol. 75: 179-185.

Mantoura, R.F.C. and C.A. Llewellyn. 1983. Anal. Chim. Acta. 151, 297-314.

Trees, C.C., M.C. Kennicutt and J.M. Brooks. 1985. *Mar. Chem.* 16: 1-12.

Trees, C.C., R.R. Bidigare, and J.M. Brooks. 1986. *J. Plankton Res.* 8, 447-458.

Wright, S.W. and S.W. Jeffrey. 1987. *Mar. Ecol. Prog. Ser.* 38: 259-266.

Yentsch, C.S. 1983. In Remote Sensing Applications in Marine Science and Technology, A.P. Cracknell (ed.), D. Reidel Pub. Co., pp. 263-297.

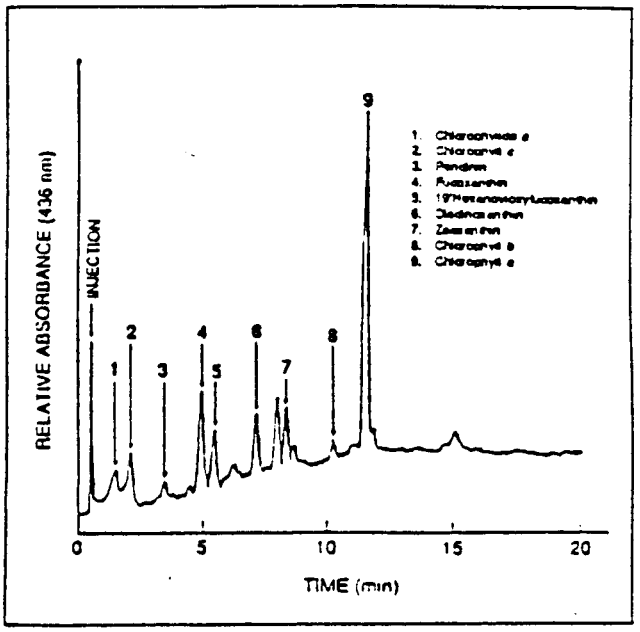

Figure 4. HPLC absorbance sample chromatogram.

Table 1. Station Locations for GSP Cruise (13 May - 9 June 1987)

Station	Latitude	Longitude
28	74.253°N	5.597°E
29	74.252°N	6.327°E
30	74.253°N	6.408°E
31	74.248°N	6.567°E
32	74.247°N	6.748°E
34	74.248°N	7.803°E
61	74.482°N	9.520°E
63	74.490°N	8.435°E
65	74.498°N	7.308°E
66	74.495°N	7.012°E
67	74.488°N	6.737°E
71	74.500°N	5.077°E
87	75.000°N	4.158°E
90	74.912°N	5.810°E
92	74.868°N	6.682°E
94	74.833°N	7.203°E
101	74.993°N	6.643°E
103	75.087°N	7.367°E
105	75.112°N	6.790°E
107	75.163°N	5.975°E
113	75.412°N	2.008°E
115	75.472°N	0.002°W
117	75.582°N	1.993°W
132	77.385°N	5.750°W
133	77.570°N	3.522°W
135	77.743°N	2.080°W
136	77.748°N	1.632°W
137	77.760°N	1.285°W
138	77.778°N	0.903°W
139	77.815°N	0.120°W
143	77.975°N	3.193°E
149	77.978°N	4.497°W
150	78.028°N	3.660°W
151	78.063°N	3.138°W
153	78.133°N	1.462°W
155	78.198°N	0.067°W
157	78.290°N	2.117°E
159	78.337°N	0.993°W
168	78.310°N	2.695°W
169	78.392°N	1.727°W
171	78.522°N	0.207°W
173	78.610°N	1.780°E
174	78.610°N	3.988°W
177	78.670°N	3.178°W
179	78.825°N	0.318°W

Appendix A. HPLC Derived Phytoplankton Pigment Concentrations from ARK 4/1 Cruise in the Greenland Sea; Station Data

Sta. No.	Depth	Chl a	Chl b	Chl c	Chlide a	Peridinin	Fuco	Hex	Diadino	Carotene
28	0	692	312	117	38	16	264	106	165	69
28	6.5	602	308	116	45	0	203	120	122	30
28	11	412	180	80	32	0	132	73	68	37
28	16	1377	1313	213	123	0	425	439	287	316
28	28	1710	652	306	177	40	807	360	197	34
28	43	1140	354	217	231	0	801	237	147	16
29	0	1037	337	240	157	55	67	402	348	57
29	10	1043	309	220	144	55	56	362	287	45
29	20	1141	385	291	200	49	128	430	234	38
29	30	879	369	237	163	30	137	347	72	36
29	40	607	325	142	95	0	130	208	98	51
29	50	445	308	97	74	0	144	83	14	27
30	0	613	357	108	45	0	107	135	137	48
30	7	647	341	101	39	0	91	121	157	56
30	13	540	336	101	46	0	74	127	164	66
30	20	973	467	204	96	37	171	226	218	12
30	31	1338	584	318	146	57	269	307	184	56
30	49	932	400	186	163	0	376	169	91	16
31	0	562	240	124	36	0	198	87	185	49
31	5	780	295	117	0	0	216	110	195	69
31	8	681	285	142	39	0	227	109	204	62
31	12	610	173	130	40	0	193	103	204	39
31	19	734	326	126	0	0	206	0	206	85
31	30	1296	551	305	110	25	356	272	208	31
32	0	261	201	48	0	0	55	77	81	23
32	5	381	279	52	0	0	0	109	85	37
32	8	435	329	64	37	0	68	133	103	55
32	13	334	280	55	24	0	52	89	83	46
32	21	423	268	78	30	0	77	102	98	37
32	50	817	355	188	107	0	273	212	93	46
34	0	1361	310	162	130	29	54	411	239	96
34	9	587	273	146	142	0	62	297	64	0
34	14	509	112	117	96	18	56	220	50	5
34	23	500	274	147	124	0	40	292	159	21
34	35	514	235	158	134	0	0	309	169	26
										38
61	0	1225	324	292	185	45	165	416	210	62
61	5	1015	167	228	154	30	127	284	118	47
61	9	1334	303	295	188	47	174	394	209	66
61	14	1151	315	263	173	32	160	378	189	60
61	23	2096	529	265	178	34	167	400	211	110
61	35	923	301	190	124	0	135	283	158	67
63	1	1165	360	313	210	44	156	559	293	51
63	6	1620	358	364	245	47	181	691	342	89
63	10	1610	386	333	226	56	163	656	330	87
63	17	1198	328	319	227	34	137	570	277	31
63	26	1132	165	293	201	0	131	505	271	56
63	41	1177	344	304	217	68	117	504	277	52

Appendix A. HPLC Derived Phytoplankton Pigment Concentrations from ARK 4/1 Cruise in the Greenland Sea; Station Data

Sta. No.	Depth	Chl a	Chl b	Chl c	Chlide a	Peridinin	Fuco	Hex	Diadino	Carotene
65	1	1787	293	550	345	37	383	528	315	83
65	5	1876	323	575	371	33	412	550	327	111
65	9	1886	287	563	342	0	416	560	336	85
65	16	2586	369	675	414	40	542	689	412	109
65	23	2435	402	606	394	52	530	697	396	99
65	35	1561	366	345	231	0	253	464	244	77
66	1	1523	255	398	310	0	174	701	255	76
66	8	1373	321	402	308	35	152	683	339	84
66	13	1463	338	390	306	30	146	680	340	85
66	21	1536	206	448	367	41	139	724	290	94
66	32	1082	395	301	255	0	158	545	227	74
67	0	1340	392	343	290	0	109	668	288	74
67	5	1413	397	355	297	18	125	688	291	60
67	8	1508	408	378	318	31	136	721	292	74
67	13	1325	392	327	271	22	114	649	273	82
67	27	1076	295	281	221	0	95	562	214	46
67	32	1051	213	286	228	0	138	594	204	110
71	0	2967	623	810	314	0	1596	453	444	128
71	4	3456	641	976	398	0	1896	558	504	122
71	8	1192	404	252	78	0	408	220	122	61
71	12	2493	683	531	104	0	1035	376	301	128
71	19	1960	710	432	125	0	783	347	264	103
71	30	2030	571	432	130	0	868	299	222	94
87	0	2237	740	396	170	0	872	343	328	84
87	5	2002	601	428	178	0	808	317	319	78
87	8	1940	642	399	166	0	780	311	308	86
87	12	1734	581	363	144	0	723	284	285	68
87	19	1764	541	386	150	0	764	290	289	92
87	30	1490	483	343	162	0	710	254	240	55
90	0	1424	581	326	138	0	443	311	266	49
90	5	1293	494	294	132	0	418	281	245	74
90	8	1562	554	327	139	0	489	285	256	78
90	12	1572	494	311	117	0	542	273	264	99
90	19	1594	508	314	123	0	564	269	253	91
90	30	1802	555	326	160	0	646	291	210	70
92	0	1273	370	348	299	0	149	665	328	58
92	10	1875	495	469	410	0	217	926	454	96
92	20	1566	416	443	389	0	191	846	429	35
92	30	1688	408	450	395	0	195	864	370	60
92	40	1474	402	384	339	0	180	790	327	74
92	50	1857	452	426	374	0	224	890	278	82
94	0	2285	328	688	515	56	401	802	467	85
94	7	2307	361	644	495	60	424	754	468	98
94	13	2238	342	665	483	47	432	758	461	87
94	20	3578	492	1036	715	85	708	1174	569	123
94	32	2304	379	668	487	39	446	844	335	100
94	49	1665	371	480	413	0	318	667	230	74

Appendix A. HPLC Derived Phytoplankton Pigment Concentrations from ARK 4/1 Cruise in the Greenland Sea: Station Data

Sta. No.	Depth	Chl a	Chl b	Chl c	Chlide a	Peridinin	Fuco	Hex	Diadino	Carotene
101	0	1266	647	188	107	0	238	276	231	107
101	10	748	407	144	86	0	146	194	174	54
101	20	1197	436	224	126	29	323	235	202	58
101	25	898	361	180	134	0	394	156	156	34
101	30	1060	276	198	196	0	537	208	144	38
101	40	1343	385	328	311	0	521	470	189	58
103	0	1484	354	410	232	27	424	428	398	77
103	5	1577	386	420	246	38	451	474	406	70
103	9	1694	379	412	229	43	443	457	398	79
103	13	668	313	178	120	0	126	207	165	37
103	21	1262	280	501	333	0	364	477	244	4
103	33	1155	318	329	285	0	296	455	121	35
105	0	912	490	165	98	0	177	235	215	86
105	5	834	439	157	93	0	140	200	193	70
105	9	1007	514	172	97	0	188	227	198	86
105	15	997	477	200	106	0	221	231	177	82
105	23	887	451	231	114	27	245	201	118	54
105	35	1316	406	338	234	56	439	297	128	54
107	0	976	333	237	81	56	246	224	292	63
107	5	1004	350	248	83	74	267	237	313	75
107	9	1028	341	240	84	69	262	225	302	84
107	15	994	359	246	92	54	207	248	285	73
107	23	1000	217	250	102	47	261	166	128	57
107	35	1015	528	198	103	0	231	187	60	69
113	0	358	0	61	47	0	43	94	125	33
113	12	314	0	64	43	0	44	91	139	16
113	21	282	0	68	45	0	84	110	0	16
113	34	349	0	98	64	0	75	137	201	0
113	53	621	0	187	150	0	260	125	97	22
113	75	522	0	118	112	0	267	54	26	23
115	2	1382	275	383	267	0	749	230	160	48
115	9	777	253	186	107	0	304	146	136	0
115	16	586	281	119	63	0	221	104	136	42
115	26	611	287	107	49	0	218	96	175	46
115	40	465	90	92	58	0	146	0	116	30
115	62	696	300	128	75	0	208	161	205	46
117	1	2333	222	484	463	0	1565	310	187	74
117	9	980	348	202	78	0	425	0	225	63
117	13	1026	290	242	89	0	453	132	189	39
117	18	845	288	175	80	0	350	146	257	58
117	31	742	266	159	73	0	300	153	230	56
117	44	1018	327	202	101	0	388	213	292	71
132	0	587	346	117	81	0	160	113	0	48
132	20	333	297	64	50	0	117	63	0	24
132	31	212	230	35	53	0	86	0	0	22
132	49	50	0	0	0	0	0	0	0	0
132	76	103	0	0	0	0	0	0	0	0

Appendix A. HPLC Derived Phytoplankton Pigment Concentrations from ARK 4/1 Cruise in the Greenland Sea; Station Data

Sta. No.	Depth	Chl a	Chl b	Chl c	Chlide a	Peridinin	Fuco	Hex	Diadino	Carotene
132	100	74	0	0	0	0	0	0	0	0
133	1	290	0	47	19	0	0	0	0	20
133	11	247	0	40	0	0	0	0	0	19
133	30	93	0	0	0	0	0	0	0	0
133	45	79	0	20	0	0	0	0	0	0
133	70	53	0	0	0	0	0	0	0	0
135	0	1820	182	662	424	0	309	963	341	78
135	5	1982	215	677	449	0	0	1034	297	81
135	9	1967	510	703	470	0	691	727	266	113
135	13	2110	627	729	523	0	913	577	216	119
135	21	2096	582	780	537	0	1062	572	219	100
135	33	913	385	230	172	0	312	273	59	46
135	75	474	120	158	148	0	182	0	0	0
136	0	1354	286	259	99	0	376	254	353	84
136	5	1747	543	447	186	0	567	505	432	111
136	10	2079	650	669	335	0	660	684	387	114
136	13	2366	798	736	359	0	767	647	346	174
136	20	3145	949	112	612	0	1278	66	300	174
136	32	1437	807	340	240	0	433	416	0	75
136	74	286	223	61	54	0	88	100	0	17
137	0	776	396	141	43	0	136	231	158	58
137	8	1297	545	329	148	0	333	386	169	48
137	14	2122	796	572	306	0	675	487	210	106
137	22	2973	974	752	442	0	947	553	239	146
137	35	1599	718	347	220	0	440	295	117	72
137	56	501	141	132	108	0	166	0	0	0
138	0	846	360	184	86	0	170	267	187	76
138	6	1359	450	330	162	0	280	402	254	84
138	10	1530	498	410	200	0	335	444	0	89
138	16	1400	497	398	220	0	454	367	198	73
138	25	1917	776	506	332	0	664	400	175	101
138	38	704	327	186	163	0	251	0	0	49
139	0	1710	576	416	210	0	373	435	243	96
139	5	2424	655	798	448	0	757	568	275	119
139	9	2664	702	916	529	0	946	654	313	134
139	15	2847	727	1013	642	0	1108	717	304	140
139	23	1028	379	545	402	0	632	567	179	110
139	35	433	281	111	81	0	144	0	0	40
143	0	1481	470	442	365	0	152	967	470	74
143	5	1566	432	556	460	0	0	1166	435	0
143	8	1688	428	575	487	0	0	1309	441	72
143	12	1915	438	633	574	0	201	1377	452	98
143	19	1130	293	365	327	0	360	633	171	58
143	30	723	238	210	193	0	301	282	84	29
143	75	397	0	79	83	0	214	0	0	22
149	0	344	0	99	64	0	105	86	24	17

Appendix A. HPLC Derived Phytoplankton Pigment Concentrations from ARK 4/1 Cruise in the Greenland Sea; Station Data

Sta. No.	Depth	Chl a	Chl b	Chl c	Chlide a	Peridinin	Fuco	Hex	Diadino	Carotene
149	12	339	0	96	60	0	42	42	0	0
149	21	237	0	59	37	0	78	99	0	0
149	34	221	0	29	0	0	0	0	0	0
149	53	163	0	42	33	0	51	0	0	0
149	81	89	0	19	0	0	0	0	0	19
149	100	109	0	0	0	0	0	0	0	0
150	0	1275	616	260	124	0	273	334	265	90
150	6	2215	660	586	309	0	700	560	366	124
150	10	2357	640	596	341	0	684	580	293	116
150	16	2828	712	729	409	0	970	642	343	145
150	25	2475	830	706	443	0	919	556	208	160
150	38	1026	470	287	194	0	361	272	106	58
150	75	1177	756	248	171	0	0	342	0	0
151	0	1594	378	360	180	0	412	408	124	96
151	7	2417	593	598	331	0	744	552	158	139
151	11	3260	746	825	484	0	1099	693	223	184
151	18	3091	629	871	568	0	1400	680	176	147
151	28	2457	856	549	354	0	819	399	97	138
151	43	1536	603	390	256	0	436	323	96	64
151	75	304	0	93	89	0	84	0	0	0
153	0	2765	267	865	483	0	906	1070	410	130
153	4	3040	233	968	545	0	975	1087	286	173
153	6	3462	322	934	635	0	1225	1099	320	135
153	10	3379	298	1078	718	0	1369	1116	270	130
153	16	2806	356	865	613	0	1108	901	185	101
153	24	1099	230	258	239	0	340	384	23	59
153	75	492	108	102	99	0	173	96	0	51
155	0	1472	245	406	210	0	164	164	217	88
155	3	2634	741	794	543	0	363	1505	801	146
155	5	2678	743	827	554	0	334	1141	675	152
155	8	2287	545	669	495	0	256	1163	561	112
155	12	2211	311	595	431	0	217	1126	510	110
155	19	3047	511	894	896	0	744	628	73	17
157	0	3122	808	958	970	0	1070	756	265	116
157	4	3891	751	1233	1122	0	1326	545	289	129
157	7	3972	716	1310	1217	0	1362	876	209	142
157	11	4202	839	1321	1407	0	1676	1180	315	145
157	18	3932	874	1210	1197	0	1455	561	237	138
157	27	3149	622	869	1047	0	1191	469	232	112
157	75	971	295	222	271	0	418	252	113	65
159	0	2217	508	615	278	0	700	404	351	155
159	5	3507	362	1437	704	0	1892	784	370	139
159	10	6380	554	2714	1422	0	3232	1351	793	291
159	15	2117	169	648	273	0	1044	392	104	104
159	20	2587	377	727	274	0	1331	546	151	123
159	30	734	274	175	140	0	251	154	0	9
168	0	1858	424	731	373	0	908	302	277	102

Appendix A. HPLC Derived Phytoplankton Pigment Concentrations from ARK 4/1 Cruise in the Greenland Sea; Station Data

Sta. No.	Depth	Chl a	Chl b	Chl c	Chlide a	Peridinin	Fuco	Hex	Diadino	Carotene
168	6	1936	167	738	398	0	673	301	48	70
168	10	3035	363	1290	732	0	1659	704	324	142
168	16	4115	395	1720	1018	0	2297	887	360	188
168	25	1481	264	600	364	0	879	348	134	78
168	38	850	272	286	216	0	491	217	89	47
168	75	306	0	84	78	0	144	62	0	8
169	0	2284	680	748	429	0	904	776	389	117
169	5	2485	560	854	496	0	1104	774	273	114
169	10	2856	634	998	576	0	1336	958	232	137
169	15	1174	377	361	208	0	592	448	101	56
169	25	706	282	186	124	0	342	271	0	40
169	40	296	0	60	44	0	130	0	0	22
171	0	1797	432	469	255	0	604	422	462	93
171	5	2059	401	587	321	0	790	314	377	87
171	8	1411	357	456	249	0	622	488	261	82
171	19	1237	186	526	305	0	712	157	107	44
171	30	312	204	94	63	0	158	85	44	0
171	50	143	0	38	34	0	0	0	0	0
173	0	1938	536	441	283	53	502	452	300	110
173	5	4327	837	479	324	72	552	442	346	258
173	12	2276	568	493	392	47	564	427	242	112
173	19	1708	441	477	515	0	627	298	122	50
173	30	1263	305	313	439	0	588	213	102	38
174	0	537	0	133	120	0	414	0	87	28
174	12	926	0	253	217	0	645	152	119	44
174	21	488	0	146	100	0	297	106	77	30
174	34	177	0	53	37	0	83	50	5	0
174	53	152	0	38	0	0	64	39	7	0
174	81	178	0	39	0	0	64	30	19	17
177	0	1450	287	408	120	0	700	170	329	60
177	7	1208	249	365	142	0	574	150	246	43
177	11	906	245	289	124	0	406	120	173	40
177	18	619	245	173	91	0	294	120	101	30
177	28	541	220	180	138	0	305	114	80	27
177	43	582	248	170	160	0	356	119	81	27
179	0	3513	511	1297	820	0	1696	464	326	109
179	4	4268	521	1500	947	0	1866	778	506	165
179	7	1628	425	433	297	0	780	230	119	48
179	11	1059	318	313	242	0	599	183	83	54
179	18	880	352	200	212	0	457	162	73	45
179	27	735	203	190	202	0	411	132	52	31

APPENDIX B: OPTICAL VARIABILITY DURING GREENLAND SEA PROJECT CRUISE (ARK IV/1) ON THE RV POLARSTERN

Technical Memorandum

10 March 1988

OPTICAL VARIABILITY DURING GREENLAND SEA PROJECT CRUISE (ARK IV/1) ON THE RV POLARSTERN

13 May - 9 June 1987

Charles C. Trees
Institute of Marine Resources
Scripps Institution of Oceanography
University of California, San Diego
La Jolla, CA 92093 USA

Sta.	*Diffuse Attenuation Coefficient (488nm)				Model	Cast Depth (m)	Ave. K(488) to 100m	Secchi Disc Depth (m)
28	0.069 30	0.0738/46		0.0499	two layer with hump	140	0.0606	24.6
30	0.046o/40	0.0719/56		0.0409	two layer with hump	105	0.0485	36.4
31	0.0661/31			0.0868	two layer with hump	56	–	25.7
61	0.0702/41	0.0285/65		0.0376	two layer with inverse	123	0.0498	24.2
63	0.0653/39	0.0413/61		0.0315	two layer with inverse	115	0.0462	26.0
65	0.0947/24	0.0778/50		0.0460	three layer	110	0.0656	18.0
66	0.0762/41			0.0410	two layer	125	0.0556	22.3
67	0.0649/49			0.0367	two layer	119	0.0496	26.2
90	0.0795/61			0.0372	two layer	166	0.0647	21.4
91	0.0813/62			0.0421	two layer	118	0.0664	20.9
92	0.0819/52			0.0544	two layer	96	0.0689	20.8
94	0.0890/54	0.0750/82		0.0404	three layer	117	0.0763	19.1
101	0.0669/40	0.0886/63		0.0656	two layer with hump	82	0.0717	25.4
103	0.0760/17	0.1322/39		0.0334	two layer with hump	136	0.0625	22.4
105	0.0619/41	0.1076/59		0.0402	two layer with hump	138	0.0613	27.5
107	0.0657/29	0.0531/81		0.0410	three layer	143	0.0545	25.9
113				0.0392	single layer	192	0.0392	43.4
117	0.0657/76			0.0348	two layer	180	0.0573	25.9
132	0.0780/31			0.0365	two layer	168	0.0503	21.8
133	0.0640/22			0.0310	two layer	193	0.0388	26.6
134	0.0674/18			0.0301	two layer	92	0.0363	25.2
135	0.1061/44			0.0342	two layer	150	0.0665	16.0
136	0.0827/16	0.1406/34		0.0328	two layer with hump	103	0.0619	20.6
143	0.0808/16	0.1432/29		0.0360	two layer with hump	168	0.0560	21.0
149	0.0639/50			0.0333	two layer	168	0.0493	26.6
150	0.1078/50			0.0421	two layer	100	0.0753	15.8
151	0.0964/9	0.1468/23	0.0860/45	0.0434	three layer with hump	93	0.0724	17.6
152	0.1112/10	0.1601/22	0.0887/41	0.0455	three layer with hump	93	0.0749	15.2
157	0.1841/23	0.1407/49		0.0704	three layer	49	–	9.2
159	0.1478/8	0.2100/20	0.0712/35	0.0326	three layer with hump	96	0.0703	11.5
168	0.0906/29	0.0450/72		0.0350	three layer	193	0.0562	18.8
169	0.1733/27			0.0350	two layer	94	0.0737	9.8
171	0.0866/24			0.0369	two layer	141	0.0493	19.6
174	0.0782/22			0.0490	two layer	148	0.0556	20.5
177	0.1110/13	0.0497/49		0.0321	three layer	151	0.0488	15.3

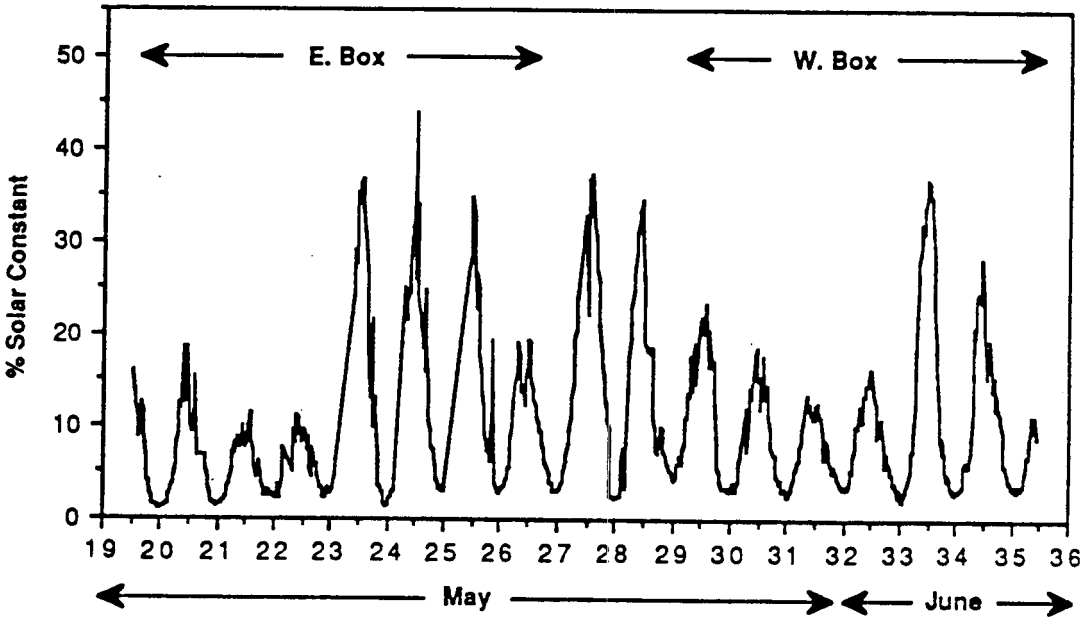
E. Box
W. Box
% Solar Constant
50
40
30
20
10
0
19 20 21 22 23 24 25 26 27 28 29 30 31 32 33 34 35 36
May
June

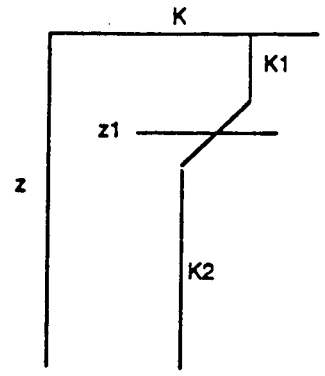

(a) Two Layer Model

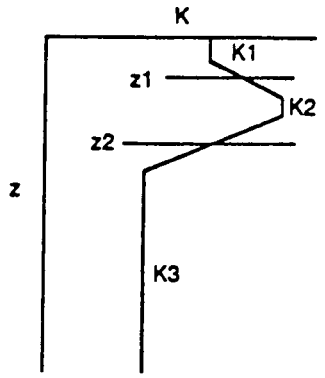

(b) Two Layer Model with Hump

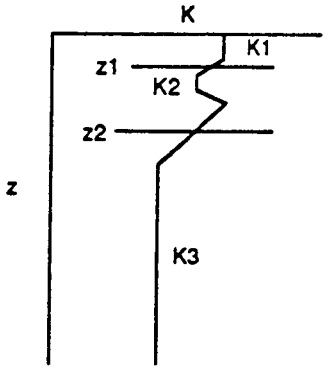

(c) Two Layer Model with Inverse

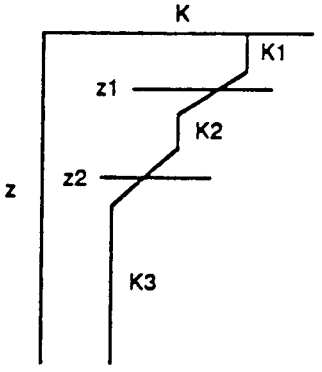

(d) Three Layer Model

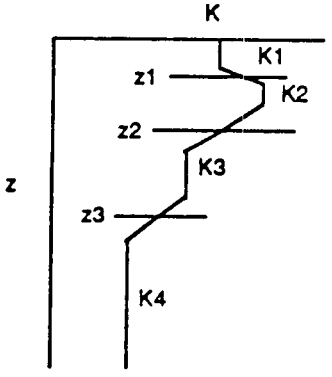

(e) Three Layer Model with Hump

Figure 1. Types of K profiles encountered on GSP Cruise

DATA ANALYSIS:

*Derived K (diffuse attenuation coefficients) profiles computed from the cruise data can be characterized as one of five general curves. These five typical types of curves are shown in Figure 1 and identified as:

(a) two layer model
(b) two layer model with hump
(c) two layer model with inverse
(d) three layer model
(e) three layer model with hump

The data from any station can be generally categorized by, starting at the surface, giving the surface K value, the transition depth, the next K value, the transition depth, etc.

Secchi disc depths were calculated from the K values in the upper surfaces waters using the formula of 1.7/Secchi disc depth = K (Poole and Atkins, 1929; J. Mar. Biol. Ass. U.K.).

APPENDIX C

MARS POST-MISSION CALIBRATION and CHARACTERIZATION

The MARS instrument was radiometrically calibrated by viewing a flat Barium-Sulfate plate which was illuminated by laboratory standard lamp traceable to an NBS standard source. The calibration lamp was fixed at a distance of 50 cm from the plate, and was surrounded by light baffles to prevent stray illumination, e.g. reflected from the walls in the laboratory, from reaching the reflectance plate. The source was positioned normal to the reflectance plate, the MARS viewed irradiance reflected from the plate at an angle 45 degrees from the normal, and the voltage response in each MARS channel was recorded. Given the known value E(ch) of irradiance from the lamp for the wavelength of each MARS channel ch, reflectance of the plate (0.95), and the voltage response V(ch) of each channel, the radiance sensitivity

$$F(ch) = PI * V(ch) / [\ 0.95 * E(ch)\ ]$$

was calculated. To convert MARS voltage output to radiance units, the MARS software divides by F.

The instrument was calibrated both before and after the Greenland Sea deployment in May-June 1987. However, the first calibration was done when the sphere was coated with PTFE (halon). During air shipment to West Germany, the halon coating detached from the interior of the sphere. The sphere was then recoated with Barium-Sulfate immediately prior to deployment to Spitzbergen, thus invalidating the pre-mission calibration. The calibration values used in the present analysis were determined in mid-June 1987, immediately after the instrument was returned to San Diego. The gain sensitivity factors F for this calibration are listed in Table C-1.

The spectral bandpass of each channel was obtained by passing the illumination from a laboratory standard lamp through a grating monochromator, and by recording the MARS output in each channel as the monochromator was scanned through the appropriate range of wavelengths. The wavelengths of peak response and at the positions of half-power response were recorded for each channel and used to determine the centroid wavelength and spectral bandwidth (full-width half-power). The resulting wavelength characterization is also listed in Table C-1.

The Biospherical Instrument Inc. electronics boards used in the MARS feature an autozero function which clamps the output voltage to remove dark current biases as determined prior to takeoff on

each flight. Additional dark current readings were recorded during most of the flights to determine any drift in this baseline during the flight. The mean values from each of the dark-reading data segments were averaged and are listed here in Table C-2. These values must be subtracted from the calibrated radiance data in the ASCII data files on the 9-track magnetic tape which accompanies this report.

Table C-1

MARS Post-Mission Calibration Summary - June 1987
Greenland Sea Deployment (21 May thru 2 June 1987)

Performed by: Jack Varah
Visibility Laboratory
Scripps Institution of Oceanography
University of California, San Diego
La Jolla, CA 92093

Channel	F volts/radiance*	Center Wavelength nm	Spectral Bandpass nm (HPFW)
1	0.00361	409	13.9
2	0.00827	438	11.3
3	0.02667	487	10.5
4	0.02337	519	10.0
5	0.04389	549	9.9
6	0.07100	586	12.1
7	0.08001	630	13.0
8	0.10138	666	13.8
9	0.09638	680	14.4
10	0.08322	726	19.0

* radiance units are mW/(cm**2 sr micro-m)

Table C-2

MARS Dark Current Readings in mw/(cm**2 sr μm)

Date	Channel	Dark Radiance
jun01		
	1	0.000000e+000
	2	0.000000e+000
	3	4.469790e-005
	4	0.000000e+000
	5	6.735909e-005
	6	3.358008e-006
	7	0.000000e+000
	8	0.000000e+000
	9	1.484241e-006
	10	5.729839e-007
jun02		
	1	0.000000e+000
	2	0.000000e+000
	3	1.119235e-003
	4	3.199318e-003
	5	3.107210e-004
	6	9.261386e-004
	7	3.528154e-004
	8	6.217979e-004
	9	3.581968e-004
	10	4.578141e-004
may21		
	1	3.090856e-003
	2	0.000000e+000
	3	1.401726e-003
	4	7.008711e-003
	5	2.172874e-005
	6	1.141723e-004
	7	8.605836e-004
	8	1.767091e-003
	9	8.188063e-004
	10	1.652485e-003
may25		
	1	3.156900e-003
	2	0.000000e+000
	3	0.000000e+000
	4	0.000000e+000
	5	0.000000e+000
	6	0.000000e+000
	7	0.000000e+000
	8	0.000000e+000
	9	0.000000e+000
	10	0.000000e+000

Table C-2 continued

MARS Dark Current Readings in mw/(cm**2 sr um)

Date	Channel	Dark Radiance
may29		
	1	9.960000e-003
	2	0.000000e+000
	3	4.000000e-005
	4	4.816000e-003
	5	1.168000e-003
	6	8.840000e-004
	7	6.550000e-004
	8	8.950000e-004
	9	4.950000e-004
	10	1.012000e-003
may30		
	1	1.492593e-003
	2	5.765866e-006
	3	0.000000e+000
	4	0.000000e+000
	5	0.000000e+000
	6	0.000000e+000
	7	0.000000e+000
	8	0.000000e+000
	9	0.000000e+000
	10	0.000000e+000
may31		
	1	2.919142e-003
	2	2.208327e-003
	3	0.000000e+000
	4	1.428267e-005
	5	4.769458e-004
	6	1.296191e-004
	7	0.000000e+000
	8	3.292425e-006
	9	8.905446e-006
	10	2.429452e-004

APPENDIX D

DATA FORMATS

The MARS data for each flight segment illustrated in Section 6 are available as ASCII files on magnetic tape. One copy of of the data tape has been furnished to NASA GSFC with this report. Additional copies of the MARS GSP data tape may be requested from the authors at:

SDSU CHORS
6505 Alvarado Rd; Suite 206
San Diego, CA 92128

Ph: 619/594-2272

For each flightline, the MARS data are provided in two files. The first file for each trackline contains the calibrated radiances (which must, however, be corrected for dark current readings - Appendix C; radiance values for channels 1 and 2 should also be scaled by factors 0.83 and 0.95 respectively - Section 5). A second file contains the estimate of chlorophyll-a concentration (micro-grams per liter) calculated by the methods described in Sections 3, 4 and 5 for all valid data points (i.e. no clouds or ice flagged by a brightness anomaly in channel 10) in each trackline.

The tape contains 82 files, which are identified in Table D-1. The file names comprise the month, day and track segment, with ".dat" appended to denote calibrated radiance data files, and ".chl" appended to denote estimated chlorophyll-a data files. Comments identify files containing sea ice segments and Polarstern stations (denoted PS Sta # times = tttttt,...), where times are in seconds. The times in these data records are GMT + 4 hrs, which was dictated by the time to which the Dornier's Inertial Navigation System was set (we are mystified concerning the motive for this choice of time zone, but it's of no importance).

RADIANCE FILE FORMAT (mmmdd_x.dat files - Table D-1):

The first 41 files on the MARS GSP-87 data tape are calibrated radiance files (see Table D-1).

These files are formatted, fixed-block ASCII files.

The blocksize is 4590 bytes.

There are 30 logical records, each containing 153 bytes, in each block (physical record). Each logical record ends in an ASCII newline character '\n'.

The final block in each file is padded with ASCII blanks ' ' to maintain the fixed blocksize at 4590 bytes.

The first logical record in each file is an ASCII text label which identifies the file type, date of data acquisition, and trackline id letter; the record is then padded with blanks and a newline to length 153.

The remaining records in the file are MARS radiance records with annotated navigation data. Using FORTRAN conventions, each record is given in the following format:

Variable Identification	Type	Name	Format
Record Number	integer	REC	I5
A Colon ':'	character	C	A1
Time in Sec (GMT + 4 hrs)	real*8	TIME	F9.2
MARS RADIANCE (Ch 1..10) in mW/(cm**2 sr um)	real*4	RAD(10)	10F9.4
Latitude (dec. deg; + => N)	real*4	LAT	F10.3
Longitude (dec deg; + => E)	real*4	LON	F10.3
Ground Speed (knots)	real*4	SPEED	F9.1
Course Angle (degress from true North; + clockwise)	real*4	COURSE	F9.1
Altitude (feet)	real*4	ALT	F9.1

CHLOROPHYLL FILE FORMAT (mmmdd_x.chl file - Table D-1):

The last 41 files (42..82) contain chlorophyll-a concentrations estimated from the MARS alongtrack data (see Table D-1).

These files are formatted, fixed-block ASCII files.

The blocksize is 3250 bytes.

There are 50 logical records, each containing 65 bytes, in each block (physical record). Each logical record ends in an ASCII newline character '\n'.

The final block in each file is padded with ASCII blanks ' ' to maintain the fixed blocksize at 3250 bytes.

The first logical record in each file is an ASCII text label which identifies the file type, date of data acquisition, and trackline id letter; the record is then padded with blanks and a newline to length 65.

The remaining records in the file are MARS chloropyll, yellow index, and color index records with annotated navigation data. Using FORTRAN conventions, each record is given in the following format:

Variable Identification	Type	Name	Format
Record Number	integer	REC	I6
Time in Sec (GMT + 4 hrs)	real*8	TIME	F10.2
Ice Flag (0 => open water)	integer	ICE	I3
Latitude (dec. deg; + => N)	real*4	LAT	F9.3
Longitude (dec deg; + => E)	real*4	LON	F9.3
Chlorophyll-a Conc (ug/l)	real*4	CHL	F7.2
Yellow Index [Lw(410)/Lw(550)]	real*4	YELLOW	F10.4
Color Index [Lw(440)/Lw(550)]	real*4	COLOR	F10.4

TABLE D-1

MARS GSP-87 DATA TAPE CONTENT

File #	File Name	Comments
1	jun1_a.dat	
2	jun1_b.dat	
3	jun1_c.dat	Sea Ice; PS Sta 159 times = 59237, 59405, 59565 & 59735
4	jun1_d.dat	PS Sta 159 time = 62766
5	jun1_e.dat	
6	jun1_f.dat	
7	jun1_g.dat	
8	jun2_a.dat	
9	jun2_b.dat	
10	jun2_c.dat	
11	jun2_d.dat	
12	jun2_e.dat	PS Sta 169 times = 61444, 61551, 61661, 61766 & 61842
13	may21_b.dat	
14	may21_c.dat	
15	may21_d.dat	
16	may23_a.dat	PS Sta 92 times = 57835, 58010 & 58210
17	may23_b.dat	
18	may23_c.dat	
19	may23_d.dat	
20	may23_e.dat	
21	may25_a.dat	
22	may25_b.dat	
23	may25_c.dat	
24	may25_p.dat	
25	may29_a.dat	Includes Sea Ice Segments
26	may29_b.dat	PS Sta 133 times = 60998, 61100 & 61222
27	may29_c.dat	
28	may29_d.dat	
29	may29_t.dat	
30	may30_a.dat	PS Sta 143 times = 53834, 54014 & 54168
31	may30_b.dat	
32	may30_c.dat	
33	may30_d.dat	
34	may30_e.dat	
35	may31_a.dat	PS Sta 151 times = 57835, 57900 & 58043
36	may31_b.dat	
37	may31_c.dat	
38	may31_d.dat	
39	may31_e.dat	
40	may31_f.dat	
41	may31_g.dat	

TABLE D-1 (Cont'd)

MARS GSP-87 DATA TAPE CONTENT

File #	File Name	Comments
42	jun1_a.chl	
43	jun1_b.chl	
44	jun1_c.chl	
45	jun1_d.chl	
46	jun1_e.chl	
47	jun1_f.chl	
48	jun1_g.chl	
49	jun2_a.chl	
50	jun2_b.chl	
51	jun2_c.chl	
52	jun2_d.chl	
53	jun2_e.chl	
54	may21_b.chl	
55	may21_c.chl	
56	may21_d.chl	
57	may23_a.chl	
58	may23_b.chl	
59	may23_c.chl	
60	may23_d.chl	
61	may23_e.chl	
62	may25_a.chl	
63	may25_b.chl	
64	may25_c.chl	
65	may25_p.chl	
66	may29_a.chl	
67	may29_b.chl	
68	may29_c.chl	
69	may29_d.chl	
70	may29_t.chl	
71	may30_a.chl	
72	may30_b.chl	
73	may30_c.chl	
74	may30_d.chl	
75	may30_e.chl	
76	may31_a.chl	
77	may31_b.chl	
78	may31_c.chl	
79	may31_d.chl	
80	may31_e.chl	
81	may31_f.chl	
82	may31_g.chl	